On the Decellularization and Recellularization of Tissue Engineered Heart Valves

By

Mitchell Charles VeDepo

Submitted to the Bioengineering Program and the Graduate Faculty of the
University of Kansas in partial fulfillment of the requirements
for the degree of Doctor of Philosophy.

Committee Members:

_____
Chair: Dr. Arghya Paul, Ph.D.

_____
Co-Chair: Dr. Gabriel Converse, Ph.D.

_____
Dr. Richard Hopkins, M.D.

_____
Dr. Michael Detamore, Ph.D.

_____
Dr. Clay Quint, M.D., Ph.D.

_____
Dr. Jennifer Robinson, Ph.D.

_____
Dean Michael Roberts, Ph.D.

Date Defended: February 16, 2018

ACCEPTANCE PAGE

The dissertation committee for Mitchell Charles VeDepo certifies that this is the approved version of the following dissertation:

On the Decellularization and Recellularization of Tissue Engineered Heart Valves

_____
Chair: Dr. Arghya Paul, Ph.D.

_____
Co-Chair: Dr. Gabriel Converse, Ph.D.

Date Accepted: February 16, 2018

ABSTRACT

The overall objective of this thesis was to fill critical knowledge gaps for the development of the tissue engineered heart valve (TEHV). Heart valve tissue engineering is a promising solution for the currently unmet need of an ideal prosthetic heart valve. However, the TEHV still faces a number of challenges ranging from scaffold creation to the lack of consistent recellularization. Therefore, the progression of this thesis was designed around the pathway leading to the THEV and focuses on addressing some of the key challenges. There are the three principal steps in TEHV development: scaffold formation through decellularization, seeding a patient specific cell population, and conditioning through culture in a bioreactor. The current body of work followed these steps with three aims focused on valve decellularization, cell seeding, and bioreactor conditioning, respectively. The first aim provided a detailed investigation into the species-specific effects of decellulzation on human and ovine aortic heart valves. The tested multi-detergent decellularization process lead to cell free scaffolds for both human and ovine heart valves; however, decellularization was found to more greatly affect ovine tissue than human tissue. The next aim of this thesis investigated the ability for recellularization, and the potential mechanism by which recellularization occurred for four cell populations: MNCs, low dose MSCs, high dose MSCs, and VICs. The higher dose of MSCs showed the greatest cellular infiltration compared to MNCs or VICs and maintained a phenotype similar to native cells. The final aim of the thesis was to develop bioreactor-conditioning protocols to increase the recellularization of cell seeded valves. Detailed investigations into bioreactor conditioning were performed individually for valves seeded with MNCs and MSCs. Bioreactor conditioning for MNC seeded valves focused on the duration of bioreactor culture and found three weeks of culture resulted in proliferation of the MSC sub-population and partial recellularization. The

investigation into bioreactor conditioning for MSC seeded valves focused on non-physiologic parameters of chamber pressure and hypoxic conditioning to increase recellularization into the distal leaflet. Hypoxic conditions greatly increased the infiltration of seeded cells while cyclic negative pressure conditioning better maintained stem cell gene markers. The goal driving this thesis was the clinical application of a TEHV and the described methodologies were developed to be translatable to the clinic. The current body of work offers real, obtainable advances for the field of heart valve tissue engineering.

ACKNOWLEDGEMENTS

I first became interested in pursing a doctorate in bioengineering during a conversation with my undergraduate advisor, Dr. Paul Ogg. He told me, “a successful doctor may help thousands of patients in a lifetime, but a successful bioengineer may help millions.” I am continually motivated by those words and I would not be on this path without him. So, I would like to start by sincerely saying, thank you Dr. Ogg. Rest in peace. The pursuit of this Ph.D. has been the most interesting and rewarding dream I have ever set out to accomplish. However, I could have never made it a reality without the gracious contributions from various people. Therefore, in the next few pages, I would like to continue to thank those people who aided me and guided my research. Equally as important, I would like to thank the individuals who have supported me personally and helped me find so much happiness.

I would like to thank my research advisors, Dr. Gabe Converse and Dr. Richard Hopkins. Thank you both for helping me discover my potential and mold that into the current thesis. It is through your guidance and insight that this dream became a reality. I would also like to thank you both for very different reasons. Gabe, thank you for being ‘hands on’, for providing daily guidance on the minute details, for showing incredible patience though my many mistakes, and for helping me navigate the Ph.D. process. Dr. Hopkins, thank you for being ‘hands off’, for offering wisdom for the difficult challenges, for keeping in mind the 10,000 ft view, and for providing the vision of making the TEHV a reality. Together, your complimentary mentoring styles offered everything I needed to accomplish this goal and I am forever grateful to you both.

I am also grateful to the other members of the Cardiac Regenerative Surgery Research Lab: Kari Neill, Gayathri Acharya, Matthew Armstrong, Chris McFall, and Eric Buse. Thank you for sharing your knowledge to teach me new techniques that were crucial to the completion

of this work. I would like to especially thank Eric for his help with decellularization techniques and for his willingness to help me suture heart valves, even in the early hours of the morning.

I would like to thank my committee members, Dr. Arghya Paul, Dr. Clay Quint, Dr. Michael Detamore, Dr. Jennifer Robinson, and Dean Michael Roberts for your willingness to serve on my committee and your guidance as I navigated the unique challenges associated with my research position, various personnel changes, and unforeseen lab closures. I am sincerely thankful to Dr. Detamore for the continued support, even after your departure. You have exceeded the call of duty to provide academic and personal guidance and the mentorship I have received has been inspiring.

I would also like to thank those people or groups that provided contributions to the work presented in this thesis. While the presented work as a whole is my own, certain tasks or portions of tasks were accomplished by others. A portion of the valve suturing was performed by Eric Buse, Gabe Converse accomplished some of the mechanical testing, Gabe Converse also designed the experiments in Chapter 5, the CMH histology lab mounted and cut slide sections, and the HPLC/mass spectroscopy in Chapter 3 was performed by Todd Williams and the KU Mass Spectrometry Lab. While I am responsible for all other work contained herein, I would like to thank the previously listed people for their contributions.

Furthermore, I am thankful to the sources of funding I received during completion of my project. Thank you to the National Institute of Health for funding the work presented in Chapter 5 and to the Children's Mercy Hospital for the unique research position and financial support.

In addition to the academic and financial support I received over the past years, I was fortunate to receive so much personal support in the pursuit of this goal and I am very thankful to the many individuals helped me find so much happiness throughout this process. I want to begin

by thanking my mom and dad. Dad, the most valuable lesson you taught me has been the importance of hard work and that the reward is always greater when it doesn't come easy. Mom, you then gave me the tools to accomplish the necessary hard work through great attention to detail and determination. None of this would be possible without your encouragement and support, so thank you both so much. I also want to thank my sister, Delanie. As my 'first best friend', I am so grateful to you for the love you have always shown me as you inspire me to be the best version of myself.

Of course, I am tremendously thankful to my girlfriend Maggie. I am still surprised that you even agreed to go on this crazy ride with me and let me pursue my dream. You have shown an incredible degree of the patience over the last 4 ½ years and I am forever thankful for the love you have given and for the kindness I haven't always deserved. You have been my venting place when life got tough, my cheerleader when life went right, and above all else, a constant source of support in whatever goals I strive for. Whether a climbing route or a personal stumble, you have always caught my falls and helped me reach new heights.

I must also acknowledge the Apex community. You all have become a second family and have helped me find myself through leadership, hard work, and good times. I am thankful for every bit of support I have received and for the encouragement to better myself outside of academics. I must especially thank Phil and the Ratterman family, for supporting me as a friend, a coach, a training partner, and an adopted family member.

And lastly, thanks to God, for the ability and the opportunity.

TABLE OF CONTENTS

LIST OF FIGURES

CHAPTER 6:

CHAPTER 7:

SUPPLEMENTAL FIGURES

LIST OF TABLES

CHAPTER 1: INTRODUCTION TO THESIS

The overall objective of this thesis was to fill critical knowledge gaps for the advance of a biologically and physiologically practical tissue engineered heart valve (TEHV). The ultimate clinical goal driving this work was the development of a heart valve prosthetic capable of optimal hemodynamics and growth after implantation. There is a significant unmet need for an ideal prosthetic heart valve and the TEHV has the potential to create a new paradigm in the field valve replacement. However, a number of challenges remain before the TEHV may be realized. Therefore, the progression of experiments in this body of work was designed around a clinically realistic pathway leading to the THEV and focused on addressing some of the key challenges. There are the three principal steps in TEHV development: scaffold formation through decellularization, seeding a patient specific cell population, and conditioning through culture in a bioreactor (Figure 1.1). This project addresses a major challenge in each step through the following three specific aims: (1) characterize the effects of a multi-detergent decellularization protocol, (2) compare candidate seeding cell populations for recellularization potential, (3) develop a bioreactor conditioning protocol to enhance valve recellularization.

The first aim of this thesis focused on challenges concerning the safety of decellularized valve scaffolds by elucidating and comparing the effects of decellularization on both human and ovine aortic valves. The second aim addressed the primary challenge of valve recellularization by investigating the mechanisms of scaffold repopulation associated with various cell populations. The third aim further investigated the challenge of recellularization by identifying bioreactor conditioning parameters that may be utilized to increase the recellularization of valve scaffolds. The third aim was broken down into two parts, with one part focused on tuning bioreactor conditions for MNC seeded heart valves and the other part focused on the bioreactor

conditions for MSC seeded heart valves. The chapters that follow reflect the progression of these aims.

Chapter 2 provides background on the current state of heart valve tissue engineering through a literature review of the existing methods for the decellularization and subsequent recellularization techniques that have been employed for heart valve tissue engineering. This review focuses on the broad approaches for TEHV processing and lays the groundwork for describing the two mechanisms of recellularization: *in situ* recellularization through host cell recruitment and *in vitro* recellularization through seeded cell proliferation. Chapter 2 addresses the entire thesis as it provides valuable insight into the previously explored methods for heart valve tissue engineering.

Chapter 3 covers the first aim of the project and the first step on the pathway to the TEHV, scaffold creation through heart valve decellularization. This chapter provides a detailed investigation comparing the species-specific effects of heart valve decellularization. Human and ovine aortic valves were subjected to an identical decellularization protocol and the results were described and compared through mechanical and biochemical means. Therefore, the results of this chapter are relevant to the remainder of the current thesis as the second and third aim utilized decellularized valves as scaffolds for TEHVs.

Chapter 4 begins to address the primary challenge of the TEHV: recellularization of the leaflet interstitium. This chapter focused on the cell seeding step in the pathway to the TEHV and offers a comparison of various cell populations for valve seeding. Decellularized valve scaffolds were seeded with mononuclear cells (MNCs), low dose of mesenchymal stem cells (MSCs), high dose of MSCs, or valve interstitial cells (VICs). The tissue engineered valves were then analyzed for cellular repopulation, mechanical properties, matrix remodeling, and cytokine

production. The results of this chapter provided insight for Chapter 5 and Chapter 6, where bioreactor conditioning parameters were developed for individual cell populations.

Chapter 5 covers the first part of the third aim, which tackled the third step in the pathway to a TEHV: enhancing valve recellularization through bioreactor conditioning. The design of this study was built off of the findings of Chapter 4 and further investigated MNC seeded heart valves. Decellularized valve scaffolds were seeded with MNCs and underwent various durations of bioreactor culture to examine the phenotypic evolution of the seeded cell population. This chapter provided a more comprehensive analysis than Chapter 4 for MNC seeded valves and gave insight into the effects of extended bioreactor culture on the extent of scaffold repopulation and cell phenotype.

Chapter 6 describes the second part of Aim 3, wherein the bioreactor conditioning for MSC seeded heart valves was explored. In this chapter, conditioning parameters were identified for increasing recellularization of MSC seeded heart valves using non-physiologic forces. After cell seeding, heart valves were conditioned under negative/positive cyclic pressure cycles and hypoxic/normoxic conditions. As the last step in the pathway to the TEHV, the design of chapter 6 serves as a culmination of previous chapters. The results from this chapter suggest a bioreactor conditioning protocol that may be used to further enhance the recellularization of valve scaffolds.

Finally, Chapter 7 provides concluding remarks regarding the body of work as a whole. It summarizes the key findings from the previous chapters and then presents a recommended protocol for developing a TEHV based on those findings. Lastly, an opinion on the future directions of heart valve tissue engineering is discussed.

Overall, the work conducted in the current thesis provides innovative, potential solutions to overcome key challenges still facing clinical realization of the TEHV. Specifically, TEHV

development has been hindered by the safety concerns of using decellularized valves as tissue engineering scaffolds and in the difficulty of establishing a phenotypically appropriate cell population throughout the entire valve structure. The work described herein offers a characterization of the effects of a decellularization protocol, provides evidence of cellular repopulation of decellularized valve scaffolds, and proposes recommended bioreactor conditioning protocols to further increase valve recellularization. While the design of this thesis followed the pathway to developing a TEHV, certain aspects fell outside the scope of the project, which include *in vivo* functional implant testing. Therefore, although the work presented in this thesis did not lead to the complete development of a TEHV, it provides many valuable leads for advancing the field of heart valve tissue engineering and approaches the challenge of valvular heart disease with a focus on the clinical translation of an ideal heart valve replacement.

CHAPTER 2: RECELLULARIZATION OF DECELLULARIZED HEART VALVES; PROGRESS TOWARDS THE TISSUE ENGINEERED HEART VALVE*

2.1 Abstract

The tissue engineered heart valve (TEHV) portends a new era in the field of valve replacement. Decellularized heart valves are of great interest as a scaffold for the TEHV due to their naturally bioactive composition, clinical relevance as a stand-alone implant, and partial recellularization *in vivo*. However, a significant challenge remains in realizing the TEHV: assuring consistent recellularization of the entire valve leaflets by phenotypically appropriate cells. Many creative strategies have pursued complete biological valve recellularization, however identifying the optimal recellularization method, including *in situ* or *in vitro* recellularization and chemical and/or mechanical conditioning, has proven difficult. Furthermore, while many studies have focused on individual parameters for increasing valve interstitial recellularization, a general understanding of the interacting dynamics is likely necessary to achieve success. Therefore, the

* Published as **VeDepo, M. C.**, Detamore, M., Hopkins, R. A. and Converse, G. L. Recellularization of decellularized heart valves: Progress toward the tissue-engineered heart valve. Journal of Tissue Engineering, 8, 2041731417726327, 2017. doi:10.1177/2041731417726327.

purpose of this review is to explore and compare the various processing strategies used for the decellularization and subsequent recellularization of TEHVs.

2.2 Introduction

Valvular heart disease continues to be a global cause of morbidity and mortality worldwide.[38] Approximately 2.5% of the US population suffers from aortic heart valve disease, and that value skyrockets to 13.2% for the population ≥75 years old.[61, 121] There are many etiologies for heart valve disease, including congenital defects, rheumatic fever, infective endocarditis, and valve calcification, yet after medical therapy is exhausted, the multiple options for repair or replacement each have limitations. The annual number of patients requiring heart valve surgery is estimated at 290,000 globally, and as the world population continues to grow and age, that number is expected to triple in the next five decades to over 850,000.[185] Despite decades of pursuing the ideal heart valve prosthetic, such a valve still does not exist. Mechanical valves have poor hemocompatability, requiring a lifetime of anticoagulation therapy. Xenogeneic bioprosthetic valves and biological valves such as homografts lack durability and often require replacement in ~10 years due to calcification and/or degeneration.[21, 72, 149] Children are even more restricted in the suitable options for heart valve replacement, and although pediatric patients represent only a subset of the total heart valve replacement population, the clinical need for an ideal pediatric valve is far greater.[70] The complications inherent to each class of valve substitute currently available for clinical use are amplified in children, which can necessitate reoperation in as little as 2-5 years. The current standard valve replacement for children is the cryopreserved allograft, yet this is not without problems due to the shortage of available grafts and patient-valve size mismatch. Most importantly, no current replacement option allows for somatic growth after implantation, necessitating multiple reoperations in children and impacting

surgical strategies such as timing, sequence of surgeries, serial valve selections, etc.[70] Therefore, there is a significant unmet clinical need for a truly successful heart valve replacement option, especially for pediatric patients.

Tissue engineering is a promising approach that may lead to novel constructs that will satisfy this unmet need and overcome the limitations of current valve prosthetics. The tissue engineered heart valve (TEHV) will be constructed using a combination of a porous scaffold, a cell population, and signaling factors and has the potential to provide 1) excellent hemodynamics, eliminating the need for anticoagulation therapy, 2) active tissue remodeling, preventing degeneration and 3) growth characteristics, preventing the need for reoperation.

The two primary types of valve scaffolds for the TEHV are natural scaffolds, such as decellularized tissue or biological materials, and synthetic constructs fabricated from degradable polymers.[22] Each type has inherent benefits and challenges, but decellularized heart valves are of significant interest. Decellularized heart valves are composed of biological materials that can positively impact cell differentiation and serve as building blocks during the remodeling process.[77, 100] Additionally, decellularized valves do not necessitate complete biodegradation and often maintain the mechanical anisotropy of the native valves from which they are derived.[5, 32, 97, 101, 173] Decellularized heart valves have been more clinically relevant than polymeric valves thus far, as they have been implanted as stand-alone valve substitutes and as TEHVs in animals and humans, albeit with mixed results.[45, 48-51, 131, 133, 154, 179] However, decellularized heart valves are not without their limitations. Decellularized valves require human or animal tissue for manufacture, which is limited in supply, and necessitates cryopreservation for storage. Freeze-drying of biologic heart valves has been explored to facilitate long-term storage; however, freeze-drying leads to collapse of the ECM structure and disruption of biomolecules. Research

with lycoprotectants may overcome this limitation in the future.[177] Additionally, the success of decellularized heart valves is highly reliant upon the decellularization process and the potential immune response following implantation.

On the other hand, man-made scaffolds, fabricated from synthetic or biological materials, do not require donor tissue but have struggled to recreate the macro and micro valve anatomy and mechanical anisotropy.[5] Fabricated scaffolds must also undergo complete biodegradation in synchrony with the production of extracellular matrix to remain functional. Fabricated or synthetic scaffolds have been used as a TEHV in animals, but have seen far less use clinically than decellularized valves.[93, 184] Therefore, decellularized valve scaffolds have the greatest potential for expeditious development of a the TEHV due to the regulatory history, long clinical experience with homografts, as well as a deep research focus by many groups.[31, 45, 70]

Before the TEHV is realized, a primary challenge must be overcome: the establishment and growth of a physiologically appropriate cell population within the leaflet tissue. In pursuit of this aim, researchers have employed numerous strategies for recellularization. From these strategies the two main approaches that have emerged are *in vitro* recellularization, the traditional tissue engineering approach, and *in situ* recellularization, also known as guided tissue regeneration.[22, 117] However, despite the many strategies that have been employed, it is uncertain which has the greatest potential for success and reliable recellularization of the TEHV has yet to be realized. Therefore, the purpose of this review is to explore and compare the various processing strategies used for the decellularization and subsequent recellularization for tissue engineered heart valves.

2.3 Heart valve decellularization

In the simplest terms, decellularization is the process of removing cellular (including nuclear) material from the extracellular matrix (ECM) of biological tissues. The remaining ECM provides a semi-porous scaffold that retains the complex geometry of the native tissue and is composed of natural components that provide cues for cell migration and differentiation, resulting in constructive remodeling.[36, 60, 100] Despite the clinical use of decellularized tissue for more than a decade, it is only within the last 5 years that quantifiable minimum criteria defining adequate decellularization have been generally accepted in the field.[36] These include, 1) <50 ng dsDNA per mg ECM dry weight, 2) <200 base pair DNA fragment length and 3) the lack of visible nuclear material in tissue sections stained with DAPI or H&E.[36] These criteria lay out basic metrics to be met as endpoints for decellularized tissues, since ineffective decellularization can affect the immunological response through macrophage polarization and inhibit the constructive remodeling outcome.[7, 8, 89] While decellularization does preserve the geometry of the native tissue, it has been shown to affect the structure and protein composition, often in a negative manner, depending on the decellularization methods used.[36] Additionally, methods of decellularization differ in their effectiveness to remove antigens from the ECM scaffold, such as cellular and nuclear material, as well as lipids and carbohydrates which can also function as antigens.[180] Methods of decellularization include the use of detergents, biologic agents, and physical forces. Extensive details on methods of decellularization and the effects on general tissue can be found in the reviews by Crapo *et al.,*[36] and Gilbert.[60]

2.3.1 Methods for heart valve decellularization

In the context of heart valve decellularization, additional consideration must be given to the effects of processing on the mechanics of the heart valve leaflets. Healthy heart valves,

particularly the aortic and mitral valves, which control systemic blood flow, are under extreme environmental demands. They experience ~100,000 loading cycles per day, equating to ~3 billion cycles in an average lifetime.[22] These physiological forces must be considered during heart valve decellularization since the process can affect the structural and mechanical properties of the remaining extracellular matrix. Furthermore, the effect decellularization has on the extracellular matrix is process specific (Table 2.1**;** Figure 2.1).

Detergent valve decellularization. Of the various decellularization methods, the most common utilize detergents for the removal of cells. Ionic and non-ionic detergents are effective decellularization agents because they are able to solubilize cell membranes, lysing the cells and dissociating DNA. The anionic detergents sodium dodecyl sulfate (SDS) and sodium deoxycholate (SD) are often used in valve decellularization and have proven effective in removing cells and DNA from the extracellular matrix, however prolonged chemical exposure during decellularization has been shown to disrupt collagen fiber structure in valve leaflets.[19] The disruption in the ECM leads to an associated deterioration of mechanical properties, observed through increased areal strain and decreased flexural stiffness.[101] This is despite preservation of the primary structural proteins found in valves: glycosaminoglycans (GAGs), collagen, and elastin fibers (Figure 2.1f). SDS is also particularly difficult to completely remove from the tissue and residual detergents can adversely affect cell adhesion and repopulation.[194] Non-ionic detergents, such as Triton X-100, have also proven effective at cell and DNA removal. In addition to cell removal, Triton X-100 has been shown to delipidize tissue, reducing the concentration of GAGs (Figure 2.1h). GAGs are often attributed to the viscoelastic behavior of tissue and indeed, following decellularization with Triton X-100, a decrease in the stress relaxation of valve leaflet tissue has been observed.[32, 173] Researchers have also successfully

employed multi-detergent decellularization strategies. Studies using a combination of Triton X-100 and SD reported complete cell removal with less damage to the valve extracellular matrix, when compared to other methods.[87, 190] However, neither study employed mechanical testing analysis of the decellularized leaflets and only described the extracellular matrix preservation using qualitative histologic methods. A combination of osmotic shock, Triton X-100, and the anionic detergent N-lauroylsarcosine sodium (NLS) salt has been used to successfully decellularize (>97% dsDNA removal) both pulmonary and aortic heart valves from a variety of species, including ovine, porcine, and human.[32, 131, 173] The elastin and collagen components of the extracellular matrix were preserved, yet a loss of GAGs associated with Triton X-100 was observed. Biaxial mechanical testing indicated increased areal strain, increased peak stretch ratios, and decreased stress relaxation for ovine pulmonary valves.[32] Interestingly, the same trend was observed for ovine aortic valves, yet no change in the areal strain or peak stretch ratio was observed in human aortic valves.[173] The authors speculated that the species-specific effect of identical decellularization methods was the result of a loss of collagen crosslinking components and an initial higher cellularity in the ovine valves.[173]

Enzyme valve decellularization. Enzymatic agents such as nucleases or trypsin have also been utilized in valve decellularization to breakdown biologic molecules and facilitate cell removal. Nucleases cleave nucleic acid sequences into shorter segments, expediting their removal from the extracellular matrix and the inclusion of nucleases, such as DNases or RNases, in a decellularization process is so commonplace their use was not specified in Table 2.1. Trypsin is another common enzyme used in valve decellularization. Trypsin, a serine protease, hydrolytically cleaves proteins and is used to digest cellular proteins in the decellularization process. However, the fibrous structural proteins of the valve extracellular matrix have limited

resistance to trypsin cleavage and are often affected as well. Decellularization of heart valves using trypsin often results in visible histologic damage to the extracellular matrix as well as large alterations to valve mechanics (Figure 2.1**c**). Compared to detergents, trypsin decellularization is slower to remove cells, causes greater disruption to the elastin and collagen structure, but has a better preservation of GAGs.[63, 101, 157] Complete cell removal by trypsin alone actually requires lengthy decellularization protocols and the prolonged exposure has been shown to disrupt the remaining extracellular matrix beyond practical use.[145]

Miscellaneous valve decellularization. Additional creative strategies for valve decellularization have been explored, with varying levels of success. Osmotic shock can be used to lyse cells; however, osmotic shock by itself is ineffective at removing the hydrophobic cell membranes and remnants and is therefore not recommended as the sole decellularization technique.[116, 157] It is often used in combination with detergent or enzymatic based methods as an initial step, reducing the required detergent/enzyme concentrations an/or exposure times.[32, 157, 194] Mechanical forces such as pressure gradients can also aid in decellularization, as perfusion of decellularizing solutions through the valve conduit has been shown to increase the removal of cellular material from the valve wall compared to immersion protocols.[151] Glycol radiation, using a polyethylene glycol detergent and gamma irradiation, has proven effective, resulting in >92% DNA removal in the valve cusps while not affecting ultimate tensile strength and collagen content.[122] Additionally, the gamma irradiation effectively removed the galactose-α(1,2)-galactose (α-Gal) epitope and the porcine endogenous retrovirus.[122] Decellularization by sequential antigen solubilization is another effective method for the removal of cellular and antigeneic material from xenogeneic tissues.[180] Based on shared physiochemical properties, antigens are removed by sequential solubilization techniques targeting hydrophilic and lipophilic

proteins.[181, 182] Using this method, researchers have demonstrated the successful decellularization of bovine pericardium and porcine aortic heart valve leaflets.[130, 181, 182] In addition to the removal of cellular material, sequential antigen solubilization also successfully removes the α-Gal and major histocompatibility complex I (MHC I) antigens while preserving the structural and mechanical properties of the native, untreated tissue.[130, 180] Another unique approach to decellularization utilizes supercritical fluid solution of carbon dioxide and ethanol as a cell extraction medium.[143] The high permeability and high transfer rate of the supercritical fluid makes this an effective method, resulting in a visible lack of cell nuclei and a 90% reduction in phospholipids, the primary component of cell walls. However, a stiffening and dehydration of the ECM has also been observed, likely attributed to the high ethanol exposure.[143]

2.3.2 Clinical use of decellularized heart valves

In vivo animal models using stand-alone decellularized valves have seen success, with subject survivability out to nine months with patent, functioning valves.[13, 46] However, clinical studies using stand-alone decellularized valves have seen only mixed results. In clinical practice, xenogeneic valves would be preferred to allogeneic valves due to the scarcity of human tissue, yet clinical experience using xenograft, decellularized valves has not been encouraging. The initial iteration of the SynerGraft valve (Cryolife Inc., Kennesaw, GA), a porcine xenograft, showed promising preliminary results in adults, but elicited a severe immune response and catastrophic failure in children.[62, 154] Subsequent studies identified the presence of ECM associated antigens, particularly the α-Gal epitope, following processing.[86] AutoTissue (Berlin, Germany) has developed the other clinical xenograft, the Matrix P line of decellularized porcine pulmonary valve replacements, using a sodium deoxycholate decellularization method. This valve line has been CE certified since 2004. Both positive and negative clinical outcomes have

been reported with freedom from reoperation ranging broadly from 48% at 19 months to 90% at 4 years.[95, 176] Overall, decellularized xenogeneic valves have performed equivalent to, or worse, than standard cryopreserved allografts, though advances in decellularization protocols or better pre-implant conditioning may increase efficacy.

On the other hand, clinical experience with decellularized human allografts has been more successful, with three options currently available worldwide. The CryoValve SG valve is the decellularized human allograft from CryoLife Inc. Comparisons between the CryoValve SG and standard cryopreserved allografts have not yet found a clear benefit from SynerGraft decellularization.[14, 23, 96, 139] It is speculated that the CryoValve SG valve may be more durable, though longer follow up studies are still necessary to verify these claims.[14, 23, 96, 139, 153, 168] During a 2014 FDA panel to discuss the classification of decellularized valves, CryoLife presented data indicating a 93% freedom from reoperation at 10 years in patients using the CryoValve SG.[37] Other studies using the CryoValve SG have reported freedom from valve dysfunction at approximately 85% at 5 years or 75% at 10 years.[96, 139] A multi-institutional review by Bibevski *et al.*[17] observed decreased freedom from valve dysfunction and re-intervention in SynerGraft valves compared to cryopreserved homografts. However, it is worth noting that within their study, the mean follow-up time was only 5 years and in comparing the SynerGraft and cryopreserved homograft groups, patients receiving SynerGraft valves were significantly older, received significantly larger valves, and more often underwent valve replacement as part of a Ross procedure.[17] It is not yet clear whether the durability of the allogeneic version of the SynerGraft valve will be significantly prolonged compared to more classical homografts when HLA-ABO donor recipient matching is optimized and critical conflicts avoided. The other two clinical uses with decellularized human allografts have seen relative success observing positive

early and midterm results. Haverich *et al.* has implanted 131 decellularized allografts since 2005 and they have observed 100% freedom from explant at 10 years follow-up (compared to 84% freedom from explant for cryopreserved allografts).[28, 142] Da Costa *et al.* have also seen encouraging results using decellularized aortic allograft replacements, the first of its kind, and has reported 100% freedom from reoperation of the graft at 3 years, although early hospital mortality was 7%.[39] Despite the early success by Haverich and Da Costa using decellularized allografts, long term results are not yet available (10-20 years), which is the crucial time when the majority of cryopreserved grafts fail. Additionally, without the presence of a viable cell population within the valve leaflets, the decellularized valves are anticipated to suffer the same valve dysfunction fate as standard cryopreserved valves. However, it is worth noting that all three groups using decellularized allografts report an increased freedom from valve dysfunction or replacement compared to standard cryopreserved allografts.[17, 28, 39, 96, 139, 142]

2.3.3 Limitations of decellularized heart valves

Thus far, complete autologous recellularization of implanted decellularized heart valves has not been realized (see *Guided Tissue Regeneration* section). Autologous recellularization of decellularized valves has been limited to the valve wall with only endothelial recellularization observed on the leaflet surface (Figure 2.2). This is far superior compared to cryopreserved valves, which undergo massive degeneration and leukocyte infiltration throughout the valve as evident in Figure 2.2. However, the fact that recellularization of decellularized valves is limited to the valve surface is problematic since the leaflet is the primary location of valve dysfunction in implanted cryopreserved valves. Without a viable cell population capable of ECM remodeling inside the valve leaflet, decellularized heart valves are anticipated to undergo the same fate as cryopreserved valves and ultimately suffer from valve degeneration.[70] Decellularized valves are

an important improvement above the standard cryopreserved allograft due to reduced antigencity, but without restoration of the cell population within the interstitium of the leaflet and the ability for matrix repair and remodeling, the decellularized valve likely will not be the sought after "ideal" heart valve. Therefore, additional processing strategies must be employed to encourage recellularization of the entire valve, including the distal portions of the leaflet.

2.4 Recellularization and conditioning

Ultimately, the recellularization of a tissue engineered valve should mimic the cell population of a native valve, which is made up of valvular endothelial cells (VECs) and valvular interstitial cells (VICs).[41] VECs provide a non-thrombotic monolayer over the valve surface, which plays a key role in valve hemodynamics.[25] VICs are active in the remodeling of the extracellular matrix (ECM) of the valve ensuring both tissue durability and growth characteristics.[105] Together, these cell populations create a non-thrombotic, durable, living valve. One of the primary challenges to realizing the TEHV is the recellularization of both VICs and VECs to create a physiologically appropriate cell population. There is evidence of a strong relationship between the two cell types, as VECs have been shown to regulate VICs toward a more native-like phenotype when in co-culture compared to VICs in isolated culture.[25] However, the exact pathways of valve repair and interaction between the two populations remain largely unknown. Further complexities are introduced since cell populations differ between valves in the heart, so a recellularization method may need to be optimized for each valve type.[41] Fortunately, the challenge of recellularization is lessened since there is strong evidence that following implantation, properly prepared valves have the potential for partial recellularization by native cells, particularly re-endothelialization along the valve surface.[13, 39, 48, 75, 131, 133] As demonstrated in Figure 2.2, re-endothelialization occurs across all valve surfaces while interstitial

recellularization is limited to the valve wall and sinus. Therefore, the remaining challenge lies in repopulating the distal leaflet interstitium with VIC-like cells.

Native VICs have been sub-classified into 5 distinct phenotypes, primarily quiescent VICs (qVICs) and activated VICs (aVICs).[105] qVICs are the dominant cell phenotype within the valve leaflet during normal valve function and it is believed they help maintain homeostasis through marginal matrix production and degradation. During valve injury or abnormal stress, qVICs become stimulated by VECs to become aVICs, which actively produce and degrade extracellular matrix for valve remodeling.[26] aVICs are more easily identified than qVICs with a myofibroblast-like phenotype that is characterized by positive expression of alpha-smooth muscle actin (αSMA).[105] Following injury repair and valve remodeling the aVICs are eliminated by apoptosis. However, if the activation signals persist or there is dysfunction in the apoptotic process the aVICs can become osteoblastic VICs (obVICs), which promote angiogenesis, chronic inflammation, fibrosis, and calcification leading to valve disease.[105] aVICs are therefore responsible for both valve remodeling and the potential for clinical valve disease. Many heart valve recellularization studies use aVICs, or αSMA positive cells, as the target phenotype for successful recellularization, since aVICs are more easily identified by αSMA and are responsible for valve remodeling. However, it is unknown if qVICs will ultimately replace the aVIC population and there is a lack of information on the potential for obVIC differentiation. Since initial recellularization is still a primary challenge, no studies have yet investigated the long-term fate of seeded cells, but it must be considered in the future. Regardless, progress in valve recellularization has been made and two main recellularization approaches have emerged: *in situ* recellularization and *in vitro* recellularization. Within these two approaches a number of creative

strategies have been employed to address initial cellular repopulation of the decellularized heart valve over the past two decades.

2.4.1 In situ recellularization

In situ recellularization of heart valves relies upon the natural regenerative capabilities of the host to repopulate a valve scaffold. In contrast to the typical tissue engineering paradigm, this approach does not attempt to create living tissue *ex vivo*. Instead, it aims to encourage the tissue healing and remodeling process through the implantation of a biomimetic scaffold capable of stimulating host cell recruitment and self-regeneration. For this reason, the decellularized valve scaffold is well suited, compared to polymer valve scaffolds, as it provides the chemical and mechanical cues of a natural heart valve. The two general approaches for *in situ* recellularization are implantation of stand-alone decellularized valves or implantation of chemically modified valve grafts.

Tissue guided regeneration. The most obvious, and most attempted, approach to *in situ* recellularization, has been the implantation of stand-alone decellularized valve grafts without any further chemical or mechanical modification. This approach has come to be known as tissue guided regeneration. As mentioned previously, decellularized valve grafts have been implanted in animal and clinical applications with varying results in terms of survival and growth (see *Clinical Use of Decellularized Heart Valves)*. In this section, the focus is the *in situ* recellularization of the implanted valve scaffolds (Table 2.2). A more thorough review on the tissue guided regeneration of heart valves is available by Iop *et al.*[76]

Currently, the *in situ* autologous recellularization of implanted decellularized valves is limited and variable. As mentioned previously, many studies have observed complete re-endothelialization and recellularization of the valve wall up to the leaflet base, yet the distal

subsurface leaflet remains mostly acellular. This prevents tissue growth and remodeling in the valve leaflets, ultimately leading to valve degeneration. James *et al.* reported an exception to this limited recellularization using a mouse model.[79] At 3 months implant, they observed a thickening of the decellularized mouse leaflets and repopulation by αSMA^+ cells, though by 6 months the leaflets appeared normal and the number of αSMA^+ cells decreased.[79] This may be the first study demonstrating a state of valve remodeling after implant transitioning into a quiescent, healthy state. While the study by James *et al.* is significant, the implant model presents challenges for clinical translation and the recellularization success is likely due to the thinness of the mouse leaflets, expediting cell infiltration.[79] Additionally, it appears that leaflet recellularization typically decreases as higher order animals are used as implant models (Table 2.2). Furthermore, it appears that if the decellularized replacement valve is more robust than the original, native valve, the recellularization of the leaflet is better. For example, porcine valves implanted in canines led to good recellularization, as did porcine aortic valves implanted in a porcine pulmonary valve model.[75, 78]

The *in situ* recellularization of decellularized valves in clinical use has been less successful than in pre-clinical studies. Decellularized allografts have functioned better than decellularized xenografts, as previously mentioned; however, no evidence has been presented demonstrating successful *in situ* autologous recellularization. Biopsies of the valve conduit taken from decellularized allografts during non-valve related reoperation in humans have shown repopulation of the conduit, though such recellularization is in accordance with similar animal studies.[39, 48] During the FDA panel meeting in 2014 to re-evaluate decellularized heart valve classification, CryoLife Inc. presented results of their explanted decellularized allografts.[37] The explanted valves had partial recellularization of the distal conduit but an absence of cellularity in

the decellularized leaflet up to 11 years *in vivo*.[37] Leaflet repopulation was demonstrated during clinical use of the Matrix P line of valves, a decellularized xenograft; however, the repopulating cells appear to be inflammatory rather than phenotypically appropriate valve cells.[95, 127, 138, 176]

Chemical conditioning for in situ recellularization. As autologous recellularization of decellularized valves is limited, a number of studies have investigated the use of chemical conditioning, or other chemical modifications, before implantation to increase valve recellularization (Table 2.3). This approach applies cytokine or signaling molecules to modulate the healing response of the host. Specifically, conditioning can be applied that is targeted at increasing cell attachment/migration, decreasing the immune response, increasing biologic activity, or increasing mechanical integrity. One approach designed to increase cell attachment has been the pre-implant conditioning of decellularized valves with fibronectin (FN), either alone or in combination with another growth factor.[6, 57, 122] In all examples, the valves treated with fibronectin performed better than the respective decellularized or cryopreserved control valve groups.[6, 57, 122] Fibronectin treatment alone led to increased recellularization of the luminal side of the treated graft in a small animal model, though no information was given on specific leaflet recellularization.[6] Fibronectin in combination with stromal cell derived factor 1α (SDF-1α), increased the surface and interstitial leaflet recellularization of valves implanted in sheep, as well as decreased the calcification, pannus formation, and immune response.[57] Fibronectin plus hepatocyte growth factor (HGF) was used to achieve good recellularization *in situ*.[94] Ota *et al.* treated decellularized porcine aortic valves with FN+HGF and after one month implantation in canines they observed great recellularization of the valve cusps with gene expression of vimentin comparable to native valves.[122]

Another approach using chemical conditioning and *in situ* recellularization has investigated the conjugation of antibodies onto decellularized valve scaffolds to encourage *in situ* cell attachment. Antibody conjugation is an interesting method because it allows for selective attachment for the cell phenotype of interest. One group has explored conjugating CD133 antibodies onto decellularized valve scaffolds with the purpose of selectively targeting hematopoietic stem cells and endothelial progenitor cells from circulating blood.[83, 179] After 3 months implantation in the RVOT of sheep, the antibody-conjugated valves showed increased recellularization throughout the leaflet compared to non-conjugated and cell seeded controls, including a vWF^+ surface cell layer and an $aSMA^+$ cell population in the leaflet interstitial tissue.[83] Additionally, explanted valves showed an increase in collagen, glycosaminoglycan, and MMP-9 concentrations compared to non-conjugated valves, indicating both matrix production and remodeling.[83] A follow up study found that $CD133^+$ cells were present by 3 days implant, but from 30 to 90 days most cells were $CD133^-$, $aSMA^+$, and VIM^+, demonstrating the transition and differentiation of the cell population from progenitor cell adhesion to mature valve like cells (Figure 2.3).[179] However, the increased expression of $aSMA^+$ cells, compared to native controls, is noteworth since aSMA indicates an aVIC phenotype that may lead to valve disease.[179]

Another chemical conditioning strategy has been employed that aims to restore the mechanical properties of the decellularized scaffold and to make the ECM more hospitable for recellularization. This chemical treatment was accomplished by normalizing tissue pH, rehydrating the collagen helix moisture envelope, compacting collagen fibrils, and restoring soluble proteins by treating decellularized valves in a conditioning solution composed of citric acid, hyaluronic acid, lauryl alcohol, and species-specific protein.[32, 71, 131, 132] Biomechanical evaluation revealed that the conditioning solution restored the stress relaxation behavior toward

that of the native valve properties.[32] In an ovine allograft valve implant model, the conditioning process led to better hemodynamic performance, compared to cryopreserved and decellularized valves implanted without conditioning.[131, 132] Improved re-endothelization and matrix recellularization was observed following conditioning, though the interstitial sub-surface repopulation was limited to the proximal portion of the leaflet.[131, 132] Similar results were observed using a baboon model and conditioned human valves to simulate human paradigms.[71] Re-endothelialization and cusp base recellularization was observed in conditioned human valves after 26 weeks, as well as a decrease in class I and class II antibody production compared to cryopreserved valves, indicating reduced antigenicity.[71] In all of the above-mentioned animal studies, the conditioned valves performed better than the decellularized and cryopreserved valve controls, indicating they may function better clinically than the current standards of care. However, because the distal portions of the leaflet do not completely recellularize, the potential for a lifelong valve replacement without full leaflet active ECM remodeling is likely limited.

2.4.2 In vitro recellularization

In vitro recellularization, the other proposed method of recellularization for tissue engineered heart valves, typically follows the traditional paradigm in tissue engineering in which cells are introduced on to a scaffold that is then subjected to *in vitro* conditioning. This approach relies upon using an appropriate cell source and providing conditioning signals to drive cell proliferation and differentiation in a bioreactor. The exact mechanisms that modulate valve cell phenotype are not clear, but there is evidence supporting the role of both mechanical and biochemical cues. *In vitro* recellularization leverages these cues to drive a seeded cell population into a mature cell population. The approaches that have been explored using *in vitro* cell seeding can be broken down into three groups, those that did not use any further conditioning, those that

applied mechanical conditioning, and those who applied chemical conditioning. Numerous cell sources have been explored for heart valve tissue engineering including VICs, VECs, mesenchymal stem cells (MSCs), bone marrow mononuclear cells (MNCs), myofibroblasts (MFs) smooth muscles cells (SMCs), endothelial cells (ECs) and endothelial progenitor cells (EPCs). A more thorough review on the seeding cell sources for heart valve tissue engineering is available by Jana *et al.*[80]

In vitro seeding without conditioning. Early work in the field of *in vitro* cell seeding of heart valves investigated the effect of seeding under static culture conditions without added mechanical or chemical conditioning (Table 2.4). Some of these first efforts studied the potential for leaflet repopulation by isolating the decellularized leaflets and statically seeding cells in culture flasks or well plates. A primary objective of this work was re-creating a healthy endothelial layer; therefore, seeded endothelial cells were often used in these studies.[18, 63, 135] Endothelial cell seeding resulted in a confluent monolayer of cells on the leaflet surface that stained positive for vWF, but lead to little to no cell penetration into the leaflet. Interestingly, the study by Rieder *et. al.* found that the decellularization protocol and chemicals used greatly affected the re-endothelialization of decellularized leaflets, with SDS having cytotoxic effects and Triton X-100 leading to the best endothelial coverage.[135] The value of *ex-vivo* (and especially under static conditions) endothelial seeding seems low since proper decellularization and pre-implant conditioning seems to encourage autologous re-endothelialization (presumably effected by circulating endothelial progenitor cells). In addition, without an interstitial cell population, *in vitro* endothelial cell layers typically delaminate and are rapidly lost under physiologic flow conditions.

Other studies investigating cell seeding on isolated leaflets have attempted to repopulate the leaflet interstitium using fibroblast-like cells such as cardiac stromal cells (CStCs) and neonatal dermal fibroblasts with moderate success.[40, 94, 191] Dainese *et al.* seeded isolated leaflets with CStCs and observed up to 90% of native cellularity within 50 μm of the leaflet edge, yet they observed only 30% of native cellularity in the inner leaflet regions.[40] These studies demonstrate the efficacy of introducing cells onto decellularized leaflet samples and they led to the seeding of intact decellularized valves. Kim *et al.*[90] and Steinhoff *et, al*.[161] both seeded myofibroblasts and endothelial cells onto decellularized pulmonary valves and subsequently implanted them into animal models without further *in vitro* conditioning. Kim *et, al.* used an allogeneic model and seeded canine MFs and ECs onto decellularized canine pulmonary valves and implanted them in the pulmonary position of dogs.[90] Steinhoff *et, al.* used a xenogeneic animal model and seeded ovine MFs and ECs onto decellularized porcine pulmonary valves before implanting them in the pulmonary position of sheep.[161] Neither group used chemical or mechanical conditioning before implantation, but allowed 6-7 days of static culture after seeding for cell adhesion and proliferation.[90, 161] Following the longest implant periods evaluated, both studies demonstrated complete endothelialization and partial recellularization of the leaflet interior, though notably less than compared to native leaflet tissue.[90, 161]

An interesting study by Vincentelli *et al.* compared the efficacy of MSCs and MNCs for heart valve tissue engineering by directly injecting the cells into the arterial wall and annulus of decellularized valve scaffold, followed immediately by implantation in lambs.[175] After 7 days *in vivo*, the injected cells in both groups had scattered throughout the matrix and host cells were also observed. At 4 months, both cell groups showed re-endothelialization but had markedly different recellularization responses. The MNC seeded valves had thickened and retracted

leaflets with calcified nodules and a high presence of CD68+ cells. The MSC seeded valves had thin leaflets partially recellularized with $aSMA^+$ cells and showed no signs of calcification. While MSC seeding elicited a more favorable *in vivo* response in this study, it is worth noting that the applicability of MNCs towards heart valve tissue engineering has been explored more recently using polymeric scaffolds in which seeded MNCs induced an inflammation-mediated recellularization response *in vivo*.[55, 178] Considering the potential for regenerative paracrine signaling by seeded MNCs, it is not entirely clear if the CD68+ inflammatory cells present in the MNC seeded valves in the study by Vincentelli *et al.* were exhibiting an M1 or M2 inflammation response, or if they would eventually be replaced by VIC-like cells. However, the condition of the leaflets and the presence of calcified nodules in the MNC seeded valves was not encouraging.[175]

In vitro seeding and mechanical conditioning. Mechanical conditioning of tissue engineered heart valves utilizes bioreactors and mechanical stimulation with the goal of achieving a mature cell population *in vitro* (Table 2.5). Physiologic conditions of high fluid shear and pressure have been shown to encourage the VEC and VIC phenotypes, support cell proliferation, and encourage extracellular matrix remodeling.[1, 9, 114, 115, 134, 169, 186] Mechanical conditioning in bioreactors can simulate the physiological forces of heart valves and drive the differentiation and proliferation of seeded cells down the appropriate pathways.

Using a dynamic bioreactor, Lichtenberg *et al.* explored the effects of mechanical conditioning after seeding pulmonary heart valves with vascular endothelial cells.[103, 104] They demonstrated that culturing seeded valves under physiological pulmonic conditions (2.0 L/min, 60 bpm, 25 mmHG mean system pressure) can lead to complete re-endothelialization; however, care should be taken when introducing the seeded valve scaffolds to increased shear stress.[104]

Rapid increases in the pulsatile bioreactor flow (0.1 L/min to 2.0 L/min; 0.35 L/min increases) led to significant interruptions of the endothelium.[103] Conversely, a stepwise, gradual increase in pulsatile flow (0.1 L/min to 0.5 L/min; 0.1 L/min increases) resulted in a nearly complete endothelial layer.[103] These studies showed no recellularization of the leaflet interior, though it was not expected since they seeded endothelial cells. A study by Schenke-Layland *et, al.* also investigated physiologic mechanical conditioning on valve recellularization.[144] Myofibroblasts were seeded onto trypsin decellularized porcine pulmonary valves and cultured under pulmonic conditions (3.0 L/min, 60 bpm, 60/40 mmHg), followed by subsequent seeding with endothelial cells. After culture, the tissue engineered leaflets were very well recellularized, to an extent comparable with native valves. Cells repopulating the leaflet interior were αSMA^+ and VIM^+ while the cells on the leaflet surface were vWF^+. After recellularization and conditioning, tissue engineered valves were also mechanically more similar to native valves than their decellularized-only counterparts. Indeed, the only noticeable difference between the tissue engineered valves and native valves was the presence of αSMA^+ cells throughout the tissue engineered leaflets, likely due to the seeded myofirbroblasts. While these results are promising, the high αSMA expression is indicative of aVICs, which are responsible for tissue remodeling but their prolonged activation can also lead to valve disease.[105]

A different approach using mechanical conditioning under non-physiological conditions has been investigated as a means of repopulating the interstitium of the decellularized leaflet. Converse *et al.* studied the effects of cyclic negative and positive pressure on the recellularization of decellularized valves seeded with bone marrow derived MSCs.[34] After seeding with MSCs, the valves were either cultured in a static bioreactor for 24h, conditioned in negative cyclic pressure (5 to -20 mmHg) for 72 h, or conditioned at the same negative cyclic

pressure for 72 h followed by an additional 10 days conditioning at positive pressure up to 50 mmHg. Static cultured resulted in clumping of the cells on the valve surface and minimal cell infiltration. Mechanical conditioning under negative pressures resulted in a more even distribution of cell coverage on the surface of the leaflet and limited infiltration of cells into the interstitium of the leaflet. Valves subjected to a combination of negative and positive pressure conditioning exhibited further improved cell coverage and displayed moderate cell infiltration, though still less than native. The repopulated interior cells stained positive for CD90, CD29, HSP47, VIM, and αSMA. Biaxial mechanical testing also revealed that increased culture under positive pressure resulted in mechanical properties more similar to cryopreserved valves.[34]

Despite encouraging bench-top studies, mechanically conditioned, *in vitro* seeded valves implanted in animal and pediatric models have only seen moderate recellularization success.[85, 171] Tudorache *et al.* seeded ovine aortic valves with ovine endothelial cells followed by pulsatile flow conditioning up to 1.0 L/min over the course of a week.[171] After conditioning, the tissue engineered valves showed a complete endothelial layer on the leaflet surface though no interstitial cells were present. The conditioned valves were implanted in the descending aorta of sheep for three months, at which time all valves exhibited normal function. A complete endothelial layer was observed, as expected, however there was very minimal leaflet interstitial recellularization.[171] In this study, mechanical conditioning resulted in endothelialization in the bioreactor, yet the benefit remains unclear since implanted decellularized valves will re-endothelialize autologously, especially in sheep.[131, 133] One case study investigated pediatric clinical use of mechanically conditioned tissue engineered valves. Cebotari *et al.* implanted tissue engineered valves in two pediatric patients using decellularized human pulmonary valve scaffolds seeded with autologous MNCs isolated from peripheral blood.[27] After seeding, the

valves were cultured in a continuous perfusion bioreactor using a very low flow rate (15 mL/min) for 21 days.[27] Pre-implant histology revealed a confluent monolayer of cells along the leaflet surface with markers positive for endothelial cell types. At 3.5 years of follow up, both patients had recovered normally and had experienced somatic growth, valve annulus growth, and no signs of degradation, stenosis, or cusp thickening. These are highly encouraging results; however, the sample size is very limited and no further follow up data has been provided so the long-term outcome remains unclear.

In vitro seeding and chemical modification. Another common approach to increase the recellularization of *in vitro* seeded tissue engineered heart valves has been to chemically modify the decellularized valve scaffolds prior to seeding (Table 2.6). Chemical modification utilizes cytokines, chemokines, growth factors, antibodies, and polymers to support phenotype-specific cellular attachment, bolster valve mechanics, and drive cell differentiation.

As discussed previously, decellularization can have deleterious effects on the mechanics of the valve leaflet ECM. Chemical crosslinking has been explored as a means of improving the structural and mechanical integrity of the decellularized ECM. Conventional crosslinking methods using glutaraldehyde block immunogenic antigens, yet glutaraldehyde is also cytotoxic preventing cellular ingrowth and therefore is not appropriate for recellularizing valve scaffolds. Other crosslinking methods have been explored using procyanidin, quercetin, and nordihydroguaiaretic acid (NDGA), which have been found to improve the mechanics of the valve leaflets and are not cytotoxic at low concentrations.[107, 192, 193] After crosslinking, the treated leaflets had increased ultimate tensile strength (UTS) and elastic modulus compared to untreated decellularized leaflets and in some cases greater than comparable fresh leaflets or glutaraldehyde treated leaflets.[107, 192, 193] The recellularization potential after leaflet crosslinking remains largely

unknown however, as only NDGA treated valves have been briefly seeded with ECs for 24h, though in that time ECs showed adhesion and proliferation on the crosslinked leaflets.[107]

Other chemical modifications that can bolster the mechanical integrity of valve leaflets are the incorporation of polymers into the decellularized valves to create hybrid valve scaffolds. These hybrid valves have improved mechanical properties compared to decellularized valves and the polymer additions can act as a transport mechanism for drug delivery. The biodegradable polymer poly(3-hydroxybu-tyrate-co-4-hydroxybutyrate) (P3/4HB) has been applied to decellularized porcine aortic valves through impregnation into the tissue or electrospinning onto the valve surface.[68, 160] Hybrid valves created through P3/4HB electrospinning followed by seeding with MSCs under static conditions had a greater maximum load carrying capacity, ultimate tensile strength, and elastic modulus than their decellularized-only counterparts; however, recellularization was similar between groups and limited to the leaflet surface.[68] Impregnated P3/4HB hybrid valves also had increased biomechanics and could support the culture of mouse myofibroblasts, human myofibroblasts, and human endothelial cells, but only on the valve surface.[160] A more common polymer for creating hybrid valves is polyethylene glycol (PEG) because it is highly hydrophilic, water soluble, and has active functional groups that facilitate peptide conjugation.[42, 73, 123, 195, 196] Two groups have investigated modifying decellularized porcine aortic valve leaflets with PEG conjugated with TGF-β1, VEGF, and/or RGD.[42, 73, 195, 196] They found that PEGylation of decellularized valves resulted in mechanical properties similar to native valves and that conjugation of various peptides increased surface recellularization after seeding with rat myofibroblasts or human umbilical cord vascular endothelial cells.[42, 195, 196]In fact, in all studies the PEG-peptide modified valves showed greater surface cell density than valves treated with PEG only or decellularized control valves; however,

none of the PEG-peptide modified valves resulted in repopulation of the leaflet interstitium.[42, 195, 196]

Another group has explored chemical modification of decellularized valves by applying polyelectrolyte multilayers (PEM) composed of heparin plus VEGF, chitosan, or SDF-1α.[187, 188, 197] Decellularized porcine aortic valves treated with PEM of heparin-chitosan or heparin-VEGF were subsequently seeded with endothelial progenitor cells and it was observed that both PEM coatings improved hemocompatability, showing decreased platelet adhesion and activation.[187, 188] Although seeding with endothelial progenitor cells did not result in leaflet interstitial recellularization, valves modified with heparin-chitosan were able to support an EC population while valves modified with heparin-VEGF actually had better adhesion, proliferation, and migration of ECs compared to decellularized control valves.[187, 188] Zhou *et al.* applied a PEM of heparin-SDF-1α to decellularized rat aortic valves prior to seeding with rat bone marrow MSCs and observed increased proliferation and migration of MSCs on the modified scaffolds.[197] Zhou *et al.* also implanted unseeded, heparin-SDF-1α modified valves in rats and observed luminal re-endothelialization of the aortic wall; however, there was no indication of leaflet recellularization.[197]

Other efforts involving chemical modification of *in vitro* seeded decellularized valve scaffolds have aimed at increasing the adhesion of both the seeded cells and host cells *in vivo*. Theodoridis *et al.* coated decellularized ovine pulmonary valves in CCN1, a matricellular protein associated with cell adhesion, proliferation, and differentiation, before seeding them with ovine ECs and implanting them in sheep.[170] At explant, the modified valves had greater cell surface coverage and partial interstitial recellularization by VIM^+ and αSMA^+ cells.[170] Similarly, Ye *et al.* conjugated decellularized porcine aortic valve leaflets with an anti-human CD90 antibody and

then cultured them in a shear flow bioreactor with media containing an MSC population.[189] The modified leaflets had a greater cell population distributed evenly across the surface than the un-modified controls samples.[189] These approaches demonstrate that conjugation of peptides and antibodies can increase the adhesion of cells onto valve surfaces. However, this approach has not yet resulted in the complete repopulation of the leaflet interior. Increasing surface cell density through chemical modification may encourage cell infiltration to a small degree, but other chemokines may be required to repopulate the entire leaflet.

Decellularized valves have also been treated with fibronectin (FN) before *in vitro* cell seeding. FN has been shown to promote differentiation into a VIC phenotype by human MSCs and to reduce the formation of calcific nodules by VICs, particularly in combination with vascular endothelial growth factor (VEGF).[64, 74] Individual decellularized leaflets treated with FN showed only moderate recellularization when seeded with VICs or MSCs, though immunohistochemistry revealed appropriate differentiation into the correct cell phenotypes (surface cells were vWF^+ and interstitial cells were αSMA^+ and VIM^+).[16, 77] Dohmen *et al.* treated decellularized porcine pulmonary valves with FN, seeded them with autologous ovine endothelial cells, and implanted them in the pulmonary position of sheep for 6 months.[47] At explant, FN-treated/EC seeded valves had a complete EC monolayer throughout the valve and good internal recellularization of the leaflet, while valves treated with FN but not seeded had only a partial EC layer and minimal leaflet recellularization.[47] The same group also performed a small clinical study using the same *in vitro* seeding and FN treatment approach. Between 2000 and 2002, 11 patients underwent pulmonary valve replacement with a tissue engineered pulmonary heart valve treated with ProNectin F (a synthetic FN alternative) and seeded with autologous ECs.[49-51] At 10 years follow up, there was a 100% survival rate and transthoracic

echocardiography showed patent and functioning valves in all patients.[50] At 3 months, one patient required a non-related re-operation, during which a small biopsy was taken from the conduit of the tissue engineered heart valve.[48] Histology of the biopsy revealed repopulation of the conduit wall by $CD31^+$ and vWF^+ surface cells and fibroblast-like interstitial cells.[48]

2.5 Discussion and future directions

Many challenges have been encountered in the pursuit of a TEHV. In the context of engineering a viable TEHV using a decellularized valve scaffold, the most pressing challenge is achieving recellularization of the entire valve, including distal portions of the leaflet, with an appropriate cell population. Upon analysis of the various recellularization strategies that have been employed, it is apparent that all approaches are not equally effective. Chemical conditioning with fibronectin has been one of more successful approaches and has lead to increased leaflet recellularization in both *in situ* and *in vitro* studies.[6, 47, 49-51, 57, 122] Other chemical treatments that target increased cell adhesion, including conjugation of CD133 and CCN1 to the decellularized scaffold, have led to increased recellularization of the leaflet surface and the leaflet interstitium by phenotypically appropriate cells.[83, 170, 179] Mechanical conditioning has a positive effect on recellularization in general, although the most effective parameters for mechanical conditioning have yet to be determined and may vary by valve position. Conditioning parameters of pressure and flow similar to native *in situ* conditions seem to be the most obvious choice, yet mechanical conditioning at pulmonary conditions has had mixed results and conditioning using non-physiological forces has also resulted in limited recellularization.[34, 85, 103, 104, 144, 171] Complicating matters, the cell population within the TEHV must ultimately mimic that of the native valve. Justifiably so, αSMA is often used as the marker of choice to evaluate the appropriateness of scaffold repopulation since aVICs express αSMA during the

remodeling of valve extracellular matrix, and matrix remodeling is a basic requirement for a functioning TEHV. However, as discussed previously, the prolonged expression of αSMA and activation of VICs can lead to valve fibrosis, inflammation, and calcification.[105] As evidenced above, several groups have shown excellent scaffold repopulation by αSMA^+ cells, but the cell population should ultimately transition to a quiescent state. The study by James *et al.* provided one example of this successful transition in a decellularized valve graft implanted in a mouse model, however similar results have not yet been observed in larger animal implant models.[79] One of the crucial tasks in proving the safety of the TEHV will be proving that a seeded cell population that is initially αSMA^+ is capable of transitioning into a quiescent state after valve remodeling is complete.

Successful strategies have been employed for both of the two main approaches for heart valve recellularization (*in situ* & *in vitro*) and have resulted in recellularization of the interstitial tissue of the distal leaflet. In particular, the studies by Ota *et al.,*[122] Jordan *et al.,*[83] Iop *et al.,*[77] and Schenke-Layland *et al.*[144] demonstrate good recellularization of an appropriate valve cell phenotype using a variety of methods. However as we continue to progress the field of heart valve tissue engineering, we must be mindful of the potential clinical and regulatory challenges associated with successful recellularization strategies. *Ex vivo* cell seeding maintains the ability to directly influence cell infiltration by the choice of the seeding cells and by applying bioreactor conditioning parameters through mechanical or biochemical means. But, the same bioreactor conditioning associated with relatively complete *in vitro* recellularization requires lengthy valve and cell culture, limiting the potential for off-the-shelf availability and clinical relevance. Short term *in vitro* seeding protocols have numerous practical advantages (e.g. sterility) but are challenging in assuring target recellularization populations are achieved. In either case, *in vitro*

seeding will have associated regulatory challenges with assuring correct lineage and phenotype stability of the seeded and subsequent proliferated cells, particularly if MSCs or other stem cells are used. Therefore, the future direction of heart valve tissue engineering may follow the paradigm of guided tissue regeneration and *in situ* recellularization. That is, the greatest possibility for success lies in developing bioengineered scaffolds and conditioning methods to create 'smart', bioactive heart valves that harness the patient's own regenerative capabilities to recellularize the construct after implantation. The inherent elegance of *in situ* recellularization is the simplification between the TEHV product (manufacture, distribution, inventory, and patient allocation) and the clinical event (actual treatment of individual patients.) It is worth noting that there are still significant regulatory hurdles associated with *in situ* recellularization since many of the signaling molecules may be pro-neoplastic and may cause difficulties in sterilization. Lastly, it is worth noting that the two recellularization approaches of *in vitro* and *in situ* are not mutually exclusive and the benefits of both may be leveraged. For example, short term seeding of a 'pilot' cell population *in vitro* may provide the signaling cues necessary to induce complete valve repopulation by host cells *in situ*. Such approaches have already realized recellularization success in vascular tissue engineering and with polymeric heart valve scaffolds.[137, 178]

As discussed previously, decellularized heart valve scaffolds are of significant interest moving forward with the tissue engineered heart valve. However, other scaffold options are being explored that may soon over-come the limitations of decellularized valves. One such scaffold is a polymeric valve under development by XELTIS, a European based company that started the first clinical trial evaluating a synthetic, biodegradable scaffold in October 2016.[129, 183] The XELTIS valve is a non-cell seeded scaffold that allows host cell repopulation and new tissue formation. This valve is promising because of the unlimited supply of a synthetic valve, though

long-term follow up studies are necessary determine the success of the XELTIS valve implants. Another noteworthy scaffold option comes from decellularizing 'man-made' engineered tissue. For example, Tranquillo *et al.* have created valve and leaflet shaped collagen scaffolds by seeding fibrin gels with dermal cells followed by decellularization.[164-166] These engineered tissues show potential for both *in situ* recellularization in sheep and *in vitro* recellularization after seeding with MSCs.[164-166] Similar to synthetic scaffolds, these engineered scaffolds have potential for unlimited supply but further studies are needed to ensure clinical safety. Until then, the decellularized heart valve is still the scaffold currently in the best position to move forward as a clinically useful TEHV. As advances continue in materials science and in the understanding of heart valve structure, the challenges facing synthetic and engineered scaffolds may be overcome and an artificial scaffold may one day be preferred for bioengineered valve replacements with the attendant manufacturing advantages. However, the timeline for that reality is uncertain and decellularized valve scaffolds have the greatest potential for the expeditious development of a TEHV due to the regulatory history, long clinical experience with homografts, as well as a deep research focus by many groups. [31, 45, 70] Utilizing the decellularized heart valve as a tissue engineering scaffold offers advantages in terms of both immediate function and overall safety, as the worst case scenario results in a valve similar to the homograft for which the natural history is well known and clinical advantages are appropriate for specific patient populations.

In addressing the challenges associated with the TEHV, researchers must be mindful of the ultimate goal: improving the clinical management of congenital heart defects and other structural valve diseases. Success in the laboratory does not necessarily equate to successful translation to clinical practice. While the regulatory guidelines for non-viable prosthetic valve

substitutes are well defined, the guidelines for FDA approval of a viable combination device (cells + scaffold) such as a TEHV are evolving and no such construct has yet been approved. Valve functional safety will certainly be paramount; however, assurance of consistent recellularization with phenotypically appropriate cell populations could be more challenging to demonstrate *in vivo* and non-destructively, potentially necessitating new technologies for analyzing recellularization. Ultimately, the challenge remains regarding scaffold repopulation and the success of the TEHV may be reliant upon developing new performance markers, including *in vitro* cell population monitoring, not just performance monitoring by echocardiography and traditional MRI methods. Thus, successful heart valve tissue engineering strategies will require elegant science to meet the design criteria of the TEHV, survive regulatory scrutiny, and achieve clinical success eclipsing current valve replacement options.

CHAPTER 3: SPECIES-SPECIFIC EFFECTS OF AORTIC VALVE DECELLULARIZATION[†]

3.1 Abstract

Decellularized heart valves have great potential as a stand-alone valve replacement or as a scaffold for tissue engineering heart valves. Before decellularized valves can be widely used clinically, regulatory standards require pre-clinical testing in an animal model, often sheep. Numerous decellularization protocols have been applied to both human and ovine valves; however, the ways in which a specific process may affect valves of these species differently have not been reported. In the current study, the comparative effects of decellularization were evaluated for human and ovine aortic valves by measuring mechanical and biochemical properties. Cell removal was equally effective for both species. The initial cell density of the ovine valve leaflets (2036 ± 673 cells/mm^2) was almost triple the cell density of human leaflets (760 ± 386 cells/mm^2; $p < 0.001$). Interestingly, post-decellularization ovine leaflets exhibited significant increases in biaxial areal strain ($p < 0.001$) and circumferential peak stretch ($p < 0.001$); however, this effect was not observed in the human counterparts ($p > 0.10$). This

[†] Published as **VeDepo, M. C.,** Buse, E. E., Quinn, R. W., Williams, T., Detamore, M. S., Hopkins, R. A. and Converse, G. L. Species-Specific Effects of Aortic Valve Decellularization. Acta Biomater, 2017. doi: 10.1016/j.actbio.2017.01.008. PubMed PMID: 28069510.

species-dependent difference in the effect of decellularization was likely due to the higher initial cellularity in ovine valves, as well as a significant decrease in collagen crosslinking following the decellularization of ovine leaflets that was not observed in the human leaflet. Decellularization also caused a significant decrease in the circumferential relaxation of ovine leaflets ($p < 0.05$), but not human leaflets ($p > 0.30$), which was credited to a greater reduction of glycosaminoglycans in the ovine tissue post-decellularization. These results indicate that an identical decellularization process can have differing species-specifc effects on heart valves.

3.2 Introduction

None of the current treatment options for heart disease requiring valve replacement are ideal, including mechanical, bioprosthetic, and biological (primarily cryopreserved homograft) valves. Mechanical valves run the risk of embolism and require a lifetime of anti-coagulation therapy.[117, 140] Bioprosthetic and homograft valves have a limited lifespan due to structural degradation, calcification, and immunological inflammation.[70, 106, 117, 140] These complications are compounded in children, resulting in multiple revision surgeries throughout the patient's life. Decellularized heart valve options possess great potential as a valve replacement option and/or as a scaffold for tissue engineering. As a stand-alone valve substitute, the design of decellularized valves is well proven and the acellular nature reduces the immunological response and host rejection. However, in clinical application decellularized valves have been met with varying levels of success, with decellularized allogeneic valves performing better than xenogeneic valves.[27, 28, 56, 62, 119, 127, 154] Decellularized valves are a promising scaffold for the tissue engineered heart valve (TEHV) due to excellent, intrinsic hemodynamic function and structure.[117] The TEHV conceptually would combine the optimal hemodynamic performance of

the homograft valve with early active tissue remodeling, perhaps allowing for somatic growth after implantation.[56, 99, 133] However, before decellularized valves are used as stand-alone replacements or TEHV scaffolds, the effects of the decellularization process must be fully understood.[32, 65, 117]

Decellularization has been shown to affect the mechanical and biochemical properties of human, ovine and porcine valve tissue; however, the species-specific effects of decellularization have not been elucidated due to differences in tissue processing protocols.[32, 81, 101] Species-specific differences in native valve tissue have already been reported between ovine, porcine, and aged, human valve leaflets.[111] Martin et al. found there are significant mechanical differences between the three species and qualitatively observed less collagen type I and collagen alignment in the ovine leaflets.[111] These reported findings warrant a comparative analysis of decellularization across species, as species-specific differences in the effect of decellularization may have down-stream consequences.

The effects of decellularization on the valve extracellular matrix are highly dependent on the individual decellularization protocol.[36] A study by Liao et al. measured the biaxial mechanical and structural effects of three different decellularization protocols on porcine aortic valves.[101] All three decellularization protocols were found to increase leaflet extensibility, though to differing degrees, with the Triton X-100 process having the greatest effect.[101] Other studies have also compared the effects of different decellularization methods, yet they have found that processes using Triton X-100 or other detergents caused the least harm to the extracellular matrix, while methods using the enzymatic agent trypsin caused the most harm.[87, 116, 157, 172] We have previously investigated the effects of a low concentration, multi-detergent decellularization process on the biaxial, mechanical properties of ovine heart valve leaflets and

found an increase in leaflet extensibility and areal strain along with a reduction in relaxation following decellularization.[32, 34] It was proposed that the increase in leaflet extensibility was due to an increased mobility of collagen fibers.[101] However, it remains unclear whether other factors contribute to changes in mechanical behavior following decellularization. Taken together, these reports indicate that the mechanical and biochemical behavior of a decellularized leaflet is dependent upon the decellularization protocol and therefore each decellularization protocol should be analyzed and validated for the species and tissue that it will ultimately process.

The end-goal of characterizing decellularized tissue is to develop a fundamental understanding of tissue composition and properties, which may, in turn, facilitate clinical translation. However, regulatory guidelines require pre-clinical testing in animal models. Sheep are considered the regulatory standard for valve implantation due to the similar cardiac and growth characteristics of the ovine model to human children[59], yet due to species- transplantation antigen mismatch it is not useful to implant human valves in sheep. Therefore, good scientific practice requires characterizing pre-implant decellularized human and ovine valves. Previous studies have investigated the effects of decellularization on ovine valve tissue and the performance of those valves in sheep.[131-133] However, to our knowledge, no studies have evaluated the comparative effects of equivalent decellularization protocols between ovine and human valves. The ovine valve model was designed to test calcific degradation of glutaraldehyde crosslinked bioprosthetic valves, thus the similarities to human hosts for evaluating other biological valves is less well understood. Therefore the purpose of this study is to compare the effects of a multi-detergent decellularization process on human and ovine aortic valves. The underlying causes for changes in the mechanical behavior of the extracellular matrix (ECM) were evaluated using histology, collagen crosslinking analysis, and biochemical content assays.

3.3 Materials and Methods

3.3.1 Tissue preparation

Ovine aortic valves were obtained from juvenile sheep under approved IACUC protocols and in accordance with *Guide for Care and Use of Laboratory Animals* (National Institutes of Health Publication No. 85-23). Ovine samples were cryopreserved 72 h after harvest to simulate clinical tissue handling methods. Human aortic valves were obtained from a tissue banking facility (LifeNet health, Virginia Beach, VA) from male donors aged 16-26 years old. All samples were stored in cryopreserved state until use. The cryopreservation procedure was modeled after clinical tissue handling protocols. Briefly, samples were frozen in a cryoprotectant (RPMI w/10% FBS and 10% DMSO) at 1 °C min^{-1} using a controlled rate freezer (2100 Series, Custom BioGenics Systems, Romeo, MI) before being stored in a cryofreezer at -180 °C. Cryopreserved valves were selected as the standard comparison against decellularized valves since cryopreserved valves are used clinically and are the closest to in-situ native valves that can be easily obtained. In total, seven ovine cryopreserved, six ovine decellularized, six human cryopreserved and six human decellularized aortic heart valves were used to complete this study.

3.3.2 Valve decellularization

Ovine and human aortic valves were thawed from cryopreservation and decellularized using a reciprocating osmotic shock and non-ionic detergent wash protocol similar to that described previously.[133] Under continuous mild shaking, valves were immersed in a series of solutions including, hypertonic salt solution (HSS), 0.05% Triton X-100 (Sigma-Aldrich), deionized water, *N*-lauroylsarcosine sodium salt (Sigma-Aldrich), and Benzonase® (EMD Chemicals, Gibbstown, NJ). Afterwards, organic soluble material was extracted via recirculating sterile water through ion exchange resins (Amberlite, Sigma-Aldrich; Mixed Bead Resin TMD-

8, Sigma-Aldrich; Dowex Monosphere, Supleco) for 40 hours. Following decellularization the valves were cryopreserved using the procedure described above. The effectiveness of decellularization was determined via histologic imaging and double-stranded DNA (dsDNA) analysis. Assays for dsDNA were performed using the Quant-it Kit, High Sensitivity (Invitrogen, Carlsbad, CA) and measured using a fluorescence plate reader (Synergy HT, Bio-Tek Instruments Inc., Winooski, VT) at 486/528 nm excitation/emission wavelengths. dsDNA content was calculated as ng mg^{-1} of wet tissue.

3.3.3 Biaxial mechanical testing

The quasi-static and time dependent mechanical behavior of cryopreserved and decellularized, human and ovine valve leaflets were measured using planar biaxial mechanical testing, using methods similar to those previously described.[32] Leaflets were dissected from their regional position (left coronary (LC), right coronary (RC), or non-coronary (NC)) and a 9 x 6 mm rectangular specimen was cut from the belly region of the leaflet. The rectangular samples were then attached to tissue grips using small fishing hooks and line, with four attachment points per side. The tissue grips were submerged in phosphate buffer saline (PBS) at 37 °C and mounted on a four motor biaxial test system (LM1 TestBench, Bose, Eden Prairie, MN) such that the loading axes aligned with the circumferential and radial directions of the sample.

Equibiaxial loading was performed on cryopreserved and decellularized leaflet samples (n = 9). Ovine specimens were loaded to tensions of 30 N m^{-1} using a rise time of 10 s and human specimens were loaded to 60 N m^{-1} using a rise time of 10 s. A lower tension was used on ovine samples to prevent failure at attachment points based on previous experience.[32] Specimens were preconditioned for 10 loading cycles prior to data collection. Strain was measured using a digital video extensometer. Peak stretch ratios were calculated from strain data in the

circumferential (λ_C^{peak}) and radial (λ_R^{peak}) directions. Anisotropy ratios (λ_R^{peak}/ λ_C^{peak}) were also calculated for each specimen. Areal strain was used as a measure of net extensibility and was calculated from equibiaxial data as (λ_C^{peak} x λ_R^{peak} – 1) x 100%. Following quasi-static testing, all samples underwent relaxation testing. Samples were loaded to the same equibiaxial tension used previously at a rate of 8 mm s^{-1} along the radial axis. The displacement rate along the circumferential axis was adjusted so the overall rise time of both axes was equal. Specimens were held at a constant displacement and allowed to relax for 1000 s, while load data was collected. Relaxation data is reported as per cent relaxation at multiple time points (i.e., 1, 10, 100 and 1000 s). Additionally, the time after initial loading at which differences in relaxation between cryopreserved and decellularized became statistically significant was determined. It is worth noting that the same specimens used for mechanical testing were also utilized for GAG, collagen, elastin analysis. Between tests, the specimens were stored at -80 °C.

3.3.4 Biochemical Assays

The effects of decellularization on the leaflet extracellular matrix were evaluated using biochemical assays, specifically by measuring the collagen, elastin, sulfated glycosaminoglycan (sGAG), and total protein concentrations. Collagen and total protein concentrations were measured using the QuickZyme Total Collagen Assay and QuickZyme Total Protein Assay, respectively (QuickZyme Biosciences, Leiden, The Netherlands). Samples (~15 mg, n = 9) were prepared by overnight hydrolysis in 6M HCl at 90 °C. The resulting hydrolysates were used for the collagen and total protein assays, as well as for collagen cross-linking analysis. The collagen and total protein assays used colorimetric quantification to measure the hydroxyproline and free amino acid concentrations, respectively. Samples were analyzed using a UV/Vis spectrophotometer (VERSAmax, Molecular Devices) at 570 nm. Elastin and sGAG

concentrations were measured using commercially available assay kits (Fastin Elastin Assay and Blyscan Sulfated Glycosaminoglycan Assay; Biocolor). Tissue samples for elastin and sGAG assays (~15 mg, n=9 each) were processed according to manufacturer protocols and the results quantified colorimetrically using a UV/Vis spectrophotometer at 513 nm and 656 nm, respectively. Total protein content is reported as μg mg^{-1} of wet tissue. Collagen, elastin, and sGAG content are reported as fraction of total protein and as μg mg^{-1} of wet tissue.

3.3.5 Collagen Cross-linking

The degree of collagen crosslinking in the human and ovine leaflets, for both cryopreserved and decellularized samples, was analyzed by measuring the mature enzymatic collagen crosslinks by the biomarkers pyridinoline (PYD) and deoxypyridinoline (DPY).[91] PYD and DPY are hydrophilic amino acid derivatives released by digestion to amino acids. PYD and DPY have a quaternary amine (pyridinium) and three carboxylic acid functional groups and are frequently measured by cation ion pair reverse phase chromatography with fluorescence detection. A modification of the general ion pair method has been adapted for reverse phase liquid chromatography and mass spectrometry (LCMS).[91] The ion pair agent, in this case 30 mM sodium salt from octane sulfonic acid, was put into each sample. When injected, each sample "refreshes" the amount of ion pair bound to the stationary phase of the C18 column for consistent retention times. Separation was done in isocratic mode with 90% 0.1% acetic acid and 10% CH3CN on a Hypersil BDS C18 column (3 μ, 2.1 mm × 100 mm) using a Waters Acquity Classic UPLC (Waters Corp., Milford MA). The injection volume was 20 ul and the column operated at 320 ul/min with the first 4 minutes of eluent diverted away from the source. Following separation, compounds were detected using a "triple" quadrupole mass spectrometer (Quattro Ultima Micromass Ltd. Manchester UK) operating in positive-ion mode with the mass

analyzers tuned to 0.8u FWHH. Cone voltage and collision induced dissociation conditions for precursor/product ion pairs were determined by post column mixing of standards infused at UPLC elution conditions. The conditions were 1) PYD m/z 429> 82 and 2) DPY m/z 413> 84, both with a cone voltage of 45 V, a collision energy of 35 V, and 150 ms dwell time. The retention times were 6.8 minutes for both compounds. Calibration curves were generated by pooling partial aliquots from all samples in a batch and spiking with PYD/DPY standards (Quidel, San Diego CA USA) at 4 concentrations in the 100s of pg/ul range. Samples for all groups were taken from the hydrolysates used in the collagen concentration assay. The hydrolysate samples were dried overnight under N_2 flow then stored at -20 °C until use, at which point they were reconstituted in H_2O. Then, the ion pair agent was added after pooled sample segregation. Remnant hydrolysis salts, amino acids, etc., did not suppress signal compared to standards with hydrolysis. PYD and DPY concentrations are reported as ng μg^{-1} of collagen. Note that a second set of valves was used for collagen cross-linking analysis. Additional collagen analysis was performed on these valves. Therefore, the collagen contents used for normalization of cross-linking compounds correspond directly to the valves used for cross-linking analysis.

3.3.6 Histology

Human and ovine valve leaflet samples for histology were dissected and sectioned along the radial plane. Hematoxylin and eosin (H&E) staining was used to evaluate leaflet architecture and cell removal. Following H&E staining, cellularity of the cryopreserved ovine (n=12) and human (n=6) leaflets was determined by counting the cells in a calculated area using Axiovision software. Cell density was measured at the base, middle, and tip region of the leaflet and an average for the whole leaflet was calculated. Leaflets were also stained with Movat's

pentachrome to evaluate the ECM biochemical structure and collagen architecture.

3.3.7 Statistical Analysis

To determine the effect of decellularization within each species, statistical comparisons were made between the cryopreserved and decellularized samples of that species. A statistical comparison was also made for the initial cellular density between human cryopreserved and ovine cryopreserved samples in an effort to elucidate a possible reason for differences in effect observed between species. Normality within groups was determined by the Shapiro-Wilk test. Data between cryopreserved and decellularized groups was evaluated with parametric (Student's t-test) and non-parametric (Mann-Whitney Rank Sum Test) methods as appropriate (SigmaStat 3.5, Systat Software, Inc., Chicago, IL.). Differences between groups were considered statistically significant at $p < 0.05$. Error values reported as the standard deviation of the mean.

3.4 Results

3.4.1 Decellularization and Histology

For all decellularized samples, dsDNA content was below the detection limit of 0.007 ng/mg wet tissue, indicating a >99.9% reduction in nuclear material from both human and ovine leaflet tissue. Effective decellularization is further supported by histologic acellularity observed in all regions of both human (Figure 3.1) and ovine (Figure 3.2**)** decellularized valve leaflets. The lamellar structure of the leaflet was preserved following decellularization; however, the extracellular matrix was more porous due to the removal of cells (Figure 3.1 C, D and Figure 3.2 C, D).

The average number of cells in cryopreserved tissue was measured by leaflet region (Figure 3.3). Both ovine and human leaflets had a significantly greater density of cells in the tip

of the leaflet compared to the base and the middle. Overall leaflet averages indicated that the cellular density in the ovine leaflet was nearly three-fold that measured in the human leaflet, with 2036 ± 673 and 760 ± 386 cells/mm^2 in ovine and human tissues, respectively ($p < 0.001$).

3.4.2 Planar biaxial mechanical testing

The mechanical behavior of ovine and human aortic valve leaflets was highly anisotropic under biaxial loading (Figure 3.4). Mechanical testing revealed several species-specific effects of decellularization (Figure 3.5). As determined by equibiaxial testing, decellularized ovine leaflets exhibited a statistically significant increase in areal strain compared to cryopreserved samples ($p < 0.001$), while no significant difference was measured in human samples ($p = 0.11$). Decellularized ovine leaflets had an areal strain of 158.1 ± 15.4% while cryopreserved ovine leaflets exhibited 124.5 ± 19.7%. Decellularized and cryopreserved human leaflets exhibited areal strains of 93.3 ± 12.3% and 84.0 ± 11.3%, respectively. Ovine leaflets also exhibited a significant increase in the circumferential peak stretch ratio of decellularized leaflets compared to cryopreserved leaflets ($p < 0.001$). Ovine leaflets had a circumferential peak stretch ratio of 1.36 ± 0.07 and 1.22 ± 0.06 for decellularized and cryopreserved samples, respectively. No significant change in circumferential peak stretch ratio was seen in human samples ($p = 0.23$). Human leaflets had a circumferential peak stretch ratio of 1.16 ± 0.08 and 1.10 ± 0.08 for decellularized and cryopreserved samples, respectively. There was also no significant difference in the radial peak stretch ratio between decellularized and cryopreserved leaflets for ovine ($p = 0.28$) or human ($p = 0.73$) samples. Ovine radial stretch ratios for decellularized and cryopreserved samples were 1.90 ± 0.11 and 1.84 ± 0.14, respectively, and human radial stretch ratios were 1.66 ± 0.07 and 1.65 ± 0.07, for decellularized and cryopreserved respectively. Ovine cryopreserved and decellularized leaflets exhibited anisotropy ratios of 1.51 ± 0.14 and

1.41 ± 0.12, respectively; however, the difference was not statistically significant ($p < 0.11$). Human cryopreserved and decellularized leaflets exhibited anisotropy ratios of 1.49 ± 0.16 and 1.44 ± 0.13, respectively; however, as with the ovine samples, the difference was not statistically significant ($p = 0.43$).

Relaxation testing revealed that decellularization effected the time-dependent behavior of leaflet; however, the effect was more pronounced in the ovine leaflet (Figure 3.6**,** Figure 3.7). Decellularization caused significantly decreased relaxation of valve leaflets in both ovine and human tissues in the radial direction at 1000 s ($p < 0.001$ ovine; $p = 0.04$ human). Ovine decellularized and cryopreserved leaflets respectively exhibited 25.8 ± 1.7% and 30.7 ± 2.9% relaxation in the radial direction at 1000 s, while human decellularized and cryopreserved leaflets respectively exhibited 25.9 ± 1.1 % and 27.7 ± 2.0%. However, in the circumferential direction, only ovine tissue exhibited a significant decrease in relaxation at 1000 s ($p < 0.01$). Ovine leaflets exhibited 26.9 ± 2.0% and 31.53 ± 2.9% relaxation in the circumferential direction at 1000 s for decellularized and cryopreserved samples, respectively. No significant change in circumferential relaxation was observed in human tissue ($p = 0.21$). At 1000 s, human tissue exhibited circumferential relaxation of 25.6 ± 1.2% and 27.1 ± 3.3%, for decellularized and cryopreserved samples respectively. Statistically significant differences in relaxation between decellularized and cryopreserved ovine leaflets emerged 2 and 4 s after initial loading in the radial and circumferential specimen directions, respectively. In the radial specimen direction at 2 s, cryopreserved and decellularized ovine leaflets exhibited 16.9 ± 2.9% and 14.3 ± 1.9 relaxation, respectively ($p = 0.04$). In the circumferential specimen direction at 4 s, cryopreserved and decellularized ovine leaflets exhibited 19.7 ± 2.9% and 17.2 ± 1.4 relaxation, respectively ($p = 0.04$). These differences in ovine samples remained statistically significant

throughout the remainder of relaxation period ($p < 0.03$); however, a statistically significant difference in relaxation of human samples in the radial direction did not emerge until 100 s after initial loading (Figure 3.7).

3.4.3 Biochemical Assays

The decellularization process was found to slightly affect the biochemical composition of the extracellular matrix of the valve leaflets (Table 3.1). Collagen, the primary structural protein of the leaflet matrix, was not significantly altered by decellularization in ovine or human samples ($p = 0.59$; $p = 0.39$, respectively). Interestingly, decellularization did cause a significant decrease in the elastin concentration of human leaflets ($p < 0.05$), yet there was no significant change in ovine leaflets ($p = 0.84$). The concentration of sGAGs was also significantly decreased in decellularized samples for both ovine and human tissues ($p<0.01$; $p < 0.001$, respectively). The reported differences in sGAG content between decellularized and cryopreserved samples represent an 89.6% reduction for ovine leaflets and a 57.4% reduction for human leaflets. Overall, there was no significant change in total protein concentration of the leaflet samples for either human or ovine specimens after decellularization.

3.4.4 Collagen Cross-linking

The concentration per collagen of the mature collagen cross-links PYD and DPY was measured in the human and ovine cryopreserved and decellularized leaflet samples (Figure 3.8). Following decellularization, the concentration of DPY and PYD remained relatively unchanged in the human leaflets. The concentration of PYD in the human leaflets measured 0.17 ± 0.03 ng μg collagen^{-1} for decellularized samples and 0.18 ± 0.03 ng μg collagen^{-1} for cryopreserved samples ($p = 0.70$). The concentration of DPY in the human leaflets was 0.06 ± 0.03 ng μg

collagen^{-1} and 0.07 ± 0.01 ng μg collagen^{-1} for decellularized and cryopreserved samples, respectively ($p = 0.43$). Interestingly however, the ovine leaflets experienced a significant decrease of both collagen crosslinking markers after decellularization. Ovine leaflets had a PYD concentration of 0.21 ± 0.08 ng μg collagen^{-1} and 0.31 ± 0.06 ng μg collagen^{-1} for decellularized and cryopreserved samples, respectively ($p < 0.01$), and a DPY concentration of 0.02 ± 0.004 ng μg collagen^{-1} and 0.1 ± 0.006 ng μg collagen^{-1} for decellularized and cryopreserved sample, respectively ($p < 0.05$).

3.5 Discussion

3.5.1 Mechanical Effects of Decellularization

The primary purpose of the tested decellularization process is removal of cellular and nuclear material from the scaffold. At this, it was highly effective for both ovine and human aortic valve leaflets. In both species, the double stranded DNA content of the decellularized leaflets was lower than the detection limit of 0.007 ng/mg wet tissue, indicating greater than 99.9% removal of double stranded DNA. Decellularization was confirmed by H&E staining which showed no evidence of cells or nuclear material in the resulting extracellular matrix of human or ovine leaflet tissue.

The decellularization process was equally effective at removing nuclear material from both human and ovine valves, yet decellularization also resulted in changes in mechanical behavior of ovine valve leaflets, as we have observed previously for ovine pulmonary valve leaflets [32]. Equibiaxial and time dependent mechanical testing of the decellularized ovine leaflets revealed increased areal strain and circumferential stretch ratio, along with significantly decreased relaxation in both specimen directions, compared to the cryopreserved leaflet; however, the level anisotropy remained unchanged (Figure 3.5**,** Figure 3.7). For the human aortic

valve leaflet, only a significant decrease in relaxation in the radial specimen direction was observed. Differences before and after decellularization in the relaxation behavior of the ovine leaflet were reflected in the relaxation curves; however, this was not the case for human sample, likely due to the overall magnitude of the change (Figure 3.6**,** Figure 3.7). Statistically significant differences in relaxation between cryopreserved and decellularized leaflet tissue also emerged much more rapidly in ovine samples, compared to human samples. This illustrates a key finding of this study that, while the human and ovine valves underwent the same decellularization process, the mechanical behavior of the ovine aortic valve leaflet was affected more extensively.

Direct statistical comparisons were not made between the mechanical properties of ovine and human tissues in part because different tension levels were used for the two cohorts and also because the effect of decellularization within a given species is determined by comparing the cryopreserved and decellularized samples of that particular species. However, to gain a better understanding of the relationship in mechanical behavior between the human and ovine leaflets, stretch ratio and areal strain values for human leaflet tissues at a tension of 30 N/m were determined from the tension-stretch data (Table S1). As expected based on the tension-stretch curves (Figure 4a), stretch ratios and areal strain at 30 N/m were very similar to those at 60 N/m ($p > 0.44$), and as at a tension of 60 N/m, there were no statistically significant differences between cryopreserved and decellularized samples at a tension of 30 N/m.

3.5.2 Biochemical makeup of the ECM

Collagen, the primary structural protein of the valve leaflets, and the total protein content of the leaflets remained unchanged after decellularization indicating other factors were responsible for the change in leaflet mechanical properties in ovine samples (Table 3.1).

However, a significant decrease in sulfated GAGs was measured in decellularized samples. The loss of the bulky GAGs from the ECM may open the leaflet architecture and allow greater freedom of rotation of the collagen fibers owing to the increase in areal strain. However, a study by Eckert et al. used enzymatic digestion to test the biomechanical properties of GAGs in porcine aortic valve leaflets and it was found that the loss of GAGs had no effect on peak stretch during biaxial tensile testing.[53] Therefore, it is unlikely that the loss of GAGs contributed significantly to the changes in areal strain and peak stretch ratio of ovine leaflets in the current study. A reduction of GAG content has been linked to decreased relaxation.[20, 32, 102, 112] In the current study, decreases in relaxation were observed in both human and ovine leaflets following decellularization; however, the changes were more extensive, and emerged more rapidly, in ovine tissue. This corresponded to a larger reduction in GAG content in ovine samples, compared to human. Seemingly contrary to these results, the study by Eckert et al. reported no change in the time-dependent tensile properties of their porcine valve leaflets after the enzymatic removal of GAGs.[53] However, their study evaluated changes in hysteresis of the stress-strain relationship during cyclic loading. Therefore Eckert's results and those from this study are not directly comparable. In this study, significant differences in per cent relaxation were observed at 2-4 s after initial loading. While still longer than the cardiac cycle, the speed with which these differences emerged suggests that GAG retention during decellularization may be an important consideration.

3.5.3 Collagen Crosslinking

The trivalent collagen crosslinks PYD and DPY are the mature products of lysyl oxidase-mediated crosslinking.[128] Both compounds are primarily found in bone collagen, but they are also present in a number of soft tissues, including heart valves.[2, 11, 128] Aldous et al. found that

during the fetal-to-neonatal transition of bovine, the concentration of these mature crosslinks increased in aortic valve leaflets as the transvalvular pressure increased, indicating collagen remodeling and maturation in response to higher loads.[2] In another study. Balguid et al. found a direct correlation between the concentration of PYD and DPY in human valve leaflets and the circumferential modulus of elasticity.[11] In the current study, decellularization resulted in a significant decrease in PYD and DPY in ovine aortic valve leaflets; however, no significant changes were observed in human tissue. This species-dependent effect on collagen crosslinking likely contributed to the dissimilarities observed in the mechanical behavior between species. It isn't entirely clear why ovine valves were more susceptible to a loss of PYD and DPY crosslinks; however, all ovine valves were from juvenile sheep and human valves were from donors 16-26 years of age. There is evidence that the amount of collagen crosslinking increases with age[88, 163], which favors crosslinking in the human valves. Interestingly however, the PYD concentration measured in this study was greater in the ovine valves. Though it does not appear that age affected the concentration of collagen crosslinking, the age of the valves may effect crosslinking stability. "Mature" collagen has been thought to have stronger molecular bonds which has consequences such as less protein remodeling and stiffer collagen rich tissues. Furthermore, human valve leaflets are almost twice as thick as ovine leaflets and the decellularization process may have a greater effect on the thinner ovine leaflets.[141] It is also possible that the loss of collagen crosslinks is entirely a species-specific effect.

3.5.4 Cell density and cell loss

The number of cells per mm^2 in the cryopreserved ovine leaflets was nearly triple the amount of cells per mm^2 found in cryopreserved human leaflets. The measured difference in cellularity may partially be related to the previously mentioned age discrepancy between ovine

and human groups rather than purely species-specific. After decellularization, no cells were found in valve leaflets of either species. Valve interstitial cells (VICs) have been mechanically characterized by microaspiration and found to have their own effective elastic modulus that correlates with transvalvular pressure[115] and viscoelastic properties.[113] The contractility of VICs is thought to be too low to affect valve mechanics during normal valve function[115], and it is doubtful the cells provide significant structural stability during tensional loading. However, Liao et al. previously reported increased extensibility of porcine aortic valve leaflets following decellularization and attributed the changes to increased collagen fiber motility, reasoning that the loss of cells and other key proteins opens up the leaflet architecture allowing more freedom of movement of collagen fibers.[101] Additionally, VICs interact with the surrounding ECM through integrin-mediated adhesions, which act to transfer local micromechanical forces to the cells.[30] Therefore, the integrin binding of the VICs likely function as attachment points between collagen fibers, restricting their rotation and providing greater structural stability. It is proposed that following decellularization, the vacant regions of missing cells and the loss of cellular attachment between collagen fibers leads to greater collagen fiber rotation. Thus, the higher initial cellularity of the ovine valves likely also contributed to the discrepancy in post-decellularization mechanical properties. These results imply that the VICS within the aortic valve leaflet may provide greater structural support than previously believed, not by conveying their own mechanical properties but instead in the interaction between VICs and ECM components.

3.5.5 Insight for in vivo implantation

Taken together, the results of this study show a species-specific response to decellularization. After decellularization, ovine aortic leaflets displayed a greater change in

biaxial stretch behavior compared to their human counterparts. The underlying cause for the species-specific response in biaxial stretch is likely a contribution of multiple factors: including a loss of collagen crosslinking and greater initial cellularity in ovine valve leaflets. Additionally, ovine leaflets underwent more extensive changes in relaxation post-decellularization, which corresponds to larger GAG reduction. These results stand as a firm reminder that the ovine animal model is only a model, and that studies performed in sheep or using ovine tissue may not translate perfectly to clinically studies. However, the ovine model remains an important regulatory pre-clinical animal model due to its similar calcification and immune response analogous especially to valve replacement in pediatric patients. Since human valves cannot be implanted in sheep, the characterization of decellularized valves post-processing from both species provided by this study is essential. The success of *in vivo* ovine valve replacement studies using decellularized valves has been shown and our own decellularization protocol has been validated by *in vivo* studies using similarly decellularized valves implanted in juvenile sheep.[131-133] While the ovine model provides crucial calcification information, it is also worth considering other animal models especially if unanticipated in-vivo results occur that are at variance with in-vitro predictions of performance. Porcine valves are more anatomically and mechanically similar to humans and the papio model allows implantation of human valves.[71, 141] Ultimately, the sheep model remains the gold standard for assessing vulnerability to calcification while also providing estimates of pro-thrombotic and pro-inflammatory propensities before moving into clinical trials. The combination of relevant bench assays and the sheep chronic implant model likely provides a useful and sufficient preclinical testing regimen.

3.5.6 Study Limitations

This study is not without limitation. While planar biaxial testing has emerged as a

popular method for evaluating the mechanical behavior of the heart valve leaflet, test methodologies remain unstandardized. The reference configuration for strain monitoring in this study was selected as the unloaded state prior to specimen preconditioning, as reported previously.[32] Others have selected a reference state either after the application of a small pre-load[151] or after specimen preconditioning.[111] Thus, the mechanical properties reported here are not necessarily directly comparable to those reported by other authors. However, in the context of this comparative study, the methodology selected for biaxial testing does permit comparisons to be drawn between cryopreserved and decellularized tissues. Different strategies have also been reported for specimen attachment to the biaxial test apparatus (i.e., hooks, springs, clamps). Hooks, which inherently create stress-concentrations at the discrete attachment points, were selected for the current study. This could result in non-uniform relaxation across the leaflet; however, we note that we did not visually observe evidence of transient deformation at the attachment points (e.g., gaps in the tissue developing over time) over the course of relaxation experiments. Moreover, because the same number of attachment points per side, per specimen were used over the course of the study, any effect would be consistent across all specimens tested. The placement of tissue attachment points is also important in biaxial testing.[155] Care was taken to place hooks as uniformly as possible across leaflet samples to minimize this potential source of error. We also note that the loading rate used for relaxation testing was lower than the physiologic rate; however, Doehring *et al.* found only moderate strain-rate dependence in the relaxation of heart valve leaflet tissue.[44] Additionally, Stella *et al.* reported no strain-rate sensitivity in leaflet membrane strain energy under biaxial loading.[162] Thus, given the comparative nature of this study, the methods used here were useful in determining differences in relaxation following decellularization. Finally, the standard deviation in biochemical test data

was high in some cases. This may be due to sampling, coupled with regional variation in leaflet composition. Variability could likely be reduced through the use of larger samples for each individual assay; however, the methods used here permitted the direct evaluation of multiple biochemical properties on each leaflet sample subjected to biaxial testing.

3.6 Conclusion

This study identifies key differences in the effects of decellularization on human and ovine aortic valves. Decellularization resulted in effective cell removal for both human and ovine aortic valve leaflets. Ovine leaflets exhibited significant changes in mechanical properties that were not observed in human leaflets. Further analysis identified a number of underlying causes including the loss of collagen crosslinking and greater initial cellularity in ovine leaflets compared to human. This species-specific response to decellularization highlights the importance of validating decellularization protocols for the species and tissue for which it is intended as well as the species intended for in-vivo chronic implant testing.

CHAPTER 4: COMPARISON OF CANDIDATE CELL POPULATIONS FOR THE RECELLULARIZATION OF TISSUE ENGINEERED HEART VALVES[‡]

4.1 Abstract

Heart valve tissue engineering may provide improved treatment for valvular heart disease, yet development of a tissue engineered heart valve (TEHV) has been limited by incomplete recellularization of the valve leaflets. In this study, we compare the leaflet recellularization potential of candidate cell populations after seeding onto decellularized heart valves and two weeks of bioreactor conditioning. Four cell populations were tested: bone marrow mononuclear cells (*MNC*), 5 million bone marrow mesenchymal stem cells (*MSC*), 10 million bone marrow mesenchymal stem cells (*MSC2*), and valve interstitial cells (*VIC*). *MSC2* valves demonstrated the best recellularization of the interstitial leaflet tissue as well as an appropriate cell phenotype, mechanical properties, and biochemical composition. *MSC* valves exhibited similar leaflet repopulation, yet had decreased mechanical and biochemical properties. *MNC* seeding resulted in minimal recellularization of the leaflet, though an additional time point group found cells present after three days, which seemed to disappear at two weeks. *VIC* seeding

[‡] Submitted as **VeDepo M.C.**, Buse E., Paul A., Hopkins R.A., and Converse G. L., Comparison of Candidate Cell Populations for the Recellularization of Tissue Engineered Heart Valves, *Cellular and Molecular Bioengineering*, Submitted Dec. 23, 2017.

resulted in cell clumping on the leaflet surface and poor recellularization. The results of this study suggest mesenchymal stem cells are a preferred cell population for TEHV recellularization and demonstrate the ability for repopulation of the distal valve leaflet.

4.2 Introduction

Valvular heart disease remains a significant cause of morbidity and mortality worldwide, particularly for pediatric patients with congenital valve defects.[70] The current options for valve replacement, including mechanical valves, bioprosthetic valves, and cryopreserved allografts, all have associated limitations and cannot provide the necessary remodeling or growth after implantation.[70] Therefore, pediatric patients requiring valve replacement often undergo multiple revision surgeries throughout their lifetime.[70] The tissue engineered heart valve (TEHV) may be the ideal solution for heart valve replacement acting as a one-time intervention to create living, functional tissue capable of growth and remodeling.[70]

However, a number challenges remain before realizing the TEHV. Primarily is the difficulty in establishing a phenotypically appropriate cell population within the valve leaflet tissue. Native heart valves are populated by two cell phenotypes, valve endothelial cells on the luminal surfaces and valve interstitial cells (VICs) within the tissue matrix. Decellularized heart valves implanted as bioprosthetic replacements in human and animal models have shown complete re-endothelialization of the luminal surfaces and partial recellularization of the valve interstitial tissue including the conduit and leaflet base.[48, 131] However, despite the presence of endothelial cells, the distal free-edge of the valve leaflets exhibit an absence of VIC repopulation.[48, 131] Therefore, the challenge is establishing a VIC-like population within the distal leaflet interior.

Over the years, various methodologies for cell seeding using multiple cell sources have been explored.[80, 174] Using endothelial cells, myofibroblasts, or VICs from arterial, venous, or leaflet tissue avoids cell phenotype mismatch with the native valve; however, obtaining homologous cells for clinical use is problematic.[66, 104, 161] Bone marrow derived mesenchymal stem cells (MSCs) and mononuclear cells (MNCs) have received interest as a potentially patient-specific cell source. MSCs are an attractive option because of their differentiation potential toward a VIC lineage and their immunomodulatory capabilities.[35, 52, 158] However, the preparation MSC populations prior to seeding can be a time consuming procedure.[124] MNCs are of interest due to their potential for rapid migration and inflammation-mediated native cell recruitment through paracrine signaling.[137, 178]

Despite the variety of cell sources for heart valve seeding, there have been very few direct comparisons between cell populations to evaluate the potential for valve recellularization. One of the only comparisons (Vincentelli *et al.*) utilized a direct injection technique to transplant ovine MNCs or MSCs into the annulus and arterial wall of decellularized porcine pulmonary heart valves before implantation into sheep.[175] After 4 months *in vivo,* the MNC injected group displayed thickened leaflets, increased pressure gradients, calcification, and the presence of inflammatory cells.[175] The presence of the inflammatory cells may be in line with the inflammation-mediated recellularization described previously by MNCs, although the other reported results are not encouraging and suggest a classical inflammatory response. The injection of expanded MSCs did not elicit this negative response and a limited number of α-actin positive cells were observed in the leaflet.[175] However, cells cannot be clinically localized directly within the leaflet using this method due to the potential of damage to the delicate tissue.

Therefore, the purpose of this investigation is to provide a direct comparison between seeding cell populations for their TEHV recellularization potential. MNCs, MSCs, and VICs, were tested for their ability to repopulate the interstitial leaflet tissue of decellularized heart valves following *in vitro* bioreactor conditioning. To better evaluate the MSC seeded groups, two seeding concentrations were tested, leading to a total of four tested cell populations. Although not clinically practical, VICs were included as a positive control for cell phenotype analysis. It was hypothesized that valves seeded with MSCs at the higher concentration would lead to significantly higher recellularization of the leaflet tissue compared to other groups.

4.3 Methods

4.3.1 Tissue and tissue processing

Ovine aortic valves were harvested from juvenile sheep under approved IACUC protocols and in accordance with Guide for Care and Use of Laboratory Animals (National Institutes of Health Publication No. 85-23). Harvested valves were cryopreserved using a procedure modeled after clinical tissue handling protocols. Valve were frozen at 1 °C min^{-1} using a controlled rate freezer (2100 Series, Custom BioGenics Systems) then stored at -180 °C. Valve decellularization was performed as described previously.[133] Briefly, the valves were thawed and subjected to reciprocating osmotic shock, followed by detergent (Triton X-100, sodium-lauroyl sarcosine) and enzymatic (Benzonase®) washes to remove cellular material. Extraction of organic material was performed using recirculating water and ion exchange resins. After decellularization, the valves were again cryopreserved as described and stored at -180 °C until seeding.

4.3.2 Seeding cell populations

The decellularized ovine aortic valves were randomly divided into four groups for seeding: human MNCs (*MNC* group), human MSCs at a dose of either 5 million (*MSC* group) or 10 million (*MSC2* group) cells per valve, or human VICs (*VIC* group). Cell populations for MNC and MSC seeded valves were isolated from 25 mL human bone marrow aliquots obtained from a commercial source (Lonza) using a bone marrow filter system (Kaneka).[98] For MNC seeding, the entire mononuclear cell population was isolated from bone marrow and used for valve seeding. For seeding with MSC populations, mononuclear cells were filtered from bone marrow and the mesenchymal stem cell fraction was isolated through cell culture until sufficient cells were available. VICs were isolated from human aortic valve leaflets. Briefly, aortic valve leaflets were dissected, minced, and placed in a cell culture flask to allow the outgrowth of VIC cells. After sufficient proliferation, VICs were cryopreserved and stored at -180 °C

4.3.3 Valve seeding and conditioning

For each cell seeding group, the tissue engineered heart valves were seeded following established protocols.[34] Decellularized valves were thawed from cryopreservation and sutured onto tissue grips. The seeding cell population for each group was then suspended in 10 mL of media and seeded into the lumen of the valve which was mounted in a static bioreactor chamber containing 200 mL valve media (DMEM F12 (Life Technologies) and 10% human serum (Sigma-Aldrich)). After cell seeding, all groups underwent the same bioreactor conditioning protocol starting with 24h of static culture (37 °C, 5% CO_2) to allow cell adhesion. Valves were then transferred to a dynamic bioreactor chamber containing 500 mL valve media and were conditioned for 24h under cyclic negative pressure (-20 to 5 mmHg), followed by 24h of cyclic low positive pressure (-5 to 20 mmHg), and finally 2 weeks of cyclic high positive pressure (-5 mmHg to 120 mmHg).[34] A media change was performed on all valves after 1 week of high

positive pressure, wherein half of the bioreactor media (250 mL) was removed and replaced with 250 mL of fresh valve media. Following bioreactor conditioning, the valves were removed and dissected for analysis, including histology, immunohistochemistry (IHC), real time PCR (rt-PCR), biomechanical testing, and biochemical analysis.

After analysis of the *MNC* group revealed minimal cell infiltration, an additional sub-group was added which was seeded similarly and then conditioned in the bioreactor for only 3 days (*MNC short)* (24h static, 24h negative pressure cycles, and 24h high pressure cycles). The purpose was to elucidate temporal changes in the cell population, since previous experience has seen moderate leaflet recellularization with seeded MNCs.[33] After conditioning, the *MNC short* term valves were analyzed by histology, IHC, and PCR. *MNC short* valves were not included in the mechanical or biochemical analyses since significant changes were not expected so quickly.

4.3.4 Histology, IHC, & PCR

Samples for histology were sectioned along the radial plane of each leaflet from the valves of each group. Hematoxylin and eosin (H&E) staining was used to evaluate repopulation of the decellularized valve leaflets, specifically by the presence of cells within the leaflet tissue and on the leaflet surface. Protein expression of the seeded cells was evaluated by IHC. Unstained slides were blocked in 10% normal goat serum for 1 hour before overnight incubation at 4 °C with 1:100 diluted primary antibodies. The primary antibodies (Abcam) targeted alpha smooth muscle actin (aSMA), heat shock protein 47 (HSP47), vimentin (VIM), CD90, CD68, CD271, CD34, and CD45. Fluorescent secondary antibodies (Alexa Fluor 488 or Alexa Fluor 594; Life Technologies) were then incubated for 1 h followed by nuclear counterstaining (DAPI; Life Technologies).

Gene expression in the cell populations prior to seeding and after 2 weeks of conditioning was analyzed by rt-PCR. Pre-seeding cell samples were taken immediately before seeding. Post-seeding tissue samples were isolated from each leaflet during valve dissection and immediately frozen in liquid nitrogen before being pulverized. Tissue samples from each leaflet of the valve were combined to form one sample to measure overall gene expression across the valve. RNA was isolated using the RNeasy Micro Kit (Qiagen) and then reverse transcribed to cDNA using the High Capacity cDNA Reverse Transcription Kit (Invitrogen). rt-PCR (7300 RT-PCR system, Applied Biosystems) was performed using a custom phenotyping array (TaqMan, Life Technologies). PCR data is conveyed as the relative fold change in gene expression of the cells from tissue samples compared against the matched pre-seeding cell population. Data is presented as the mean relative fold change of all valves within a group (n=3) with standard deviation error bars.

4.3.5 Mechanical testing

The mechanical behavior of the leaflet tissue from the *MNC, MSC, MSC2*, and *VIC* groups was measured by biaxial loading. *MNC short* seeded valves were not tested. Biaxial mechanical testing was performed in phosphate buffered saline at 37 °C using methods described previously.[32] Rectangular specimens (9 x 6 mm, n=9) were cut from the middle belly region of each leaflet and mounted onto a four motor equibiaxial loading system (LM1 TestBench, Bose ElectroForce) with the radial and circumferential directions of the sample aligned to the loading axes. Samples were then loaded to an equibiaxial tension of 30 N/m with a rise time of 10s and the peak stretch ratios were calculated from strain data in the circumferential (λ_C^{peak}) and radial (λ_R^{peak}) directions. Areal strain was used as a measure of net extensibility and was calculated

from stretch data as (λ_C^{peak} x λ_R^{peak} – 1) x 100%. Results were compared against biaxial mechanical data previously reported from cryopreserved and decellularized valves.[173]

4.3.6 Biochemical analysis

The sulfated glycosaminoglycan (GAG), collagen, and total protein concentrations of the extracellular matrix of seeded valves was measured using colorimetric assays. GAG concentration was measured using the Blyscan Sulfated Glycosaminoglycan Assay (Biocolor). Tissue samples (approx. 15 mg; n=9) were processed according to manufacturer protocols and the results were measured using a spectrophotometer at 656 nm. Collagen concentration was measured using the QuickZyme Total Collagen Assay (QuickZyme Biosciences). Samples (approx. 15 mg, n = 9) were prepared by overnight hydrolysis in 6M HCl at 90 °C and the hydroxyproline concentration was measured using a UV/Vis spectrophotometer at 570 nm. Total protein concentration was measured using the QuickZyme Total Protein Assay (QuickZyme, Biosciences) and used the same hydrolysates that were prepared for collagen quantification. The GAG, collagen, and total protein concentrations are reported as μg mg^{-1} of wet tissue and are compared to previously reported values from cryopreserved and decellularized valves.[173]

The production of signaling molecules such as cytokines and chemokines from the cells of the seeded tissue engineered valves was quantified using a multiplex (Luminex) assay in accordance with manufacturer protocols. Media samples (n= 3 to 6) were taken at the end of bioreactor conditioning (2 weeks of high positive pressure) and frozen at -80°C until use. The multiplex assay identified the media concentration of FGF-2, IL-10, IL-6, MCP-1, MIP-1α, MIP-1β, TNFα and VEGF.

4.3.7 Statistical analysis

Statistical analysis was performed by ANOVA, and post-hoc comparisons were made using the Tukey test or the Kruskal-Wallis test for parametric and non-parametric data, respectively. Differences were considered statistically significant at $p < 0.05$.

4.4 Results

4.4.1 Tissue Processing

As demonstrated previously, the decellularization process resulted in complete removal of cells from the valve tissue while preserving the overall architecture of the extracellular matrix (data not shown).[32, 173] Following cell seeding and bioreactor conditioning, the valves in all groups had a normal appearance with complete and functional leaflets.

4.4.2 Histology

H&E staining of the seeded valve groups revealed differing levels of recellularization after two weeks of bioreactor culture (**Figure 1**). *MNC* seeded valves had minimal recellularization with isolated cells present only on the surface of the leaflet while the interstitial matrix remained acellular (**Figure 1 A,E**). *MSC* seeded valves showed recellularization of the leaflet matrix with a high density of cells within the leaflet matrix, though multilayered clumps of cells were present on the leaflet surface (**Figure 1 B,F**). It is worth noting that the recellularization was limited to the distal region of the leaflet, while the mid and base of the leaflet had very little cells present within the leaflet or on the surface. *MSC2* seeded valves showed similar recellularization to the *MSC* group and interestingly appeared to have less cell clumping present on the valve surface (**Figure 1 C,G**). Again, the recellularization of the *MSC2* group was primarily within the distal leaflet region. Valves seeded with *VICs* showed high

cellularity and clumping of cells on the valve surface but very little to no cellular infiltration into the leaflet interstitium (**Figure 1 D,H**).

4.4.3 Cell phenotypes

The protein expression of the seeded cells on the tissue engineered valve leaflets was evaluated by IHC (**Figure 2**). Cells from the *MNC* group were notably negative for αSMA and CD90, but showed slight positive expression of HSP47, VIM, and CD68 (**Figure 2 A,E,I**). The *MSC* and *MSC2* groups had similar protein expression and stained positive for αSMA, HSP47, VIM, and CD90, though the *MSC2* group appears to have greater protein expression (**Figure 2 B,F,J;C,G,K**) . The cells of the *VIC* group were positive for HSP47, CD90, and VIM while interestingly remained negative for αSMA, the classical marker pattern for activated VICs (**Figure 2 D,H,L**).

The gene expression of the cells from the seeded heart valves was measured by rt-PCR and evaluated as the relative fold change compared to the respectively matched, pre-seeded cell population (**Figure 3**). Valves from the *MNC* seeded group showed an up-regulation of the myofibroblast marker αSMA (ACTA2), stem cell type markers (ITGB1, SERPINH1, THY1), and markers of extracellular matrix remodeling (COL1A1, MMP1). *MNC* seeded valves also showed a general down-regulation of immune cell markers (CD14, CD163, CD4, IFNG, PTPRC) with the exception of CD206, a marker for M2 macrophages. The cells from the *MSC* group showed relatively small changes in gene expression with a general down-regulation in immune cell gene markers (CD14, CD163, CD4, PTPRC). The relative gene expression of *MSC2* valves was generally similar to the *MSC* valves, though a greater up-regulation of MMP1 was observed. The *VIC* group displayed an interesting gene expression profile with slight up-regulation of MMP1 but down-regulation of ACTA2 and COL1A1.

4.4.4 Mechanical Analysis

Biaxial testing of the tissue engineered leaflets revealed significant differences in the areal strain and directional stretch ratios between the cell seeding groups (**Table 1**). The collected data were compared to previously reported data for cryopreserved and decellularized ovine aortic valve leaflets, which act as a positive and negative control respectively.[173] Interestingly, the areal strains of *MNC* leaflets were most similar to cryopreserved leaflets (i.e. with native cells) when compared to the other tested groups, and significantly different than decellularized ($p = 0.006$), *MSC* ($p = 0.021$) and *VIC* ($p = 0.045$) groups; no significant differences were found in circumferential or radial stretch ratios between *MNC* valves and other groups. On the other hand, *MSC* seeded leaflets appeared to be most mechanically similar to decellularized leaflets when compared to other groups and were found to have significantly greater areal strain ($p = 0.024$) and circumferential stretch ($p = 0.004$) than cryopreserved leaflets. Leaflets from the *VIC* seeded group revealed no significant differences between the cryopreserved and decellularized groups, though the average properties of the *VIC* leaflets was much closer to those of the decellularized leaflets. Similarly, no significant differences in mechanical properties were found between the *MSC2* group and the cryopreserved or decellularized groups, however the areal strain and circumferential stretch ratio of the *MSC2* group was medial to the control groups.

4.4.5 Biochemical Analysis

The concentrations of GAG, collagen, and total protein in the seeded valve leaflets were measured and compared to previously reported data for cryopreserved and decellularized ovine aortic leaflets (**Table 2**).[173] The previously reported data indicated a significant loss of GAG between cryopreserved and decellularized samples. However, no other significant differences

were found in GAG concentration between other groups in this study. The average GAG concentration of all tissue engineered leaflets was within the bounds of the reported cryopreserved and decellularized concentrations. Conversely, the concentration of collagen was similar between cryopreserved and decellularized groups, yet all tissue engineered groups (*MNC, MSC, MSC2,* and *VIC*) had a significantly increased collagen concentration than either control group ($p < 0.05$). The total protein concentration in all cell seeded groups was greater than either cryopreserved or decellularized groups, although only the *MSC2* group was significantly different ($p < 0.05$).

The production of cytokines by the seeded valves was measured by analyzing the culture media after the two week culture period using multiplex assays (**Figure 4**). Cytokines were measured to estimate the potential for inflammation and/or cell recruitment. The selected cytokines represent a mix of classic inflammation signaling proteins representing an M1 macrophage response (IL-6, MIP-1α, MIP-1β, TNFα) and an assortment of tissue repair signaling proteins associated with an M2 macrophage response (FGF-2, IL-10, MCP-1, VEGF). Of the cytokines measured, IL-6, MCP-1 and VEGF were produced to the greatest concentration by all cell seeded groups. *VIC* seeded valves produced an exceptionally high amount of IL-6 compared to other valves, and a significantly greater amount than *MNC* or *MSC* seeded valves ($p < 0.05$). Similarly, *VIC* seeded valves produced more MCP-1 than the other seeded groups, and a significantly greater amount than *MSC* or *MSC2* seeded valves ($p < 0.05$). The highest VEGF concentration was produced by *MSC2* seeded valves, though there was no significant difference between any groups and there was a large variance within the *MSC2* samples. FGF2 production was relatively similar across all groups. Of the classic inflammatory signaling proteins, *MNC* valves produced higher concentrations compared to other groups. IL-10 production was greatest

in *MNC* valves and was significantly greater than the *MSC* group ($p < 0$ .05). MIP-1α and MIP-1β was also greatest in the *MNC* valves and significantly greater than the *MSC2* group ($p < 0.05$). TNFα is not included in **Figure 4** because it was below the detection limit (2.15 pg/mL) in all but one *MNC* sample, which had a TNFα concentration of 5.81 pg/mL.

4.5 Discussion

4.5.1 MNC Valve Seeding

Valves in the *MNC* group exhibited surprisingly minimal leaflet recellularization. The lack of recellularization is particularly unexpected due to the seemingly positive effect that MNC seeding had on the mechanical and biochemical properties. *MNC* valves exhibited mechanical properties most similar to cryopreserved valves (i.e. native control) compared to the other groups and the increased collagen in *MNC* valves compared to decellularized valves indicated an active cell presence during bioreactor culture. Furthermore, previous experience within our group has seen the establishment of pilot cell populations within the leaflet matrix after only three days when seeding with MNCs.[33] To investigate the short-term fate of the MNC seeded cells within this study, three additional decellularized ovine aortic valves were seeded with human MNCs and cultured in the bioreactor for three days (*MNC short*). Interestingly, histology of the *MNC short* group revealed a cell population present within the leaflet matrix (**Figure 5 A-D**). The cells were located only within the fibrosa layer of the leaflet and were not continuous, but appeared in small clusters along the length of the leaflet. IHC staining revealed the cells stained positive for CD68, CD34, or CD45 (**Figure 5 E-H**). rt-PCR of the *MNC short* valves was similar to the *MNC* two week conditioned valves, except for a general up-regulation of classic inflammatory genes compared to the pre-seeding population, specifically CD163, CD14, and TNFα.

Taken together, the *MNC short* and *MNC* valves show an evolving cell phenotype and population throughout the bioreactor culture period. Following MNC seeding, recellularization readily occurs within the fibrosa layer by macrophages, leukocytes, and hematopoietic cells. As bioreactor culture continues, those cells likely migrate or undergo cell death leading to isolated cells on the leaflet surface by two weeks. The cells remaining at two weeks were positive for CD68, HSP47, and VIM, indicating a mix of macrophage and fibroblastic phenotypes. The fibroblastic cells likely originate from the proliferation of the small population of stem cells found within bone marrow.[3] The evolving cell phenotype is supported by the rt-PCR data that shows an up-regulation of the ACTA2, SERPINH1, and THY1 genes in the *MNC* valves compared to the pre-seeding cells, although it is worth nothing there was no positive staining for CD90 or CD271 during IHC. Despite the proliferation of the stem cell population, after two weeks of bioreactor culture the leaflet interstitial tissue remained acellular indicating cell proliferation was not occurring quickly enough to repopulate the leaflet. Therefore, MNC seeding and two weeks of bioreactor culture is an impractical approach for *in vitro* TEHV recellularization as a stand-alone method.

An alternative approach may be seeding MNCs to establish a pilot cell population that can stimulate autologous recellularization *in situ*. Weber *et al.* demonstrated seeded MNCs are capable of inducing an inflammation-mediated recellularization response in polymeric heart valve scaffolds.[178] Roh *et al.* further identified that the mononuclear cells produce the signaling cytokine MCP-1, which induces the recellularization response.[137] In this study, we found the *MNC* valves produced moderate amounts of MCP-1. Although cytokine production was not measured for *MNC short* valves, it was demonstrated that MNCs can rapidly establish within the leaflet tissue and may be producing signaling cytokines much earlier than measured here. Future

investigations should investigate the temporal cytokine production of MNC seeded valves and the potential for autologous cell recruitment *in situ*.

4.5.2 MSC and MSC2 Valve Seeding

Seeding with MSCs led to the most successful recellularization of the interstitial matrix of the decellularized leaflets. Surprisingly, the difference in the seeding cell concentrations, 5 million cells for the *MSC* group versus 10 million cells for the *MSC2* group, did not lead to greatly differing degrees of recellularization (**Figure 1**). In fact, no significant differences were directly measured between the *MSC* or *MSC2* groups by any metric in this study. However, a number of dissimilarities can be inferred based on the significant differences measured between other groups. For example, the areal strain and circumferential stretch ratio of *MSC* valves was similar to decellularized valves and significantly different than cryopreserved valves, indicating that cell seeding in the *MSC* group had little to no effect on the mechanical properties. Alternatively, the *MSC2* group showed statistically similar mechanical properties to both decellularized and cryopreserved valves, indicating *MSC2* seeding had a small effect on mechanical properties. The concentrations of GAGs, collagen, and total protein was also similar between *MSC* and *MSC2* group, yet *MSC2* had significantly more total protein than either decellularized or cryopreserved valves, signifying increased protein production. IHC revealed similar protein expression between the *MSC* and *MSC2* groups, yet the staining intensity appears greater in the *MSC2* group. Comparing the *MSC* and *MSC2* groups indicate it is advantageous to seed with the higher concentration of MSCs.

Overall, these results suggest seeding with MSCs leads to better recellularization of TEHV compared to MNCs after two weeks of bioreactor culture. MSCs have shown great potential as a cell source for heart valve tissue engineering, due in part to their pluripotent

differentiation and naturally myofibroblastic phenotype similar to native VICs.[52] Additionally, MSCs possess immunomodulatory capabilities that may help reduce inflammation.[35, 158] However, the use of MSCs may raise some concerns since their multi-lineage potential can lead to the differentiation of adverse phenotypes, including osteoblasts, chondrocytes, and/or adipocytes.[52] Before the clinical application of MSC seeded devices can be realized, the underlying factors leading to cell differentiation in valve tissues must be understood and controlled so as to avoid adverse differentiation.

4.5.3 VIC Valve Seeding

Due to the difficulty in obtaining a patient matched VIC population, seeding TEHVs with autologous VICs is not a clinically viable solution. Despite this, the VIC group was included in this study under the expectation that VIC seeded valves would lead to moderate recellularization and provide an internal positive control for cell phenotype analysis. However, the *VIC* group of valves showed surprisingly minimal recellularization of the leaflet interstitial tissue and cells remained clumped on the leaflet surface. Also surprising was the lack of αSMA expression by the cells in the *VIC* group.[105]

Valve interstitial cells in a healthy, native valve remain quiescent (qVIC) until damage or injury to the valve requires repair, at which point they become activated (aVICs) and are identified by their expression of αSMA.[105] aVICs are responsible for remodeling the extracellular matrix and αSMA is often used as a marker for the VIC phenotype in tissue engineering applications since matrix remodeling is a basic requirement for a functioning TEHV. After repairing valve damage, aVICs should return to a quiescent state, but it is worth noting that prolonged VIC activation is linked to valve disease including fibrosis, inflammation, and ultimately calcification.[105]

In this study, we found VIC seeded valves did not express αSMA. We expected the seeded VICs to express an activated phenotype and begin remodeling the decellularized matrix, yet it appears the VICs remained quiescent. The apparent qVIC phenotype may explain the lack of cell infiltration in the *VIC* group since the cells may not have produced matrix remodeling proteins, such as MMPs, which would break down surrounding tissue matrix. The extracellular matrix of the valve leaflets appears compact and cells may be unable to infiltrate the leaflet without the expression of matrix remodeling proteins. Hof *et al.* similarly reported an absence of cellular infiltration after seeding VICs onto decellularized leaflet tissue due to the presence of a compact basement membrane.[67] To increase the penetrability of the leaflets, Hof *et al.* performed laser perforation or enzymatic digestion by trypsin and found laser perforation treatment led to marginal cell infiltration while trypsin treatment led to increased infiltration.[67] However, trypsin digestion led to structural alterations in the leaflet matrix, and is therefore not a clinically viable treatment option for decellularized valves.[67] In addition to the clinical impracticality of seeding valves with autologous VICs, the results of this study, and others, suggest that VIC seeding leads to poor recellularization of the leaflet tissue and is likely not applicable for the TEHV.

4.5.4 Limitations

While this study provides fundamental information regarding candidate cell populations for heart valve seeding, it is not without limitations. For example, the *in vitro* nature of this study eliminates the tissue healing milieu that is expected *in vivo*. As such, a number of factors could not be included in this study which may change the recellularization potential of the cell populations, including paracrine and endocrine signaling, the presence of local tissue repair cells, and possible inflammatory responses. Therefore, the results of this study are simply guidelines, and set the stage for future *in vivo* experiments to further elucidate TEHV recellularization.

Additionally, this study only investigated most groups at an arbitrary time point of two weeks. As evidenced by the *MNC short* group, recellularization likely changes throughout the culture period and future studies should investigate the time response curve of cell populations to further enhance recellularization.

4.6 Conclusion

This investigation was designed to provide a direct comparison of candidate cell populations for heart valve tissue engineering. We compared four different cell populations for their ability to repopulate the distal leaflet of decellularized heart valves after two weeks of *in vitro* bioreactor culture. We found that seeding with MSCs at a higher concentration delivered the best results as demonstrated by recellularization of the interstitial leaflet tissue, cell phenotype, mechanical properties, and biochemical analysis. Seeding with MSCs at a lower concentration exhibited similar leaflet repopulation, yet the mechanical and biochemical analysis were not as encouraging. MNC seeding led to minimal recellularization though an additional time point group demonstrated a cellular presence at only three days. VIC seeding resulted in cell clumping on the leaflet surface but poor recellularization of the interstitial tissue. These results confirm the hypothesis that of the tested groups, MSCs are best suited for bioreactor *ex vivo* TEHV recellularization.

CHAPTER 5: EXTENDED BIOREACTOR CONDITIONING OF MONONUCLEAR CELL SEEDED HEART VALVE SCAFFOLDS[§]

5.1 Abstract

The tissue engineered heart valve may be the ideal valve replacement option but still must overcome challenges in leaflet recellularization. This study sought to investigate the potential for leaflet matrix restoration and repopulation following MNC seeding and extended periods of bioreactor conditioning. Human aortic heart valves were seeded with MNCs and conditioned in a pulsatile bioreactor for 3 days, 3 weeks, or 6 weeks. The results of this study determined that an MNC population can be readily localized within the leaflet tissue in as little as 3 days. Furthermore, as extended bioreactor condition continued to the 3 week and 6 week time points the MSC sub-fraction within the larger MNC population proliferated and became the predominant cell phenotype. However, repopulation of the leaflet interstitium was less extensive than anticipated. Valves in the 6 week time point also exhibited retracted leaflets. Thus, while the 3 week bioreactor conditioning period used in this study may hold some promise, a bioreactor

[§] Submitted as **VeDepo M.C.**, Buse E., Quinn R., Hopkins R.A., and Converse G. L., Extended Bioreactor Conditioning of Mononuclear Cell Seeded Heart Valve Scaffolds, *Journal of Tissue Engineering*, Submitted Dec. 22, 2017.

conditioning period of 6 weeks is not a viable option for clinical translation due to the negative impact on valve performance.

5.2 Introduction

Heart valve disease is a common cause of global morbidity with etiologies ranging from congenital to degenerative.[61] Although a variety of options are available for heart valve replacement, including mechanical valves, bioprosthetic xenografts and cryopreserved homografts, the ideal heart valve substitute has yet to be developed.[70] The tissue engineered heart valve (TEHV) offers great potential as a permanent valve substitute for disorders requiring valve replacement, overcoming the limitations of the other replacement options. This is particularly true for the pediatric population for which an initial intervention using a living, growing valve would eliminate the need for multiple revision surgeries and catheter interventions as the child matures.[70] However, logistical and regulatory challenges have hindered the development of a clinically useful TEHV, including the selection of an appropriate cell line for scaffold repopulation. The ideal cell source should 1) be patient specific and readily available in the clinical setting, 2) require minimal manipulation prior to scaffold seeding and 3) offer the potential for phenotypically appropriate scaffold repopulation, either through direct proliferation of the seeded cells (prior to or following implantation) or through chemotactic recruitment of autologous cells (following implantation).[66, 80, 103]

Traditional approaches to heart valve tissue engineering have generally employed extended periods of cell culture and valve conditioning in custom bioreactors with the aim of creating end-stage living tissue *ex vivo* before theoretical or animal implantation. These approaches have used numerous cell types and sources including endothelial cells and myofibroblasts, often isolated from arterial, venous or leaflet tissue.[66, 110, 147, 161] Despite varying

degrees of success in the research arena, clinical application of these cell sources is challenged by donor site morbidity from cell harvest. Bone marrow mesenchymal stem cells (MSCs) are an alternative option for valve seeding providing autologous cells with pluripotent differentiation capabilities.[52] However, considering the low proportion of MSCs within bone marrow (0.002-0.02%), lengthy periods of *in vitro* cell expansion are required prior to valve seeding to ensure adequate cell coverage.[3]

Another option, bone marrow derived mononuclear cells (MNCs), are beginning to receive interest as a candidate for scaffold seeding. A group of European researchers has reported on the seeding of polymeric heart valve scaffolds with MNCs using fibrin as a cell carrier.[55, 146, 178] This strategy relies on the migration of seeded cells from the fibrin carrier into the polymer scaffold after implantation, followed by further recruitment of autologous cells through a paracrine signaling mechanism. Four weeks after implantation of these scaffolds in primates, seeded MNCs were no longer present; however, the presence of autologous endothelial and interstitial cells was observed.[55, 146, 178] Work by Roh *et al.* provides further evidence that a "pilot" population of MNCs may act to recruit autologous cells, as the authors reported that MNCs seeded on polymeric vascular grafts prior to implantation in mice were no longer detectable after only one week *in vivo*, though overall cellularity was maintained due to the infiltration of autologous monocytes followed by scaffold repopulation with host smooth muscle cells and endothelial cells.[137]

Of particular interest when seeding with MNCs is the persistence of MNC subpopulations, such as MSCs, macrophages and leukocytes, throughout extended conditioning periods. Since MSCs are commonly isolated from bone marrow through cell culture, it is possible that MNC seeding and extended culture will lead to expansion of the MSC population,

effectively skipping traditional cell culture methods. Additionally, all afore mentioned studies seeding with MNCs have used animal implant models to assess the potential for autologous recellularization, yet the outcome of a seeded MNC population throughout extended *ex vivo* valve conditioning remains unknown. Therefore, the purpose of this study is to investigate the fate of a MNC population seeded onto decellularized heart valves over an extended period of *ex vivo* processing. We have previously shown the ability to localize an MSC population into the leaflet matrix of a decellularized valve scaffold using a novel bioreactor and pressure conditioning. Using similar methods, it is expected that the seeded MNCs in this study will localize within the leaflet tissue of the decellularized valves and extended conditioning will lead to proliferation of the MSC population.

5.3 Methods

5.3.1 Tissues and tissue processing

Human aortic valves were obtained from a tissue banking facility (LifeNet Health) and stored in a cryopreserved state until use. The cryopreservation procedure is modeled after clinical tissue handling protocols and freezes the valves at 1 °C min^{-1} using a controlled rate freezer (2100 Series, Custom BioGenics Systems) before being stored in a cryofreezer at -180 °C. Decellularization was performed as described previously.[133] Briefly, aortic valves were subjected to reciprocating osmotic shock, followed by detergent (Triton X-100, sodium-lauroyl sarcosine) and enzymatic (Benzonase) washes to remove cellular material. Extraction of organic material was performed using recirculating water and ion exchange resins. After decellularization, the valves were again cryopreserved using the above procedure and stored at -180 °C until valve seeding.

5.3.2 Cells and valve seeding

Human bone marrow was obtained from a commercial source (Lonza) and the mononuclear cell fraction was isolated using a bone marrow filter system (Kaneka).[98] The decellularized valves were thawed from cryopreservation and then seeded with the entire mononuclear fraction isolated from the bone marrow using an established protocol.[34] Briefly, isolated mononuclear cells were suspended in 10 mL of media and seeded into the lumen of the valve which is mounted in a static bioreactor chamber containing valve media (DMEM F12 (Life Technologies) and 10% FBS). After introduction of the cells, the seeded valve was incubated in static culture (37 °C, 5% CO_2) for 24h to allow cell adhesion.

5.3.3 Valve bioreactor conditioning

After 24h static culture, the seeded valve was transferred to a pulsatile bioreactor chamber containing valve media and the assembly was placed in a linear actuator to create cyclic positive and negative pressure profiles within the bioreactor chamber. In all groups, the valves were cultured in a cyclic negative pressure profile (-20 to 5 mmHg) for 2 days, after which the 3 day group (1 day static + 2 days negative; n = 6) of valves were removed from culture and the valve leaflets were dissected for analysis. The remaining two groups were then switched to cyclic positive pressure profile (-5 to 50 mmHg) and cultured for an additional 18 days (3 week group; n = 6) or 39 days (6 week group; n = 3) before dissection and analysis. Upon dissection, samples from the valve leaflets were designated for mechanical testing and biochemical assays or histology, immunohistochemistry (IHC), and real-time PCR (rt-PCR) analysis.

5.3.4 Histology, IHC, and PCR

Samples for histology were sectioned along the radial plane of the leaflets from the 3 day, 3 week, and 6 week conditioned valves. Hematoxylin and eosin (H&E) staining was used to evaluate repopulation of the decellularized valve leaflets, specifically by the presence of cells within the leaflet tissue and on the leaflet surface. Movat's Pentachrome staining was used to evaluate the biochemical composition of the leaflet extracellular matrix. Protein expression of the seeded cells was evaluated by IHC. Unstained slides were blocked in 10% normal goat serum for 1 hour before overnight incubation at 4 °C with 1:100 diluted primary antibodies. The primary antibodies (Abcam) targeted alpha smooth muscle actin (aSMA), heat shock protein 47 (HSP47), CD29, CD90, CD45, CD34, CD68, and vimentin (VIM). Fluorescent secondary antibodies (Alexa Fluor 488 or Alexa Fluor 594, Life Technologies) were then incubated for 1 h followed by nuclear counterstaining (DAPI; Life Technologies).

Gene expression was measured by rt-PCR analysis was evaluated as the relative fold change in gene expression compared to the pre-seeding cell population. Cell samples were taken immediately before valve seeding and tissue samples from each leaflet were taken during valve dissection and frozen in liquid nitrogen. The leaflet tissue from each valve was combined to form one sample (n=3 per group) to indicate the gene expression across the valve. The frozen tissue was pulverized and the total RNA was isolated using the RNeasy Micro Kit (Qiagen) accompanied by DNase digestion (DNA-freeTM kit, Invitrogen). The RNA was then reverse transcribed to cDNA using the High Capacity cDNA Reverse Transcription Kit (Invitrogen). rt-PCR (7300 RT-PCR system, Applied Biosystems) was performed using a custom phenotyping array (TaqMan, Life Technologies). PCR data is conveyed as the relative fold change in gene expression between the matched, pre-seeding cell population and the cell population in the valve after bioreactor conditioning.

5.3.5 Mechanical Testing

The mechanical behavior of the leaflet tissue from the 3 day group and 3 week group of tissue engineered valves was measured using biaxial loading. The 6 week group of tissue engineered valves was not included for mechanical testing due to the lack of coaptation between leaflets. Biaxial mechanical testing was performed using methods described previously.[32] Rectangular specimens (9 x 6 mm, n=9) were cut from the belly region of each leaflet and mounted on a four motor equibiaxial loading system submerged in phosphate buffered saline at 37 °C (LM1 TestBench, Bose ElectroForce). Samples were mounted so that the loading axes were aligned with the radial and circumferential directions of the sample. All samples were then loaded to an equibiaxial membrane tension of 60 N/m using a rise time of 10 sec. The directional peak stretch ratios were calculated from strain data in the circumferential (λ_C^{peak}) and radial (λ_R^{peak}) directions. Areal strain was used as a measure of net extensibility and was calculated from equibiaxial data as (λ_C^{peak} x λ_R^{peak} – 1) x 100%. Results were compared against previously reported biaxial mechanical data from cryopreserved and decellularized valves.[173]

5.3.6 Biochemical

The collagen and sulfated glycosaminoglycan (GAG) concentrations of the tissue engineered leaflet extracellular matrix from the 3 week group and 6 week group was measured using colorimetric assays. The QuickZyme Total Collagen Assay (QuickZyme Biosciences) was used to measure the collagen concentration. Samples (approx. 15 mg, n = 9) were prepared by overnight hydrolysis in 6M HCl at 90 °C then prepared following the manufacturers protocol. The hydroxyproline concentration was measured using a UV/Vis spectrophotometer (VERSAmax, Molecular Devices) at 570 nm. The GAG concentration was measured using the Blyscan Sulfated Glycosaminoglycan Assay (Biocolor). Tissue samples (approx. 15 mg, n=9)

were processed according to manufacturer protocol and the results were measured using a UV/Vis spectrophotometer at 656 nm. The collagen and GAG concentrations are reported as μg mg^{-1} of wet tissue.

5.3.7 Statistical Analysis

Statistical analysis of normally distributed data was performed using one-way analysis of variances (ANOVA) (SigmaStat 3.5, Systat Software, Inc.) and post-hoc comparisons between groups were performed using the Holm–Sidak test. Differences were considered statistically significant at $p < 0.05$. Error values are reported as the standard deviation of the mean.

5.4 Results

5.4.1 Tissue Processing and Valve Seeding

As observed in previous studies, decellularization resulted in complete removal of cells from the valve tissue while preserving the overall extracellular matrix architecture (data not shown).[173] Following MNC cell seeding and bioreactor conditioning, the gross appearance of the aortic valves in the 3 day group and 3 week group was normal with functional leaflets capable of coaptation. Valves in the 6 week were incompetent due to retracted leaflets, though otherwise appeared normal.

5.4.2 Histology

Extended conditioning in the bioreactor of the MNC seeded heart valves led to differences in the recellularization of the valve leaflets, as seen by histology (Figure 1). Three day processing (1 day static and 2 days negative pressure) led to localization of cells within the interior of the leaflet tissue, though no cells were present of the surface of the leaflet (Fig. 1A,B).

After three weeks processing (1 day static, 2 days negative pressure, 18 days positive pressure), cells were still present within the leaflet tissue as well as on the surface of the leaflet (Fig. 1D,E). The cells on the surface of the 3 week group were often multilayered and clumped together. After six weeks of bioreactor conditioning (1 day static, 2 days negative pressure, 39 days positive pressure) there was a decrease in the number of cells within the leaflet tissue, though more cells were present on the leaflet surface (Fig. 1G,H). Similar to the 3 week group, the cells on the surface of the leaflets in the 6 week group were multilayered and clumped together. Movat's Pentachrome staining revealed the preservation of collagen, GAG, and elastin within the ECM for all bioreactor conditioning time points (Fig. 1C,F,I). Additionally, there was evidence of collagen production by the seeded cells in the 6 week group (Fig. 1I).

5.4.3 Protein and Gene Expression

IHC revealed a changing cell phenotype with extended periods of bioreactor conditioning (Figure 2). Previous work has shown that a MNC population isolated from bone marrow initially consists of macrophages, leukocytes, hematopoietic stem cells, and a small population of mesenchymal stem cells (MSCs) [3]. In this study, the cells on the 3 day group of seeded valves had protein expression that closely resembled the profile expected from isolated MNCs. Specifically, cells seeded on the 3 day group had positive expression of CD34 and CD68, partial expression of αSMA, HSP47, and VIM, and notably were negative for CD29 and CD90 (Fig. 2A-E). As the duration of bioreactor conditioning increased to 3 weeks the protein expression began to more closely resemble a MSC population (Fig. 2 F-J). Compared to the 3 day group, the 3 week group had increased expression of αSMA, CD90, and CD34 with decreased expression of CD68. The protein expression in the 6 week group further resembled an MSC

population with a high expression of HSP47, greater expression of αSMA, CD90, and VIM, and decreased expression of CD68 and CD34 (Fig. 2 K-O).

Gene expression by rt-PCR analysis agreed with the changing phenotype observed by IHC (Figure 3). The cells in the 3 day group showed up regulation of immune responsive cells compared to the initial seeding population (ANPEP, CD14, CD44, CD68, ICAM1, and PTPRC) and little to no up regulation of MSC or VIC related markers. However, with increased bioreactor conditioning the valves in the 3 week and 6 week groups had generally increased regulation of the MSC or VIC related markers compared to the seeding population (ACTA2, ITGB1, MCAM, NT5E, SERPINH1, and THY1). Additional gene markers were not displayed in Figure 3 because they had no expression in either the cells or the tissue. These include ADIPOQ, CD19, CD34 and TNF which were expressed in the seeded cell populations, but was not expressed by any of the valve groups. Additionally, ITGA11 and MMP1 were expressed by the 3 week valves, but had no expression in the corresponding cell populations at the time of seeding.

5.4.4 Mechanical Testing

Mechanics of the tissue engineered heart valve leaflets from the 3 day and 3 week groups were compared against each other and against leaflet samples from cryopreserved and decellularized human aortic valves (Figure 4).[173] Leaflets from the 6 week group of tissue engineered valves were not included for mechanical testing due to incompetence in the leaflets after bioreactor culture. The areal strain of the valve leaflets from the 3 day group was 90.63 ± 11.90% and the peak stretch ratios were 1.14 ± 0.08 and 1.67 ± 0.12 in the circumferential and radial directions, respectively. Valve leaflets from the 3 week group of tissue engineered valves had an areal strain of 106.30 ± 19.46% and peak stretch ratios of 1.18 ± 0.09 and 1.74 ± 0.10 in

the circumferential and radial directions, respectively. The only significant difference between groups in the measured areal strain was between the cryopreserved and 3 week group ($p = 0.012$). All other groups were statistically similar ($p > 0.05$) and no significant differences were measured between groups in the directional peak stretch ratios ($p > 0.05$).

5.4.5 Biochemical Analysis

Biochemical assays measured the collagen and GAG concentration from valves in the 3 week and 6 week groups, and those results were compared against previous results from cryopreserved and decellularized valves.[173] The 3 day group was not expected to exhibit matrix remodeling in such a short time and was therefore excluded. Cell seeding with MNCs and extended bioreactor conditioning did not have a significant effect on the biochemical composition of the decellularized heart valve leaflets (Table 1). The collagen concentration between all groups was found to be statistically similar ($p > 0.05$). As previously reported, decellularization causes a loss of GAGs within the leaflet tissue and a significant decrease in GAG concentration is found between decellularized and cryopreserved samples. Seeding with MNCs and extended bioreactor conditioning did not have a significant effect on the GAG concentration since no significant difference was found between decellularized and tissue engineered valves ($p > 0 .05$). Additionally, the cryopreserved valves retained a significantly greater GAG concentration than the tissue engineered valves from the 3 week group ($p < 0.001$) and 6 week group ($p < 0.001$).

5.5 Discussion

The purpose of this study was to investigate the fate of MNCs isolated from bone marrow seeded onto decellularized heart valve scaffolds. Specifically, we sought to evaluate the

persistence of sub-populations such as MSCs, macrophages and leukocytes on and within the valve leaflet following extended periods of bioreactor conditioning. Since MSCs are commonly isolated from bone marrow through cell culture, it was expected that MNC seeding and extended conditioning will lead to expansion of the MSC population, effectively skipping traditional cell culture methods.

The results of this study yielded both expected and unexpected outcomes. As expected, MNCs can be quickly localized into the leaflet matrix. There is evidence of MNC seeding leading to rapid recellularization *in situ,* and we now have evidence that such rapid recellularization can occur *in vitro.*[55] It was also expected that extended bioreactor processing would lead to proliferation of the MSC sub-population from the seeded MNCs. This was demonstrated by the increased expression of MSC associated genes following extended periods of bioreactor conditioning in both the 3 week and 6 week processing groups. Conversely, macrophage markers were generally down-regulated with increased processing times. This effect was also observed by IHC staining, which identified CD34, CD45, and CD68 positive cells in the three day group indicating a mixed cell population of hematopoietic stem cells, leukocytes, and macrophages. On the other hand, cells in the 3 week and 6 week groups showed positive expression of CD90, CD29, aSMA and HSP47 indicating a population of MSCs and/or myofibroblasts. The positive expression of CD34 during extended bioreactor conditioning may also indicate proliferation of the hematopoietic stem cell population, although there is evidence that MSC populations may also express CD34.[150]

Despite proliferation of the MSC population, recellularization of the leaflet matrix following extended bioreactor conditioning was not as extensive as expected. Areas of interstitial repopulation were observed at both the 3 and 6 week time points; however, a cellularity similar

to that of the cryopreserved leaflet was not achieved, and areas devoid of cells were observed. The majority of the cells present on the seeded valves following 3 weeks and 6 weeks of bioreactor conditioning were located on the surface of the leaflet. While MSC proliferation occurred during extended bioreactor processing, extensive localization of MSCs within the leaflet interstitium did not occur. Additionally, valve incompetency due to leaflet retraction was observed for these valves. Therefore, the use of long (i.e., 6 weeks) periods of bioreactor conditioning following MNC seeding is likely not a clinically viable heart valve tissue engineering strategy.

MNC seeding and bioreactor processing did not seem to have a significant effect on the mechanics or biochemical properties of the seeded heart valves. The directional strain ratios of all groups remained similar and the 3 week processing group actually displayed an increase in areal strain. Because the mechanics of valves processed for 6 weeks were clearly compromised, we did not perform biaxial mechanical testing for this group, as three additional human aortic valves would have been required and no information regarding the clinical feasibility would have been gained. Biochemical analysis did not reveal any significant changes between decellularized controls and MNC seeded samples; however, it is worth nothing some collagen deposition was observed within areas of cell localization on surface of the leaflet fibrosa at the 6 week time point (Figure 2I).The absence of any significant mechanical or biochemical changes may be due, in part, to the lack of full repopulation of the leaflet interstitium during valve seeding.

As shown by others, MNC seeded scaffolds have the potential for recellularization *in situ.* Emmert *et al.* and Weber *et al.* demonstrated that polymeric heart valve scaffolds seeded with MNCs are capable of recellularization by autologous cells in ovine and primate models, respectively.[55, 178] Roh *et al.* proposed this occurs through an inflammation-mediated mechanism

wherein seeded monocytes attract a population of autologous macrophages which incite a tissue healing response.[137] The use of MNC seeding onto decellularized scaffolds was explored by Vincentelli *et al.* who injected MNCs or MSCs into the base of the leaflet of decellularized pulmonary valves and then implanted into the pulmonary position of juvenile sheep.[175] Seven days after implantation they observed both groups had seeded cells and recruited host cells present within the scaffold, but at final explant the MNC seeded valves exhibited thickened leaflets, calcification, and CD68+ macrophage host cells in the arterial wall.[175] The results from Vincentelli *et al.* favored the MSC group, yet the presence of macrophage cells may align with the inflammation-mediated recellularization mechanism proposed by Roh *et al.*[137, 175] However, the calcification and thickened leaflets from their MNC group is troubling. The MSC favored results by Vincentelli *et al.* is further supported by evidence that seeded MSCs release a cocktail of immunomodulatory proteins that may facilitate *in situ* recellularization.[12, 175] Therefore, an MSC pilot population, such as demonstrated in our three week bioreactor conditioning group, may be better suited for valve recellularization compared to a fresh MNC population.

The results from this study provide implications towards the translation of the TEHV, as the mechanism of recellularization, whether *in vitro* cell proliferation or *in situ* autologous cell recruitment, determines the extent to which the cell-seeded decellularized heart valve must be processed prior to implantation. For example, matrix repopulation through an inflammatory-tissue healing response, in which the seeded cells serve only to attract autologous cells through paracrine signaling, would mechanistically facilitate brief *ex vivo* processing protocols. Here we demonstrated the ability to rapidly localize a MNC population into a decellularized leaflet matrix within 3 days. On the other hand, recellularization through proliferation and differentiation of the seeded population would likely require extended bioreactor processing, though different

processing methods should be considered to avoid the observed cell layering on the leaflet surface. The work proposed here segues to future large animal studies (e.g., ovine and papio) to evaluate, not only matrix repopulation, but also the hemodynamic performance and growth potential of intact tissue engineered heart valves processed by these methods.

While this study focused on extended conditioning of MNC seeded heart valve scaffolds in a bioreactor, this creates an inherent limitation such that the *in vitro* nature eliminates any tissue healing response that may be expected *in vivo*. Therefore a number of factors could not be included in this study that could ultimately effect the recellularization of the valve leaflets, including paracrine and endocrine signaling, the presence of local tissue repair cells, and possible inflammatory responses. The *in vivo* response fell outside the scope of this study, yet this investigation still provides valuable insight into the persistence of sub-populations during extended conditioning following MNC heart valve seeding.

5.6 Conclusion

This study sought to investigate the potential for leaflet matrix restoration and repopulation following MNC seeding and extended periods of bioreactor conditioning. We found that an MNC population can be readily localized within the leaflet tissue in as little as 3 days. Furthermore, the MSC sub-fraction within the larger MNC population becomes amplified with prolonged bioreactor conditioning. The effect of MSC proliferation may eliminate the need for the long term pre-seeding culture of MSC populations, although that time is replaced with extended bioreactor culture. Repopulation of the leaflet interstitium was less extensive than anticipated; however, this alone does not preclude this TEHV processing strategy from clinical use, as an incomplete cell population established ex vivo may continue to proliferate after implantation or may provide paracrine signaling to promote further autologous recellularization

in vivo. Thus, while the intermediate bioreactor conditioning period used in this study (i.e., 3 weeks) may hold some promise, a bioreactor conditioning period of 6 weeks is not a viable option for clinical translation due to the negative impact on valve performance.

CHAPTER 6: EXPLORING NON-PHYSIOLGOIC BIOREACTOR PROCESSING CONDITIONS FOR HEART VALVE TISSUE ENGINEERING[**]

6.1 Abstract

Conventional methods of bioreactor conditioning for heart valve tissue engineering have led to inconsistent results in cellular repopulation, particularly of the distal valve leaflet. The use of non-physiologic conditioning parameters within a bioreactor, such as hypoxia and cyclic chamber pressure, may lead to increased and more consistent recellularization. To investigate the effects of such bioreactor conditioning parameters, ovine aortic heart valves were seeded with mesenchymal stem cells (MSC) and cultured in one of four environments: hypoxia and high cyclic pressure, normoxia and high cyclic pressure, hypoxia and negative cyclic pressure, and normoxia and negative cyclic pressure. Analysis revealed that hypoxic conditioning led to increased cellular infiltration into the valve leaflet tissue compared to normoxic culture. Protein expression across all groups was similar, exhibiting an MSC and valve interstitial cell phenotype. Gene expression was varied between groups, with cyclic negative pressure conditioning resulting

[**] To be submitted as **VeDepo M.C.**, Buse E., Paul A., Hopkins R.A., and Converse G. L., Exploring Non-physiolgoic Bioreactor Processing Conditions for Heart Valve Tissue Engineering, *Annals of Biomedical Engineering*, 2018.

in up-regulation of gene markers for an MSC phenotype and matrix remodeling, compared to a down-regulation of similar genes for cyclic high pressure conditioning. Taken together, these results suggest the use of non-physiologic bioreactor conditioning parameters such as hypoxia and cyclic negative pressure to increase the *in vitro* cellular repopulation of TEHV leaflets.

6.2 Introduction

Heart valve tissue engineering may be the ideal solution for patients suffering from valvular heart disease and requiring valve replacement.[70] The current options for valve replacement all suffer from limitations and the pediatric population is particularly impaired by the lack of an ideal prosthetic valve substitute.[148] Mechanical prosthetic valves have poor hemodynamics requiring a lifetime of anti-coagulation therapy and tissue-based prosthetic valves are limited by poor durability often requiring re-intervention.[148] The tissue engineered heart valve (TEHV) can overcome the existing limitations of current replacement options by providing a one-time implantation of living tissue capable of optimal hemodynamics, tissue remodeling, and growth.

Unfortunately, clinical realization of the TEHV is still hindered by the difficultly in reproducibly establishing a phenotypically appropriate cell population within the tissue engineered leaflet matrix. Native heart valve leaflets are primarily populated by valve endothelial cells (VECs) on the luminal surface and valve interstitial cells (VICs) within the tissue matrix.[105] Numerous studies have attempted to recreate this two-fold cell phenotype *in vitro* by seeding heart valve scaffolds with a variety of cell populations.[174] There is evidence, however, that decellularized heart valve matrices will undergo partial autologous recellularization when implanted *in vivo.*[39, 47, 48, 131] Specifically, decellularized valves implanted in both human patients and ovine models have shown complete re-endothelialization by VECs and partial

recellularization by VICs in the valve conduit wall and leaflet base; however, the distal leaflet remains acellular.[39, 47, 48, 131] This is problematic since tissue growth requires a viable cell population throughout the leaflet tissue. Therefore, the challenge of *in vitro* recellularization should focus on recreating a cell population within the distal tip of the valve leaflet matrix.

One solution that may increase recellularization of the leaflet interstitial tissue is fine-tuning of bioreactor conditioning parameters. Bioreactor conditioning of tissue engineered heart valves can be used to apply mechanical and chemical stimuli to the valve scaffolds to drive cell proliferation, differentiation, and ultimately recellularization. Numerous studies have investigated conditioning in custom bioreactor systems to increase the recellularization of cell seeded heart valve scaffolds.[15, 103, 104, 144, 152] Many of these systems employ physiologic parameters of pressure and flow rate to mimic a systemic or pulmonary circulation environment.[103, 104, 144, 152] However, recellularization using these bioreactors has often been limited to surface re-endothelialization.[103, 104, 152] The localization of cells within the leaflet tissue remains challenging. While it is inherently logical to use physiologic parameters for bioreactor conditioning to drive cell differentiation, it may be necessary to develop novel conditioning parameters to stimulate cell infiltration into the valve leaflet.

One such solution is hypoxic conditioning, as there is evidence that culturing mesenchymal stem cells under oxygen tension can increase cell proliferation and migration.[92, 109] Additionally, in a study by Balguid *et. al,* polymeric valve scaffolds seeded with venous myofibroblasts were cultured in hypoxic conditions and exhibited increased mechanical properties compared to scaffolds cultured at normoxic conditions.[10] Cyclic champber pressurization using positive and negative pressures may also influence recellularization. Previous work in our lab has demonstrated partial recellularization of the distal valve leaflet

using cyclic positive and negative pressure cycles within the bioreactor.[34] Ovine aortic valves seeded with human MSCs showed increased recellularization following a combination of negative and positive pressure conditioning, compared to negative conditioning only or static conditioning.[34] However, the experimental design of that study made it impossible to de-couple the effects of positive versus negative pressure conditioning with the duration of bioreactor culture. Therefore, the purpose of this study was to investigate the effects of hypoxia and positive/negative bioreactor conditioning parameters on the recellularization of heart valve leaflets. Specifically, the focus is on the repopulation of the distal leaflet tip. It is hypothesized that valves cultured under hypoxic and positive pressure conditions will result in the greatest recellularization of the distal valve leaflet.

6.3 Methods

6.3.1 Tissue and tissue processing

Ovine aortic valves were harvested from juvenile sheep under approved IACUC protocols and in accordance with Guide for Care and Use of Laboratory Animals (National Institutes of Health Publication No. 85-23). Harvested valves were cryopreserved using a procedure modeled after clinical tissue handling protocols. Valve were frozen at 1 °C min^{-1} using a controlled rate freezer (2100 Series, Custom BioGenics Systems) before being stored in a cryofreezer at -180 °C. Valve decellularization was performed as described previously.[133] Briefly, the ovine aortic valves were thawed and then subjected to reciprocating osmotic shock, followed by detergent (Triton X-100, sodium-lauroyl sarcosine) and enzymatic (Benzonase) washes to remove cellular material. Extraction of organic material was performed using recirculating water and ion exchange resins. After decellularization, the valves were again cryopreserved using the above procedure and stored at -180 °C until valve seeding.

6.3.2 Valve seeding and conditioning groups

All tissue engineered valves were seeded with bone marrow derived MSCs. MSCs were isolated by filtering 25 mL bone marrow aliquots (Lonza) for the mononuclear cell fraction using a bone marrow filter system (Kaneka). The mononuclear cells were then put in culture and the MSCs were isolated as adherent cells. The cells were then cultured until sufficient numbers were available for valve seeding (approx. 10 million cells). MSC populations to be seeded in one of the groups using hypoxic bioreactor conditioning were cultured in hypoxic conditions (7% O_2, 5% CO_2, 37 °C) while MSCs to be seeded in one of the normoxic bioreactor conditioning groups were cultured in normoxic conditions (21% O_2, 5% CO_2, 37 °C). Two cell populations were isolated from a single donor with one of the matched populations being used for a hypoxic conditioning group and the other used for a normoxic conditioning group, effectively creating matched cell populations that differ based on oxygen tension conditioning. It is worth noting, the cells were effectively passage 2 at the time of valve seeding. All tissue engineered heart valves were then seeded following established valve seeding protocols.[34] The decellularized valves were thawed from cryopreservation and sutured onto tissue grips. The seeding cell population for each group was then suspended in 10 mL of media and seeded into the lumen of the valve which was mounted in a static bioreactor chamber containing 200 mL valve media (DMEM F12 (Life Technologies) and 10% human serum (Sigma-Aldrich)).

The valves were then randomly divided into one of four groups to evaluate bioreactor conditioning parameters (3 valves per group): hypoxic & high pressure (Hyp/HighP), normoxic & high pressure (Norm/HighP), hypoxic & negative pressure (Hyp/NegP), and normoxic & negative pressure (Norm/NegP). After cell seeding, all valves underwent 24h of static culture (37 °C, 5% CO_2) to allow cell adhesion the valves. Valves were then transferred to a sterile, single

use, dynamic bioreactor chamber containing 500 mL valve media and the assembly was placed in a linear actuator to create cyclic positive and negative pressure profiles within the bioreactor chamber.[34] A bioreactor conditioning protocol was then applied for 2 weeks based on the group. Valves in the hypoxic groups were cultured at 7% O_2 while valves in the normoxic groups were cultured at 21% O_2 (all valves cultured at 37 °C, 5% CO_2). After the 24 hours of static culture, valves in the high pressure groups were conditioned for 24h of cyclic negative pressure (-20 to 5 mmHg), followed by 24h of cyclic low positive pressure (-5 to 20 mmHg), and finally 2 weeks of cyclic high positive pressure (-5 mmHg to 120 mmHg). Valves in the negative pressure groups were conditioned for 9 days of cyclic negative pressure (-20 to 5 mmHg). A media change was performed on all valves after 1 week of conditioning, wherein half of the bioreactor media (250 mL) was removed and replaced with 250 mL of fresh valve media. Following bioreactor conditioning, the valves were removed and dissected for analysis, including histology, cell counting, immunohistochemistry (IHC), real time PCR (rt-PCR), and biochemical analysis.

6.3.3 Histology & Cell Counting

Samples for histology were sectioned along the radial plane of each leaflet from each of the tissue engineered valves. Hematoxylin and eosin (H&E) staining was used to evaluate repopulation of the decellularized valve leaflets, specifically by the presence of cells within the leaflet tissue and on the leaflet surface. Recellularization of the tissue engineered valves in each group (n = 9) was determined by counting the cells in a calculated area using Axiovision software. Cells within the interstitial leaflet tissue were counted but not cells on the leaflet surface. Cell density was measured at the base, middle, and tip region of the leaflet.

6.3.4 IHC & PCR

Protein expression of the cells from the tissue engineered valves was evaluated by IHC. Unstained slides cut from the samples prepared for histology. The slides were blocked in 10% normal goat serum for 1 hour before overnight incubation at 4 °C with 1:100 diluted primary antibodies. The primary antibodies (Abcam) targeted alpha smooth muscle actin (αSMA), heat shock protein 47 (HSP47), vimentin (VIM), CD90, CD73, and vWF. Fluorescent secondary antibodies (Alexa Fluor 488 or Alexa Fluor 594, Life Technologies) were then incubated for 1 h followed by nuclear counterstaining (DAPI; Life Technologies).

Gene expression was analyzed by rt-PCR and was evaluated as the fold change of the hypoxic bioreactor conditioning relative to the normoxic bioreactor conditioning, with respect to the pressure conditioning. Valves were compared based on the matched cell populations that were isolated from a single donor to minimize donor variability. Tissue sections from each leaflet were taken during valve dissection and immediately frozen in liquid nitrogen before being pulverized. The tissue sections from each leaflet of the valve were combined to form one sample to measure the gene expression across the valve. RNA was isolated using the RNeasy Micro Kit (Qiagen). The RNA was then reverse transcribed to cDNA using the High Capacity cDNA Reverse Transcription Kit (Invitrogen). Real-time PCR (7300 RT-PCR system, Applied Biosystems) was performed using a custom phenotyping array (TaqMan, Life Technologies). PCR data is conveyed as the relative fold change in gene expression of the cells from the hypoxic conditioned groups compared against their respective matched normoxic conditioned groups, with respect to pressure conditioning.

6.3.5 Biochemical analysis

The sulfated glycosaminoglycan (GAG), elastin, collagen, and total protein concentrations of the extracellular matrix from the tissue engineered valve leaflets was analyzed

using colorimetric biochemical assay kits. GAG concentration was measured using the Blyscan Sulfated Glycosaminoglycan Assay (Biocolor). Elastin concentration was measured via the Fastin Elastin Assay (Biocolor). For both the GAG and elastin assays, tissue samples (approx. 15 mg, n=9) were processed according to manufacturer protocol and the results were measured using a UV/Vis spectrophotometer (VERSAmax, Molecular Devices). at 656 nm and 513 nm, respectively. Collagen concentration was measured using the QuickZyme Total Collagen Assay (QuickZyme Biosciences). Samples (approx. 15 mg, n = 9) were prepared by overnight hydrolysis in 6M HCl at 90 °C and the hydroxyproline concentration was measured using a spectrophotometer at 570 nm. Total protein concentration was measured using the QuickZyme Total Protein Assay (QuickZyme, Biosciences) and used the same hydrolysates that were prepared for collagen quantification. The GAG, collagen, and total protein concentrations are reported as μg mg^{-1} of wet tissue and are compared to previously reported values from cryopreserved and decellularized valves.[173]

6.3.6 Statistical analysis

Statistical analysis was performed by ANOVA, and post-hoc comparisons were made using the Tukey test or the Kruskal-Wallis test for parametric and non-parametric data, respectively. Further statistical comparisons between hypoxic/normoxic groups within a given pressure conditioning, particularly for the cell density measurements, were made using the Mann-Whitney Rank Sum test. Differences were considered statistically significant at $p < 0.05$.

6.4 Results

6.4.1 Tissue, and tissue processing

As reported previously, the decellularization process resulted in complete removal of cells from the valve tissue while preserving the overall architecture of the extracellular matrix (data not shown).[32, 173] Following the two week bioreactor conditioning protocols the valves from all groups had a normal appearance and functional leaflets.

6.4.2 Histology & Cell Counting

H&E staining of the tissue engineered valve samples revealed the four bioreactor conditioning protocols lead to differing degrees of recellularization, particularly with the interstitium of the leaflet (**Figure 1**). Valves in the Hypoxic/HighP group and Hypoxic/NegP groups both showed increased cellularity within the leaflet interstitium compared to valves in the Normoxic/HighP and Normoxic/NegP group (Figure 1 A,E,C,G). This was particularly true of the distal tip of the leaflet which exhibited the greatest cell concentration, while the middle region and base of the leaflet showed less cellular infiltration. Valves in the Normoxic/HighP and Normoxic/NegP groups exhibited only minimal cellularity within the interstitial leaflet tissue, but showed a high degree of cells agglomeration on the leaflet surface (Figure 1 B,F,D,H). Similar to the hypoxic groups, the highest cell concentration was at the distal tip of the leaflet with decreased cellularity along the leaflet middle and base. These results indicate hypoxic conditions increased the recellularization of the leaflet interstitium. Pressure conditioning within the bioreactor did not seem to have an obvious effect on recellularization as visualized by histology.

The extent of matrix repopulation within each group was quantified by measuring the cell density within the leaflet tissue (**Figure 2**). As was observed by histology, all groups had an increased cellularity at the distal tip of the leaflet compared to the middle or base regions. Since the goal of this project was recellularization of the distal leaflet, and measured cell density was

greatest within the leaflet tip for all groups, the remainder of the manuscript will focus on the cell concentration within the tip region. Valves conditioned under hypoxic conditions had increased cell density compared to normoxic conditioned valves. Specifically, the Hypoxic/NegP group exhibited generally high levels of recellularization with a median cell density of 116.34 cells/mm^2 within the leaflet tip. The other hypoxic group, Hypoxic/HighP, also exhibited high recellularization with one sample showing the greatest maximum recellularization, however the results were not consistent leading to a high variance and a median cell density of 58.66 cells/mm^2. The Norm/HighP and Norm/NegP had relatively low recellularization with median values of 20.64 cells/mm^2 and 26.01 cells/mm^2 respectively. Statistical analysis by ANOVA on ranks indicated a significant difference was to be expected ($p = 0.045$), but the post-hoc comparison found no significance between individual groups. Further statistical analysis was performed using the Mann-Whitney test between hypoxic and normoxic samples within the individual pressure conditioning groups (i.e. negative pressure or high pressure). Hypoxia led to significantly increased cell density compared normoxic conditioning for both negative pressure ($p = 0.030$) and high pressure ($p = 0.042$) groups.

6.4.3 Protein and Gene Expression

The protein expression of the cells within the tissue engineered valves from the four conditioning groups was evaluated using IHC (**Figure 3**). The protein expression was similar between groups with cells from all groups displaying markers indicative of MSC or valve interstitial cell (VIC) phenotypes. Specifically, cells from all groups showed positive expression for αSMA, HSP47, VIM, and CD90. The Hypoxic/HighP group also exhibited positive expression of CD73, another MSC marker, while the other groups did not. None of the groups displayed positive expression of the endothelial cell marker vWF.

Gene expression of the tissue engineered valves was evaluated by rt-PCR (**Table 1**). The gene expression was analyzed as the fold change of the tissue engineered valves from each bioreactor conditioning group relative to the matched pre-seeded cell population. Similar to the protein expression, the gene expression between groups was relatively similar. VIC-like markers within all groups were both up-regulated (VIM) and down-regulated (ACTA2) compared to initial seeded cell population, although valves in the normoxic group showed greater down-regulation of ACTA2. Some of the MSC markers were up-regulated in all groups (CD44, ANPEP), but other MSC markers (THY1, ITGB1) exhibited increased expression in negative pressure conditioning and decreased expression in positive pressure conditioning. Interestingly, markers that indicate extracellular matrix production (HSP47, COL1A1, COL3A3) were all up-regulated in negative pressure conditioning groups and down-regulated in positive pressure conditioning groups, while the marker for extracellular matrix digestion (MMP1) was greatly up-regulated in all groups except Normoxic/NegP. The cell proliferation marker (MKI67) was down-regulated or showed no expression in all groups except Hypoxic/NegP. All groups, even valves in the hypoxic groups, showed a down-regulation of the hypoxia marker EPAS1. It is possible this was due to the pre-seeding culture of the cell populations in a hypoxic or normoxic environment depending on the group of the cell seeded valve. Endothelial markers (vWF, ENG) were partially up-regulated in most groups despite no evidence of endothelial cells by protein expression. Finally, markers for inflammatory cells (PTPRC, CD14) or signs of adverse differentiation (ACAN, ALPL, ADIPOQ) were generally down-regulated in all groups.

6.4.4 Biochemical analysis

The concentration of GAG, collagen, and total protein in the extracellular matrix of the tissue engineered valves was measured and compared to previously reported values for

cryopreserved and decellularized samples (**Table 2**) [VeDepo ref]. The biochemical analysis revealed no differences between the bioreactor conditioning groups. As reported previously, the decellularization protocol causes a significant decrease in GAG concentration. However, none of the tissue engineered valves had a significantly different GAG concentration than either decellularized or cryopreserved controls, indicating some amount of GAG production by the seeded cells. On the other hand, the collagen concentration of all tissue engineered valves from each group was significantly greater than both the cryopreserved and decellularized controls ($p < 0.05$). The concentrations of total protein in the tissue engineered valves revealed no significant differences between groups or between the cryopreserved or decellularized controls.

6.5 Discussion

The purpose of this study was to investigate the effects of oxygen tension and pressure conditioning on the recellularization of tissue engineered heart valve leaflets seeded with MSCs. The results demonstrate that the tested bioreactor conditioning parameters can positively affect recellularization. Histologic evaluation of the various groups suggested that conditioning valves in hypoxic conditions increased recellularization of the interstitial tissue of the distal valve leaflet. The positive effect of hypoxic conditioning was confirmed by quantifying the cell density within the tip, middle, and base of the leaflet. Valves cultured under hypoxia conditions resulted in significantly increased cell density within the leaflet tip compared to normoxia conditions, within individual pressure conditioning groups. Gene and protein expression revealed a relatively similar cell phenotype of MSC or VIC-like cells within all groups. Biochemical concentrations of extracellular matrix proteins were also similar between all groups.

6.5.1 Effects of cyclic pressure conditioning

The use of negative cyclic pressures versus negative and positive cyclic pressures lead to similar results in the recellularization of heart valve leaflets. The greatest observable difference was measured in the gene expression, where valves conditioned under negative pressures showed an up-regulation of MSC and matrix remodeling gene markers compared to a general down-regulation in valves conditioned at positive pressures. As mentioned, a previous study in our lab determined heart valve leaflets conditioned with a low flow, cyclic pressure conditioning protocol showed increased recellularization compared to static culture.[34] That study used the same bioreactor system as was used in the present study. This system uniquely utilizes cyclic negative and/or positive chamber pressures within the bioreactor. During the initial development of the valve seeding protocols employing this bioreactor, short (i.e., 72 h) periods of negative pressure conditioning were found to promote improved matrix repopulation, relative to similar periods of positive pressure.[34] While the exact mechanism remains unclear, it is theorized that the negative pressure cycles increase saturation of the leaflet with cell culture media and/or causes increased cell deformation, mimicking diastolic loading.[115] However, the present study suggested that the benefit of negative pressure conditioning relative to high positive pressure conditioning on cellular infiltration is transient, in that the application of extended periods of either negative or positive pressure conditioning subsequent to the initial short period of negative pressure did not impact the extent of matrix repopulation.

The more common method of bioreactor conditioning used by many other researchers attempts to mimic the physiologic forces of trans-valvular pressure and fluid flow rates experienced *in situ*. Many conventional methods using physiologic conditioning parameters have focused on re-endothelialization and therefore demonstrate minimal cellular infiltration into the leaflet tissue.[103, 104, 152] An exception is the study by Schenke-Layland *et al.* which seeded

endothelial cells and myofibroblasts onto porcine pulmonary valves followed by pulmonary physiologic conditioning (40-60 mmHg trans-valvular pressure and 3 L/min flow rate) in a bioreactor for 9 or 16 days.[144] The resulting heart valve constructs exhibited repopulation of the leaflet tissue by αSMA^+ cells within the leaflet and vWF^+ cells on the leaflet surface.[144] Conversely, seeded valves cultured under static conditions for identical time periods revealed a lack of cellular infiltration and cells remain in clusters around the leaflet surface.[144] The increased cellular infiltration in the bioreactor cultured group was likely caused by the cyclic mechanical conditioning which can promote the production and release of TGF-β1, leading to the activation of myofibroblasts and the release of proteolytic enzymes (MMPs).[126] However, it has been suggested that heart valves can be overly mechanically conditioned, potentially leading to fibrosis of the engineered tissue.[126] Therefore, mild mechanical conditioning using forces that stimulate cellular infiltration, such as a cyclic negative chamber pressure, may offer a safer means to achieve TEHV recellularization.

6.5.2 Effects of oxygen tension

Oxygen tension had the greatest effect on recellularization in this study. The study was specifically designed to mitigate the effects of donor to donor variability, so one hypoxic valve and one normoxic valve were generated from the cells of each donor. This allowed us to make comparisons between donor-matched hypoxic and normoxic valves for a given pressure conditioning protocol (**Table 3**). As seen in **Table 3**, hypoxic condition led to an increase in distal leaflet recellularization for each matched pair of valves. There was large variance in the fold change of positive pressure conditioned valves. One pair of valves exhibited greater than 8-fold increase due to hypoxic conditioning while the other two pairs of valves exhibited only a moderate increase. Conversely, negative pressure conditioned valves experienced at a least a 2-

fold increase in cell density due to hypoxia. These results suggest synergistic effects on leaflet recellularization between hypoxia and negative pressure conditioning. Of particular interest is that hypoxia greatly increased recellularization within the distal tip region of the valve leaflets. All other regions of valvular tissue (leaflet middle, leaflet base, and conduit wall) have shown evidence of autologous recellularization during the implantation of decellularized valves in human and animal models. Since the distal leaflet region has previously proven difficult to repopulate, the cellular density observed in hypoxic conditioned groups is highly encouraging.

As the results demonstrate, hypoxic conditioning significantly promotes the cellular infiltration of MSCs into the valve leaflet. However, the large variability within the hypoxic conditioned groups also indicates the inconsistent nature of TEHV recellularization. As stated previously, one of the greatest challenges remaining in heart valve tissue engineering is reproducibly establishing a phenotypically appropriate cell population within the leaflet tissue. Such inconsistency led to samples within this study demonstrating a level of recellularization similar to native leaflets, while other identically treated samples exhibited only marginal cellular repopulation. Despite the large variance, hypoxic conditioning still demonstrated a significant increase in recellularization of heart valve leaflets seeded by MSCs compared to normoxic conditioning, within a given pressure-conditioning group.

There are extensive reports on the effects of hypoxic culture on MSCs describing how a low oxygen concentration can cause cells to proliferate faster, proliferate longer, and better maintain an undifferentiated phenotype.[24, 54] However, there are fewer studies on the role hypoxia may play during tissue engineering and even fewer that focus on hypoxia in heart valve tissue engineering.[109] This is likely because human heart valves, particularly the mitral and aortic valve, do not generally exist in hypoxic conditions *in situ*. The exception of course, is during pre-

natal valve development as the uterine environment is hypoxic.[4] Amofa *et al.* described the role of changing oxygen levels on heart valve development during the neonatal transition and how such changes lead to the GAG-rich valve primordia transforming into tri-layered leaflets.[4] They further found that hypoxia can promote GAG expression in adult murine valves.[4] The latter point is of particular interest as our decellularization protocol significantly decreases GAG concentration within the leaflet ECM, however hypoxic conditioning of the tissue engineered valves within this study did not reveal an increase in GAG production. It is likely that we did not observe an increase in GAG production because the tissue engineered valves contained an MSC population compared to a VIC/myofibroblast population in native leaflets. GAG production was also observed in the study by Balguid *et al.,* in which myofibroblasts were seeded on polymeric valve scaffolds.[10] They observed GAG production to a level similar to native valves, and despite a lower collagen concentration, the resulting mechanical properties were similar to native tissue.[10]

6.5.3 Limitations

One of the primary limitations of this study is the smaller sample size within each group. Three aortic valves were processed within each group, providing nine leaflets available for analysis. While nine samples was adequate to detect the significant effects of hypoxic conditioning, the variance within the measured population was still very high. Increasing the sample size may provide more information as to the effects of bioreactor conditioning and may indicate greater synergistic effects between conditioning parameters that were not identified by this study. Another critical consequence of the low sample size is the use of a single time point for measurements rather than serial sampling. All tissue engineered valves were processed for two weeks based on previous experience with cell seeded valve constructs. However, that time

point is largely arbitrary and further work is required to determine the ideal duration of bioreactor processing. Despite the limitations, the results of this study provide invaluable leads for increasing the recellularization of TEHVs. Future studies should focus on fine-tuning the bioreactor conditioning protocol based on hypoxia and a negative pressure waveform.

6.6 Conclusion

Adjusting the bioreactor conditioning parameters for cyclic negative/positive chamber pressure and oxygen tension resulted in varying degrees of recellularization of MSC seeded TEHVs. Conditioning in a low oxygen environment led to increased cellular infiltration into the valve leaflet tissue compared to normoxic culture. Cyclic negative pressure conditioning resulted in up-regulation of gene markers for an MSC phenotype and matrix remodeling, compared to a down-regulation of similar genes for cyclic high pressure conditioning. Taken together, these results suggest the use of non-physiologic bioreactor conditioning parameters such as hypoxia and cyclic negative pressure to increase the *in vitro* cellular repopulation of TEHV leaflets. Further development of such protocols may increase the reproducibility in TEHV recellularization and ultimately usher in the development of an ideal heart valve replacement.

CHAPTER 7: CONCLUSION

Heart valve tissue engineering is a promising approach for the currently unmet need of an ideal prosthetic heart valve. However, the TEHV still faces a number of challenges ranging from optimal scaffold creation to the lack of consistent recellularization. Therefore, the current thesis explored the pathway to the TEHV and addressed challenges associated with scaffold creation through decellularization, cell seeding of valve scaffolds, and conditioning seeded scaffolds in a bioreactor.

Decellularized heart valves are a promising scaffold material for the TEHV since they are composed of biological materials that can positively impact cell differentiation and may serve as building blocks during the remodeling process.[77, 100] Additionally, decellularized valves often maintain the mechanical anisotropy of the native valves from which they are derived.[5, 32, 97, 101, 173] However, before a decelluarized valve should be used as a TEHV scaffold, the effects of the decellulrization process on the valve tissue should be characterized for all applications, including the different animal applications in which research will be performed. Therefore, the work in the current thesis began with a detailed investigation into the species-specific effects of decellulzation on human and ovine aortic heart valves. The tested multi-detergent decellularization process lead to cell free scaffolds for both human and ovine heart valves; however, decellularization was found to more greatly impact ovine tissue than human tissue. The species-specific effects were likely due to increased initial cellularity and a decrease in the collagen crosslinking of ovine leaflets. Despite the discovered effects due to decellularization, ovine valves were still used throughout the current thesis. The non-human tissue is more easily available for research purposes, and more importantly, the sheep model is the preferred FDA pre-clinical mode. The TEHV will need to be developed first in the ovine model and then translated

to clinical practice. Instead, the results from this study are relevant for use outside of the current thesis and demand attention during future pre-clinical testing of heart valve devices that incorporate decellularized tissue. Since sheep are the FDA preferred pre-clinical regulatory model for heart valve replacement, care must be given to the species-specific effects to decellularization that were identified here. This is particularly important given the potential inherent barrier to the clinical translation of such a 'combination device' (prosthetic device + biological and cellular components).

The next phase of the dissertation focused on the introduction of cells into the decellularized scaffold. As outlined in Chapter 2, decellularized valves do not completely recellularize autologously *in vivo*. Implanted decellularized valves undergo complete re-endothelialization as well as partial interstitial recellularization of the leaflet base, but the mid to distal leaflet tip remains acellular. Therefore, additional measures must be taken to encourage distal leaflet recellularization. Recellularization is proposed to take place by two mechanisms: (1) proliferation and differentiation of seeded cells or (2) autologous cell recruitment through the release of homing cytokines. The work in Aim 2 of this thesis investigated the capacity for leaflet repopulation, and the potential mechanism by which recellularization occurred for four cell populations: MNCs, low dose MSCs, high dose MSCs, and VICs. Seeding with MNCs led to initial cellular infiltration but minimal recellularization was observed at two weeks. Cytokine analysis showed increased expression of MCP-1, an inflammatory cell homing factor that others have suggested encourages recellularization through the recruitment mechanism.[12, 43, 137, 156]. On the other hand, MSC seeding at a low or high dose led to high interstitial recellularization, likely due to the cell proliferation mechanism. The higher seeding dose of MSCs led to increased native-like biochemical and mechanical properties. The increased cell population caused an

increased production of extracellular matrix proteins, which in turn likely improved the mechanical properties. Therefore, high dose seeding is recommended since it less reliant upon cell proliferation. Seeding valves with VICs was surprisingly unsuccessful. Although not clinically relevant due to the difficulty in obtaining autologous VICs, the VIC group was included under the presumption it would act as a positive control group. However, VICs achieved little recellularization, possibly because the cells could not enter an aVIC state (indicated by negative αSMA expression) and were not capable of producing matrix remodeling proteins to allow infiltration into the valve leaflet.

The final phase of the thesis was to develop bioreactor-conditioning protocols to increase the recellularization of cell seeded valves. Detailed investigations into bioreactor conditioning were performed individually for valves seeded with MNCs and MSCs. Bioreactor conditioning for MNC seeded valves was focused on the duration of bioreactor culture. The study in Chapter 4 comparing seeding cell populations indicated a changing cell phenotype in MNC seeded valves during the bioreactor culture. As observed in the previous studies, MNCs could be localized within the leaflet tissue in as little as three days using a cyclic negative and positive bioreactor pressure protocol. After three weeks of culture, an MSC cell population became the dominant phenotype as determined by gene and protein expression. As the MSC population grew, cell layering on the leaflet surface became more pronounced. Six weeks of culture of MNC seeded valves also saw an increase in the MSC population, though leaflet retraction was noted leading to incompetency of the valves. Therefore 6 weeks of culture is not recommended for MNC seeded heart valves.

Bioreactor conditioning for MSC seeded valves focused on non-physiologic parameters of chamber pressure and hypoxic conditions to increase recellularization into the distal leaflet.

The bioreactor parameters were based off of preliminary data and previous studies.[33, 34] Hypoxia led to significantly increased cell infiltration compared to normoxia, though large variations were observed. Due to the donor matched nature of each hypoxic versus normoxic conditioned valve, we can see that hypoxic conditions increased recellularization in each donor matched sample. As was observed in previous studies, negative pressure conditioning led to slightly more consistent recellularization and an increase gene expression markers associated with stem cells and matrix remodeling. Surprisingly, positive pressure cycles did not significantly out perform negative only as observed previously (converse bioreactor paper). The benefits from cyclic negative chamber pressure conditioning are encouraging but the mechanisms behind such benefits remain unclear. The negative pressure may cause increased saturation of the interstitial leaflet tissue with culture media allowing greater cellular ingrowth. Another possibility is the alternating pressure cycles may cause greater cell deformation, which in wound healing models has stimulated smooth muscle protein synthesis. Thus, cyclic deformation of the cells may enhance mobility and thus the ability to better infiltrate the dense leaflet matrix. Additionally, cell deformation may lead to increased production of matrix remodeling proteins, including proteins for matrix production and matrix breakdown, as was observed in the negative only conditioned groups from Chapter 7. Breakdown of the local matrix may enhance cellular infiltration, while production of structural matrix proteins preserves the mechanical properties.

As this thesis followed the pathway to a tissue engineered heart valve, methodologies were identified that may overcome many of the challenges remaining to the clinical realization of a TEHV. Therefore, the following protocol is suggested for TEHV development**.** Heart valve decellularization should be performed in a manner that adequately removes cellular and nuclear material, without causing structural or chemical damage to the extracellular matrix. The use of

trypsin and other aggressive enzymes is a classic example of "over processing" leading to structural damage of the valve leaflet.[63, 101, 135, 157] The low dose multi-detergent decellularization process used in the current thesis resulted in minor mechanical changes for ovine aortic valves, though human aortic valves were structurally similar. However, a loss of GAGs was noted for both ovine and human valves**.** Following decellularization, it is recommended to seed the valve scaffolds with MSCs isolated from bone marrow to establish a pilot population. MSCs showed the greatest cellular infiltration compared to other tested cell sources and the MSCs maintained a phenotype similar to native VIC-like myofibroblasts. Finally, a higher dose of MSCs is recommended, approximately 10 million cells per valve; thus, an implied cell amplification step is necessary to magnify autologous cell harvests. Lastly, it is recommended to optimize biological and mechanical conditioning within a bioreactor to increase recellularization of the valve leaflets. Specifically, hypoxic conditions and cyclic negative chamber pressures were found to be beneficial. Conditioning in a low oxygen environment led to increased cellular infiltration compared to normoxic conditioning. Cyclic negative chamber pressures resulted in greater expression of matrix remodeling gene markers compared to cyclic positive chamber pressures.

Such a protocol for generating a TEHV is suggested by the results of the sequential experiments reported in this thesis. However, there is ample room for improvement and the current thesis suggests numerous avenues for further fine-tuning of heart valve tissue engineering methodologies. This work focused on the *in vitro* recellularization of TEHVs. Therefore, the *in situ* response fell outside the scope of this study and thus remains unknown. In considering the future directions following the work in this current thesis, *in vivo* testing of TEHVs developed using the previously suggested protocol should be held paramount. Implant studies using the

described TEHV will elucidate the functionality of the valve and the host-body response to the tissue engineered device. Additionally, in lieu of extended implant studies, wear testing using a pulse duplicator may predict the long term functionality. Other options for future work concern the mechanism of recellularization. The current thesis was primarily focused on the mechanism of cell proliferation due to the *in vitro* nature of the studies. However, there is promise in leveraging *in vivo* healing capabilities through autologous recruitment driven recellularization. There is evidence that the chemo-attractant protein MCP-1 may stimulate inflammation-mediated recruitment recellularization in polymeric vascular grafts and heart valves.[55, 137, 178] The current thesis identified MCP-1 production by MNCs seeded on decellularized valves (Figure 4.4). Further analysis revealed increased MCP-1 production at 3 days and a decreased production as bioreactor conditioning continued (Figure 7.1). Therefore, seeding with an initial pilot population of MNCs or incorporation of the MCP-1 protein into the decellularized scaffold may lead to host cell recruitment and eliminate the need for bioreactor conditioning. Future work using these methods should investigate the potential for autologous recellularization by the recruitment mechanisms.

Ultimately, the work conducted in this current thesis provides innovative solutions to many of the challenges still facing clinical realization of the TEHV. The work described herein offers a species-specific characterization on the effects decellularization, compares numerous cell populations for the potential recellularization of decellularized scaffolds, and identifies bioreactor conditioning parameters to further increase valve recellularization. Additionally, methodologies identified in this thesis, specifically the use of hypoxic and negative pressure conditioning, may be applied to other tissue engineering applications to increase recellularization by myofibroblast cell types. Such conditioning may benefit any tissue-engineered application but

the use for vascular grafts, cardiac tissue, and other cardiovascular devices are of particular interest. The end-goal of the current thesis has always been the clinical application of a TEHV and the described methodologies were developed to be translatable to the clinic. As demonstrated in the current thesis, heart valve tissue engineering methods need to focus on restoring full matrix remodeling capacity through complete recellularization of the valve tissue to achieve lifelong viability. The bench-to-bedside approach adopted in this thesis offers real, obtainable advances for the field of heart valve tissue engineering and draws the reality of an ideal heart valve replacement ever closer to the present.

REFERENCES

1. Ahsan, T. and Nerem, R. M. Fluid shear stress promotes an endothelial-like phenotype during the early differentiation of embryonic stem cells. Tissue Eng Part A, 16, 3547-3553, 2010.

2. Aldous, I. G., Lee, J. M. and Wells, S. M. Differential changes in the molecular stability of collagen from the pulmonary and aortic valves during the fetal-to-neonatal transition. Ann Biomed Eng, 38, 3000-3009, 2010.

3. Alvarez-Viejo, M., Menendez-Menendez, Y., Blanco-Gelaz, M. A., Ferrero-Gutierrez, A., Fernandez-Rodriguez, M. A., Gala, J. and Otero-Hernandez, J. Quantifying mesenchymal stem cells in the mononuclear cell fraction of bone marrow samples obtained for cell therapy. Transplant Proc, 45, 434-439, 2013.

4. Amofa, D., Hulin, A., Nakada, Y., Sadek, H. A. and Yutzey, K. E. Hypoxia promotes primitive glycosaminoglycan-rich extracellular matrix composition in developing heart valves. Am J Physiol Heart Circ Physiol, 313, H1143-H1154, 2017.

5. Argento, G., Simonet, M., Oomens, C. W. and Baaijens, F. P. Multi-scale mechanical characterization of scaffolds for heart valve tissue engineering. J Biomech, 45, 2893-2898, 2012.

6. Assmann, A., Delfs, C., Munakata, H., Schiffer, F., Horstkotter, K., Huynh, K., Barth, M., Stoldt, V. R., Kamiya, H., Boeken, U., Lichtenberg, A. and Akhyari, P. Acceleration of autologous in vivo recellularization of decellularized aortic conduits by fibronectin surface coating. Biomaterials, 34, 6015-6026, 2013.

7. Badylak, S. F. Decellularized allogeneic and xenogeneic tissue as a bioscaffold for regenerative medicine: factors that influence the host response. Ann Biomed Eng, 42, 1517-1527, 2014.

8. Badylak, S. F. and Gilbert, T. W. Immune response to biologic scaffold materials. Semin Immunol, 20, 109-116, 2008.

9. Balachandran, K., Konduri, S., Sucosky, P., Jo, H. and Yoganathan, A. P. An ex vivo study of the biological properties of porcine aortic valves in response to circumferential cyclic stretch. Ann Biomed Eng, 34, 1655-1665, 2006.

10. Balguid, A., Mol, A., van Vlimmeren, M. A., Baaijens, F. P. and Bouten, C. V. Hypoxia induces near-native mechanical properties in engineered heart valve tissue. Circulation, 119, 290-297, 2009.

11. Balguid, A., Rubbens, M. P., Mol, A., Bank, R. A., Bogers, A. J., van Kats, J. P., de Mol, B. A., Baaijens, F. P. and Bouten, C. V. The role of collagen cross-links in biomechanical

behavior of human aortic heart valve leaflets--relevance for tissue engineering. Tissue Eng, 13, 1501-1511, 2007.

12. Ballotta, V., Smits, A. I., Driessen-Mol, A., Bouten, C. V. and Baaijens, F. P. Synergistic protein secretion by mesenchymal stromal cells seeded in 3D scaffolds and circulating leukocytes in physiological flow. Biomaterials, 35, 9100-9113, 2014.

13. Baraki, H., Tudorache, I., Braun, M., Hoffler, K., Gorler, A., Lichtenberg, A., Bara, C., Calistru, A., Brandes, G., Hewicker-Trautwein, M., Hilfiker, A., Haverich, A. and Cebotari, S. Orthotopic replacement of the aortic valve with decellularized allograft in a sheep model. Biomaterials, 30, 6240-6246, 2009.

14. Bechtel, J. F., Stierle, U. and Sievers, H. H. Fifty-two months' mean follow up of decellularized SynerGraft-treated pulmonary valve allografts. J Heart Valve Dis, 17, 98-104; discussion 104, 2008.

15. Berry, J. L., Steen, J. A., Koudy Williams, J., Jordan, J. E., Atala, A. and Yoo, J. J. Bioreactors for development of tissue engineered heart valves. Ann Biomed Eng, 38, 3272-3279, 2010.

16. Bertipaglia, B., Ortolani, F., Petrelli, L., Gerosa, G., Spina, M., Pauletto, P., Casarotto, D., Marchini, M., Sartore, S. and Vitalitate Exornatum Succedaneum Aorticum Labore Ingenioso Obtenibitur, P. Cell characterization of porcine aortic valve and decellularized leaflets repopulated with aortic valve interstitial cells: the VESALIO Project (Vitalitate Exornatum Succedaneum Aorticum Labore Ingenioso Obtenibitur). Ann Thorac Surg, 75, 1274-1282, 2003.

17. Bibevski, S., Ruzmetov, M., Fortuna, R. S., Turrentine, M. W., Brown, J. W. and Ohye, R. G. Performance of SynerGraft Decellularized Pulmonary Allografts Compared With Standard Cryopreserved Allografts: Results From Multiinstitutional Data. Ann Thorac Surg, 103, 869-874, 2017.

18. Bin, F., Yinglong, L., Nin, X., Kai, F., Laifeng, S. and Xiaodong, Z. Construction of tissue-engineered homograft bioprosthetic heart valves in vitro. ASAIO J, 52, 303-309, 2006.

19. Bloch, O., Erdbrugger, W., Volker, W., Schenk, A., Posner, S., Konertz, W. and Dohmen, P. M. Extracellular matrix in deoxycholic acid decellularized aortic heart valves. Med Sci Monit, 18, BR487-492, 2012.

20. Borghi, A., New, S. E., Chester, A. H., Taylor, P. M. and Yacoub, M. H. Time-dependent mechanical properties of aortic valve cusps: effect of glycosaminoglycan depletion. Acta Biomater, 9, 4645-4652, 2013.

21. Bourguignon, T., Bergoend, E., Mirza, A., Ayegnon, G., Neville, P., Aupart, M. R. and Marchand, M. Risk factors for valve-related complications after mechanical heart valve

replacement in 505 patients with long-term follow up. J Heart Valve Dis, 20, 673-680, 2011.

22. Brody, S. and Pandit, A. Approaches to heart valve tissue engineering scaffold design. J Biomed Mater Res B Appl Biomater, 83, 16-43, 2007.

23. Brown, J. W., Ruzmetov, M., Eltayeb, O., Rodefeld, M. D. and Turrentine, M. W. Performance of SynerGraft decellularized pulmonary homograft in patients undergoing a Ross procedure. Ann Thorac Surg, 91, 416-422; discussion 422-413, 2011.

24. Buravkova, L. B., Andreeva, E. R., Gogvadze, V. and Zhivotovsky, B. Mesenchymal stem cells and hypoxia: where are we? Mitochondrion, 19 Pt A, 105-112, 2014.

25. Butcher, J. T. and Nerem, R. M. Valvular endothelial cells regulate the phenotype of interstitial cells in co-culture: effects of steady shear stress. Tissue Eng, 12, 905-915, 2006.

26. Butcher, J. T., Tressel, S., Johnson, T., Turner, D., Sorescu, G., Jo, H. and Nerem, R. M. Transcriptional profiles of valvular and vascular endothelial cells reveal phenotypic differences: influence of shear stress. Arterioscler Thromb Vasc Biol, 26, 69-77, 2006.

27. Cebotari, S., Lichtenberg, A., Tudorache, I., Hilfiker, A., Mertsching, H., Leyh, R., Breymann, T., Kallenbach, K., Maniuc, L., Batrinac, A., Repin, O., Maliga, O., Ciubotaru, A. and Haverich, A. Clinical application of tissue engineered human heart valves using autologous progenitor cells. Circulation, 114, I132-137, 2006.

28. Cebotari, S., Tudorache, I., Ciubotaru, A., Boethig, D., Sarikouch, S., Goerler, A., Lichtenberg, A., Cheptanaru, E., Barnaciuc, S., Cazacu, A., Maliga, O., Repin, O., Maniuc, L., Breymann, T. and Haverich, A. Use of fresh decellularized allografts for pulmonary valve replacement may reduce the reoperation rate in children and young adults: early report. Circulation, 124, S115-123, 2011.

29. Cebotari, S., Tudorache, I., Jaekel, T., Hilfiker, A., Dorfman, S., Ternes, W., Haverich, A. and Lichtenberg, A. Detergent decellularization of heart valves for tissue engineering: toxicological effects of residual detergents on human endothelial cells. Artif Organs, 34, 206-210, 2010.

30. Chen, J. H. and Simmons, C. A. Cell-matrix interactions in the pathobiology of calcific aortic valve disease: critical roles for matricellular, matricrine, and matrix mechanics cues. Circ Res, 108, 1510-1524, 2011.

31. Cheung, D. Y., Duan, B. and Butcher, J. T. Current progress in tissue engineering of heart valves: multiscale problems, multiscale solutions. Expert Opin Biol Ther, 15, 1155-1172, 2015.

32. Converse, G. L., Armstrong, M., Quinn, R. W., Buse, E. E., Cromwell, M. L., Moriarty, S. J., Lofland, G. K., Hilbert, S. L. and Hopkins, R. A. Effects of cryopreservation,

decellularization and novel extracellular matrix conditioning on the quasi-static and time-dependent properties of the pulmonary valve leaflet. Acta Biomater, 8, 2722-2729, 2012.

33. Converse, G. L., Buse, E. E. and Hopkins, R. A. Bioreactors and operating room centric protocols for clinical heart valve tissue engineering. Progress in Pediatric Cardiology, 35, 95-100, 2013.

34. Converse, G. L., Buse, E. E., Neill, K. R., McFall, C. R., Lewis, H. N., VeDepo, M. C., Quinn, R. W. and Hopkins, R. A. Design and efficacy of a single-use bioreactor for heart valve tissue engineering. J Biomed Mater Res B Appl Biomater, 2015.

35. Corcione, A., Benvenuto, F., Ferretti, E., Giunti, D., Cappiello, V., Cazzanti, F., Risso, M., Gualandi, F., Mancardi, G. L., Pistoia, V. and Uccelli, A. Human mesenchymal stem cells modulate B-cell functions. Blood, 107, 367-372, 2006.

36. Crapo, P. M., Gilbert, T. W. and Badylak, S. F. An overview of tissue and whole organ decellularization processes. Biomaterials, 32, 3233-3243, 2011.

37.

38. d'Arcy, J. L., Prendergast, B. D., Chambers, J. B., Ray, S. G. and Bridgewater, B. Valvular heart disease: the next cardiac epidemic. Heart, 97, 91-93, 2011.

39. da Costa, F. D., Costa, A. C., Prestes, R., Domanski, A. C., Balbi, E. M., Ferreira, A. D. and Lopes, S. V. The early and midterm function of decellularized aortic valve allografts. Ann Thorac Surg, 90, 1854-1860, 2010.

40. Dainese, L., Guarino, A., Burba, I., Esposito, G., Pompilio, G., Polvani, G. and Rossini, A. Heart valve engineering: decellularized aortic homograft seeded with human cardiac stromal cells. J Heart Valve Dis, 21, 125-134, 2012.

41. Della Rocca, F., Sartore, S., Guidolin, D., Bertiplaglia, B., Gerosa, G., Casarotto, D. and Pauletto, P. Cell composition of the human pulmonary valve: a comparative study with the aortic valve--the VESALIO Project. Vitalitate Exornatum Succedaneum Aorticum labore Ingegnoso Obtinebitur. Ann Thorac Surg, 70, 1594-1600, 2000.

42. Deng, C., Dong, N., Shi, J., Chen, S., Xu, L., Shi, F., Hu, X. and Zhang, X. Application of decellularized scaffold combined with loaded nanoparticles for heart valve tissue engineering in vitro. J Huazhong Univ Sci Technolog Med Sci, 31, 88-93, 2011.

43. Deshmane, S. L., Kremlev, S., Amini, S. and Sawaya, B. E. Monocyte chemoattractant protein-1 (MCP-1): an overview. J Interferon Cytokine Res, 29, 313-326, 2009.

44. Doehring, T. C., Carew, E. O. and Vesely, I. The effect of strain rate on the viscoelastic response of aortic valve tissue: a direct-fit approach. Ann Biomed Eng, 32, 223-232, 2004.

45. Dohmen, P. M. Clinical results of implanted tissue engineered heart valves. HSR Proc Intensive Care Cardiovasc Anesth, 4, 225-231, 2012.

46. Dohmen, P. M., da Costa, F., Holinski, S., Lopes, S. V., Yoshi, S., Reichert, L. H., Villani, R., Posner, S. and Konertz, W. Is there a possibility for a glutaraldehyde-free porcine heart valve to grow? Eur Surg Res, 38, 54-61, 2006.

47. Dohmen, P. M., da Costa, F., Yoshi, S., Lopes, S. V., da Souza, F. P., Vilani, R., Wouk, A. F., da Costa, M. and Konertz, W. Histological evaluation of tissue-engineered heart valves implanted in the juvenile sheep model: is there a need for in-vitro seeding? J Heart Valve Dis, 15, 823-829, 2006.

48. Dohmen, P. M., Hauptmann, S., Terytze, A. and Konertz, W. F. In-vivo repopularization of a tissue-engineered heart valve in a human subject. J Heart Valve Dis, 16, 447-449, 2007.

49. Dohmen, P. M., Lembcke, A., Holinski, S., Kivelitz, D., Braun, J. P., Pruss, A. and Konertz, W. Mid-term clinical results using a tissue-engineered pulmonary valve to reconstruct the right ventricular outflow tract during the Ross procedure. Ann Thorac Surg, 84, 729-736, 2007.

50. Dohmen, P. M., Lembcke, A., Holinski, S., Pruss, A. and Konertz, W. Ten years of clinical results with a tissue-engineered pulmonary valve. Ann Thorac Surg, 92, 1308-1314, 2011.

51. Dohmen, P. M., Lembcke, A., Hotz, H., Kivelitz, D. and Konertz, W. F. Ross operation with a tissue-engineered heart valve. Ann Thorac Surg, 74, 1438-1442, 2002.

52. Duan, B., Hockaday, L. A., Das, S., Xu, C. and Butcher, J. T. Comparison of Mesenchymal Stem Cell Source Differentiation Toward Human Pediatric Aortic Valve Interstitial Cells Within 3D Engineered Matrices. Tissue Eng Part C Methods, 2015.

53. Eckert, C. E., Fan, R., Mikulis, B., Barron, M., Carruthers, C. A., Friebe, V. M., Vyavahare, N. R. and Sacks, M. S. On the biomechanical role of glycosaminoglycans in the aortic heart valve leaflet. Acta Biomater, 9, 4653-4660, 2013.

54. Ejtehadifar, M., Shamsasenjan, K., Movassaghpour, A., Akbarzadehlaleh, P., Dehdilani, N., Abbasi, P., Molaeipour, Z. and Saleh, M. The Effect of Hypoxia on Mesenchymal Stem Cell Biology. Adv Pharm Bull, 5, 141-149, 2015.

55. Emmert, M. Y., Weber, B., Wolint, P., Behr, L., Sammut, S., Frauenfelder, T., Frese, L., Scherman, J., Brokopp, C. E., Templin, C., Grunenfelder, J., Zund, G., Falk, V. and Hoerstrup, S. P. Stem cell-based transcatheter aortic valve implantation: first experiences in a pre-clinical model. JACC Cardiovasc Interv, 5, 874-883, 2012.

56. Erdbrugger, W., Konertz, W., Dohmen, P. M., Posner, S., Ellerbrok, H., Brodde, O. E., Robenek, H., Modersohn, D., Pruss, A., Holinski, S., Stein-Konertz, M. and Pauli, G.

Decellularized xenogenic heart valves reveal remodeling and growth potential in vivo. Tissue Eng, 12, 2059-2068, 2006.

57. Flameng, W., De Visscher, G., Mesure, L., Hermans, H., Jashari, R. and Meuris, B. Coating with fibronectin and stromal cell-derived factor-1alpha of decellularized homografts used for right ventricular outflow tract reconstruction eliminates immune response-related degeneration. J Thorac Cardiovasc Surg, 147, 1398-1404 e1392, 2014.

58. Friedrich, L. H., Jungebluth, P., Sjoqvist, S., Lundin, V., Haag, J. C., Lemon, G., Gustafsson, Y., Ajalloueian, F., Sotnichenko, A., Kielstein, H., Burguillos, M. A., Joseph, B., Teixeira, A. I., Lim, M. L. and Macchiarini, P. Preservation of aortic root architecture and properties using a detergent-enzymatic perfusion protocol. Biomaterials, 35, 1907-1913, 2014.

59. Gallegos, R. P., Nockel, P. J., Rivard, A. L. and Bianco, R. W. The current state of in-vivo pre-clinical animal models for heart valve evaluation. J Heart Valve Dis, 14, 423-432, 2005.

60. Gilbert, T. W. Strategies for tissue and organ decellularization. J Cell Biochem, 113, 2217-2222, 2012.

61. Go, A. S., Mozaffarian, D., Roger, V. L., Benjamin, E. J., Berry, J. D., Blaha, M. J., Dai, S., Ford, E. S., Fox, C. S., Franco, S., Fullerton, H. J., Gillespie, C., Hailpern, S. M., Heit, J. A., Howard, V. J., Huffman, M. D., Judd, S. E., Kissela, B. M., Kittner, S. J., Lackland, D. T., Lichtman, J. H., Lisabeth, L. D., Mackey, R. H., Magid, D. J., Marcus, G. M., Marelli, A., Matchar, D. B., McGuire, D. K., Mohler, E. R., 3rd, Moy, C. S., Mussolino, M. E., Neumar, R. W., Nichol, G., Pandey, D. K., Paynter, N. P., Reeves, M. J., Sorlie, P. D., Stein, J., Towfighi, A., Turan, T. N., Virani, S. S., Wong, N. D., Woo, D., Turner, M. B., American Heart Association Statistics, C. and Stroke Statistics, S. Heart disease and stroke statistics--2014 update: a report from the American Heart Association. Circulation, 129, e28-e292, 2014.

62. Goldstein, S., Clarke, D. R., Walsh, S. P., Black, K. S. and O'Brien, M. F. Transpecies heart valve transplant: advanced studies of a bioengineered xeno-autograft. Ann Thorac Surg, 70, 1962-1969, 2000.

63. Grauss, R. W., Hazekamp, M. G., Oppenhuizen, F., van Munsteren, C. J., Gittenberger-de Groot, A. C. and DeRuiter, M. C. Histological evaluation of decellularised porcine aortic valves: matrix changes due to different decellularisation methods. Eur J Cardiothorac Surg, 27, 566-571, 2005.

64. Gwanmesia, P., Ziegler, H., Eurich, R., Barth, M., Kamiya, H., Karck, M., Lichtenberg, A. and Akhyari, P. Opposite effects of transforming growth factor-beta1 and vascular endothelial growth factor on the degeneration of aortic valvular interstitial cell are modified by the extracellular matrix protein fibronectin: implications for heart valve engineering. Tissue Eng Part A, 16, 3737-3746, 2010.

65. Hasan, A., Ragaert, K., Swieszkowski, W., Selimovic, S., Paul, A., Camci-Unal, G., Mofrad, M. R. and Khademhosseini, A. Biomechanical properties of native and tissue engineered heart valve constructs. J Biomech, 47, 1949-1963, 2014.

66. Hoerstrup, S. P., Sodian, R., Daebritz, S., Wang, J., Bacha, E. A., Martin, D. P., Moran, A. M., Guleserian, K. J., Sperling, J. S., Kaushal, S., Vacanti, J. P., Schoen, F. J. and Mayer, J. E., Jr. Functional living trileaflet heart valves grown in vitro. Circulation, 102, III44-49, 2000.

67. Hof, A., Raschke, S., Baier, K., Nehrenheim, L., Selig, J. I., Schomaker, M., Lichtenberg, A., Meyer, H. and Akhyari, P. Challenges in developing a reseeded, tissue-engineered aortic valve prosthesis. Eur J Cardiothorac Surg, 50, 446-455, 2016.

68. Hong, H., Dong, N., Shi, J., Chen, S., Guo, C., Hu, P. and Qi, H. Fabrication of a novel hybrid scaffold for tissue engineered heart valve. J Huazhong Univ Sci Technolog Med Sci, 29, 599-603, 2009.

69. Honge, J. L., Funder, J., Hansen, E., Dohmen, P. M., Konertz, W. and Hasenkam, J. M. Recellularization of aortic valves in pigs. Eur J Cardiothorac Surg, 39, 829-834, 2011.

70. Hopkins, R. From cadaver harvested homograft valves to tissue-engineered valve conduits. Progress in Pediatric Cardiology, 21, 137-152, 2006.

71. Hopkins, R. A., Bert, A. A., Hilbert, S. L., Quinn, R. W., Brasky, K. M., Drake, W. B. and Lofland, G. K. Bioengineered human and allogeneic pulmonary valve conduits chronically implanted orthotopically in baboons: hemodynamic performance and immunologic consequences. J Thorac Cardiovasc Surg, 145, 1098-1107, 2013.

72. Hopkins, R. A., Jones, A. L., Wolfinbarger, L., Moore, M. A., Bert, A. A. and Lofland, G. K. Decellularization reduces calcification while improving both durability and 1-year functional results of pulmonary homograft valves in juvenile sheep. J Thorac Cardiovasc Surg, 137, 907-913, 913e901-904, 2009.

73. Hu, X. J., Dong, N. G., Shi, J. W., Deng, C., Li, H. D. and Lu, C. F. Evaluation of a novel tetra-functional branched poly(ethylene glycol) crosslinker for manufacture of crosslinked, decellularized, porcine aortic valve leaflets. J Biomed Mater Res B Appl Biomater, 102, 322-336, 2014.

74. Huang, W., Xiao, D. Z., Wang, Y., Shan, Z. X., Liu, X. Y., Lin, Q. X., Yang, M., Zhuang, J., Li, Y. and Yu, X. Y. Fn14 promotes differentiation of human mesenchymal stem cells into heart valvular interstitial cells by phenotypic characterization. J Cell Physiol, 229, 580-587, 2014.

75. Iop, L., Bonetti, A., Naso, F., Rizzo, S., Cagnin, S., Bianco, R., Dal Lin, C., Martini, P., Poser, H., Franci, P., Lanfranchi, G., Busetto, R., Spina, M., Basso, C., Marchini, M., Gandaglia, A., Ortolani, F. and Gerosa, G. Decellularized allogeneic heart valves

demonstrate self-regeneration potential after a long-term preclinical evaluation. PLoS One, 9, e99593, 2014.

76. Iop, L. and Gerosa, G. Guided tissue regeneration in heart valve replacement: from preclinical research to first-in-human trials. Biomed Res Int, 2015, 432901, 2015.

77. Iop, L., Renier, V., Naso, F., Piccoli, M., Bonetti, A., Gandaglia, A., Pozzobon, M., Paolin, A., Ortolani, F., Marchini, M., Spina, M., De Coppi, P., Sartore, S. and Gerosa, G. The influence of heart valve leaflet matrix characteristics on the interaction between human mesenchymal stem cells and decellularized scaffolds. Biomaterials, 30, 4104-4116, 2009.

78. Iwai, S., Torikai, K., Coppin, C. M. and Sawa, Y. Minimally immunogenic decellularized porcine valve provides in situ recellularization as a stentless bioprosthetic valve. J Artif Organs, 10, 29-35, 2007.

79. James, I., Yi, T., Tara, S., Best, C. A., Stuber, A. J., Shah, K. V., Austin, B. F., Sugiura, T., Lee, Y. U., Lincoln, J., Trask, A. J., Shinoka, T. and Breuer, C. K. Hemodynamic Characterization of a Mouse Model for Investigating the Cellular and Molecular Mechanisms of Neotissue Formation in Tissue Engineered Heart Valves. Tissue Eng Part C Methods, 2015.

80. Jana, S., Tranquillo, R. T. and Lerman, A. Cells for tissue engineering of cardiac valves. J Tissue Eng Regen Med, 2015.

81. Jiao, T., Clifton, R. J., Converse, G. L. and Hopkins, R. A. Measurements of the effects of decellularization on viscoelastic properties of tissues in ovine, baboon, and human heart valves. Tissue Eng Part A, 18, 423-431, 2012.

82. Jing, H., Wang, Z. and Chang, Q. De-Endothelialized Aortic Homografts: A Promising Scaffold Material for Tissue-Engineered Heart Valves. Cells Tissues Organs, 200, 195-203, 2014.

83. Jordan, J. E., Williams, J. K., Lee, S. J., Raghavan, D., Atala, A. and Yoo, J. J. Bioengineered self-seeding heart valves. J Thorac Cardiovasc Surg, 143, 201-208, 2012.

84. Juthier, F., Vincentelli, A., Gaudric, J., Corseaux, D., Fouquet, O., Calet, C., Le Tourneau, T., Soenen, V., Zawadzki, C., Fabre, O., Susen, S., Prat, A. and Jude, B. Decellularized heart valve as a scaffold for in vivo recellularization: deleterious effects of granulocyte colony-stimulating factor. J Thorac Cardiovasc Surg, 131, 843-852, 2006.

85. Kajbafzadeh, A. M., Ahmadi Tafti, S. H., Mokhber-Dezfooli, M. R., Khorramirouz, R., Sabetkish, S., Sabetkish, N., Rabbani, S., Tavana, H. and Mohseni, M. J. Aortic valve conduit implantation in the descending thoracic aorta in a sheep model: The outcomes of pre-seeded scaffold. Int J Surg, 28, 97-105, 2016.

86. Kasimir, M. T., Rieder, E., Seebacher, G., Nigisch, A., Dekan, B., Wolner, E., Weigel, G. and Simon, P. Decellularization does not eliminate thrombogenicity and inflammatory

stimulation in tissue-engineered porcine heart valves. J Heart Valve Dis, 15, 278-286; discussion 286, 2006.

87. Kasimir, M. T., Rieder, E., Seebacher, G., Silberhumer, G., Wolner, E., Weigel, G. and Simon, P. Comparison of different decellularization procedures of porcine heart valves. Int J Artif Organs, 26, 421-427, 2003.

88. Kasyanov, V., Moreno-Rodriguez, R. A., Kalejs, M., Ozolanta, I., Stradins, P., Wen, X., Yao, H. and Mironov, V. Age-related analysis of structural, biochemical and mechanical properties of the porcine mitral heart valve leaflets. Connect Tissue Res, 54, 394-402, 2013.

89. Keane, T. J., Londono, R., Turner, N. J. and Badylak, S. F. Consequences of ineffective decellularization of biologic scaffolds on the host response. Biomaterials, 33, 1771-1781, 2012.

90. Kim, S. S., Lim, S. H., Hong, Y. S., Cho, S. W., Ryu, J. H., Chang, B. C., Choi, C. Y. and Kim, B. S. Tissue engineering of heart valves in vivo using bone marrow-derived cells. Artif Organs, 30, 554-557, 2006.

91. Kindt, E., Rossi, D. T., Gueneva-Boucheva, K. and Hallak, H. Quantitative method for biomarkers of collagen degradation using liquid chromatography tandem mass spectrometry. Anal Biochem, 283, 71-76, 2000.

92. Kinnaird, T., Stabile, E., Burnett, M. S., Lee, C. W., Barr, S., Fuchs, S. and Epstein, S. E. Marrow-derived stromal cells express genes encoding a broad spectrum of arteriogenic cytokines and promote in vitro and in vivo arteriogenesis through paracrine mechanisms. Circ Res, 94, 678-685, 2004.

93. Kluin, J., Talacua, H., Smits, A. I., Emmert, M. Y., Brugmans, M. C., Fioretta, E. S., Dijkman, P. E., Sontjens, S. H., Duijvelshoff, R., Dekker, S., Janssen-van den Broek, M. W., Lintas, V., Vink, A., Hoerstrup, S. P., Janssen, H. M., Dankers, P. Y., Baaijens, F. P. and Bouten, C. V. In situ heart valve tissue engineering using a bioresorbable elastomeric implant - From material design to 12 months follow-up in sheep. Biomaterials, 125, 101-117, 2017.

94. Knight, R. L., Booth, C., Wilcox, H. E., Fisher, J. and Ingham, E. Tissue engineering of cardiac valves: re-seeding of acellular porcine aortic valve matrices with human mesenchymal progenitor cells. J Heart Valve Dis, 14, 806-813, 2005.

95. Konertz, W., Angeli, E., Tarusinov, G., Christ, T., Kroll, J., Dohmen, P. M., Krogmann, O., Franzbach, B., Pace Napoleone, C. and Gargiulo, G. Right ventricular outflow tract reconstruction with decellularized porcine xenografts in patients with congenital heart disease. J Heart Valve Dis, 20, 341-347, 2011.

96. Konuma, T., Devaney, E. J., Bove, E. L., Gelehrter, S., Hirsch, J. C., Tavakkol, Z. and Ohye, R. G. Performance of CryoValve SG decellularized pulmonary allografts

compared with standard cryopreserved allografts. Ann Thorac Surg, 88, 849-854; discussion 554-845, 2009.

97. Korossis, S. A., Booth, C., Wilcox, H. E., Watterson, K. G., Kearney, J. N., Fisher, J. and Ingham, E. Tissue engineering of cardiac valve prostheses II: biomechanical characterization of decellularized porcine aortic heart valves. J Heart Valve Dis, 11, 463-471, 2002.

98. Kurobe, H., Tara, S., Maxfield, M. W., Rocco, K. A., Bagi, P. S., Yi, T., Udelsman, B. V., Dean, E. W., Khosravi, R., Powell, H. M., Shinoka, T. and Breuer, C. K. Comparison of the Biological Equivalence of Two Methods for Isolating Bone Marrow Mononuclear Cells for Fabricating Tissue-Engineered Vascular Grafts. Tissue Eng Part C Methods, 21, 597-604, 2015.

99. Leyh, R. G., Wilhelmi, M., Rebe, P., Fischer, S., Kofidis, T., Haverich, A. and Mertsching, H. In vivo repopulation of xenogeneic and allogeneic acellular valve matrix conduits in the pulmonary circulation. Ann Thorac Surg, 75, 1457-1463; discussion 1463, 2003.

100. Li, F., Li, W., Johnson, S., Ingram, D., Yoder, M. and Badylak, S. Low-molecular-weight peptides derived from extracellular matrix as chemoattractants for primary endothelial cells. Endothelium, 11, 199-206, 2004.

101. Liao, J., Joyce, E. M. and Sacks, M. S. Effects of decellularization on the mechanical and structural properties of the porcine aortic valve leaflet. Biomaterials, 29, 1065-1074, 2008.

102. Liao, J., Yang, L., Grashow, J. and Sacks, M. S. The relation between collagen fibril kinematics and mechanical properties in the mitral valve anterior leaflet. J Biomech Eng, 129, 78-87, 2007.

103. Lichtenberg, A., Cebotari, S., Tudorache, I., Sturz, G., Winterhalter, M., Hilfiker, A. and Haverich, A. Flow-dependent re-endothelialization of tissue-engineered heart valves. J Heart Valve Dis, 15, 287-293; discussion 293-284, 2006.

104. Lichtenberg, A., Tudorache, I., Cebotari, S., Ringes-Lichtenberg, S., Sturz, G., Hoeffler, K., Hurscheler, C., Brandes, G., Hilfiker, A. and Haverich, A. In vitro re-endothelialization of detergent decellularized heart valves under simulated physiological dynamic conditions. Biomaterials, 27, 4221-4229, 2006.

105. Liu, A. C., Joag, V. R. and Gotlieb, A. I. The emerging role of valve interstitial cell phenotypes in regulating heart valve pathobiology. Am J Pathol, 171, 1407-1418, 2007.

106. Lovekamp, J. J., Simionescu, D. T., Mercuri, J. J., Zubiate, B., Sacks, M. S. and Vyavahare, N. R. Stability and function of glycosaminoglycans in porcine bioprosthetic heart valves. Biomaterials, 27, 1507-1518, 2006.

107. Lu, X., Zhai, W., Zhou, Y., Zhou, Y., Zhang, H. and Chang, J. Crosslinking effect of Nordihydroguaiaretic acid (NDGA) on decellularized heart valve scaffold for tissue engineering. J Mater Sci Mater Med, 21, 473-480, 2010.

108. Luo, J., Korossis, S. A., Wilshaw, S. P., Jennings, L. M., Fisher, J. and Ingham, E. Development and Characterization of Acellular Porcine Pulmonary Valve Scaffolds for Tissue Engineering. Tissue Eng Part A, 2014.

109. Ma, T., Grayson, W. L., Frohlich, M. and Vunjak-Novakovic, G. Hypoxia and stem cell-based engineering of mesenchymal tissues. Biotechnol Prog, 25, 32-42, 2009.

110. Maish, M. S., Hoffman-Kim, D., Krueger, P. M., Souza, J. M., Harper, J. J., 3rd and Hopkins, R. A. Tricuspid valve biopsy: a potential source of cardiac myofibroblast cells for tissue-engineered cardiac valves. J Heart Valve Dis, 12, 264-269, 2003.

111. Martin, C. and Sun, W. Biomechanical characterization of aortic valve tissue in humans and common animal models. J Biomed Mater Res A, 100, 1591-1599, 2012.

112. Mendoza-Novelo, B., Avila, E. E., Cauich-Rodriguez, J. V., Jorge-Herrero, E., Rojo, F. J., Guinea, G. V. and Mata-Mata, J. L. Decellularization of pericardial tissue and its impact on tensile viscoelasticity and glycosaminoglycan content. Acta Biomater, 7, 1241-1248, 2011.

113. Merryman, W. D., Bieniek, P. D., Guilak, F. and Sacks, M. S. Viscoelastic properties of the aortic valve interstitial cell. J Biomech Eng, 131, 041005, 2009.

114. Merryman, W. D., Lukoff, H. D., Long, R. A., Engelmayr, G. C., Jr., Hopkins, R. A. and Sacks, M. S. Synergistic effects of cyclic tension and transforming growth factor-beta1 on the aortic valve myofibroblast. Cardiovasc Pathol, 16, 268-276, 2007.

115. Merryman, W. D., Youn, I., Lukoff, H. D., Krueger, P. M., Guilak, F., Hopkins, R. A. and Sacks, M. S. Correlation between heart valve interstitial cell stiffness and transvalvular pressure: implications for collagen biosynthesis. Am J Physiol Heart Circ Physiol, 290, H224-231, 2006.

116. Meyer, S. R., Chiu, B., Churchill, T. A., Zhu, L., Lakey, J. R. and Ross, D. B. Comparison of aortic valve allograft decellularization techniques in the rat. J Biomed Mater Res A, 79, 254-262, 2006.

117. Mol, A., Smits, A. I., Bouten, C. V. and Baaijens, F. P. Tissue engineering of heart valves: advances and current challenges. Expert Rev Med Devices, 6, 259-275, 2009.

118. Naso, F., Gandaglia, A., Formato, M., Cigliano, A., Lepedda, A. J., Gerosa, G. and Spina, M. Differential distribution of structural components and hydration in aortic and pulmonary heart valve conduits: Impact of detergent-based cell removal. Acta Biomater, 6, 4675-4688, 2010.

119. Neumann, A., Cebotari, S., Tudorache, I., Haverich, A. and Sarikouch, S. Heart valve engineering: decellularized allograft matrices in clinical practice. Biomed Tech (Berl), 58, 453-456, 2013.

120. Neumann, A., Sarikouch, S., Breymann, T., Cebotari, S., Boethig, D., Horke, A., Beerbaum, P., Westhoff-Bleck, M., Bertram, H., Ono, M., Tudorache, I., Haverich, A. and Beutel, G. Early systemic cellular immune response in children and young adults receiving decellularized fresh allografts for pulmonary valve replacement. Tissue Eng Part A, 20, 1003-1011, 2014.

121. Nkomo, V. T., Gardin, J. M., Skelton, T. N., Gottdiener, J. S., Scott, C. G. and Enriquez-Sarano, M. Burden of valvular heart diseases: a population-based study. Lancet, 368, 1005-1011, 2006.

122. Ota, T., Sawa, Y., Iwai, S., Kitajima, T., Ueda, Y., Coppin, C., Matsuda, H. and Okita, Y. Fibronectin-hepatocyte growth factor enhances reendothelialization in tissue-engineered heart valve. Ann Thorac Surg, 80, 1794-1801, 2005.

123. Ouyang, H., Zhang, J. B., Liu, Y., Li, Q., Peng, Y. H., Kang, X. J., Wang, Y. M., Wei, X. F., Yi, D. H. and Liu, W. Y. [Research on application of modified polyethylene glycol hydrogels in the construction of tissue engineered heart valve]. Zhonghua Wai Ke Za Zhi, 46, 1723-1726, 2008.

124. Pacelli, S., Basu, S., Whitlow, J., Chakravarti, A., Acosta, F., Varshney, A., Modaresi, S., Berkland, C. and Paul, A. Strategies to develop endogenous stem cell-recruiting bioactive materials for tissue repair and regeneration. Adv Drug Deliv Rev, 120, 50-70, 2017.

125. Paniagua Gutierrez, J. R., Berry, H., Korossis, S., Mirsadraee, S., Lopes, S. V., da Costa, F., Kearney, J., Watterson, K., Fisher, J. and Ingham, E. Regenerative Potential of Low-Concentration SDS-Decellularized Porcine Aortic Valved Conduits In Vivo. Tissue Eng Part A, 21, 332-342, 2015.

126. Parvin Nejad, S., Blaser, M. C., Santerre, J. P., Caldarone, C. A. and Simmons, C. A. Biomechanical conditioning of tissue engineered heart valves: Too much of a good thing? Adv Drug Deliv Rev, 96, 161-175, 2016.

127. Perri, G., Polito, A., Esposito, C., Albanese, S. B., Francalanci, P., Pongiglione, G. and Carotti, A. Early and late failure of tissue-engineered pulmonary valve conduits used for right ventricular outflow tract reconstruction in patients with congenital heart disease. Eur J Cardiothorac Surg, 41, 1320-1325, 2012.

128. Pratt, D. A., Daniloff, Y., Duncan, A. and Robins, S. P. Automated analysis of the pyridinium crosslinks of collagen in tissue and urine using solid-phase extraction and reversed-phase high-performance liquid chromatography. Anal Biochem, 207, 168-175, 1992.

129.

130. Qiao, W. H., Liu, P., Hu, D., Al Shirbini, M., Zhou, X. M. and Dong, N. G. Sequential hydrophile and lipophile solubilization as an efficient method for decellularization of porcine aortic valve leaflets: Structure, mechanical property and biocompatibility study. J Tissue Eng Regen Med, 2016.

131. Quinn, R., Hilbert, S., Converse, G., Bert, A., Buse, E., Drake, W., Armstrong, M., Moriarty, S., Lofland, G. and Hopkins, R. Enhanced Autologous Re-endothelialization of Decellularized and Extracellular Matrix Conditioned Allografts Implanted Into the Right Ventricular Outflow Tracts of Juvenile Sheep. Cardiovascular Engineering and Technology, 3, 217-227, 2012.

132. Quinn, R. W., Bert, A. A., Converse, G. L., Buse, E. E., Hilbert, S. L., Drake, W. B. and Hopkins, R. A. Performance of Allogeneic Bioengineered Replacement Pulmonary Valves in Rapidly Growing Young Lambs. J Thorac Cardiovasc Surg, 2016.

133. Quinn, R. W., Hilbert, S. L., Bert, A. A., Drake, B. W., Bustamante, J. A., Fenton, J. E., Moriarty, S. J., Neighbors, S. L., Lofland, G. K. and Hopkins, R. A. Performance and morphology of decellularized pulmonary valves implanted in juvenile sheep. Ann Thorac Surg, 92, 131-137, 2011.

134. Rath, S., Salinas, M., Villegas, A. G. and Ramaswamy, S. Differentiation and Distribution of Marrow Stem Cells in Flex-Flow Environments Demonstrate Support of the Valvular Phenotype. PLoS One, 10, e0141802, 2015.

135. Rieder, E., Kasimir, M. T., Silberhumer, G., Seebacher, G., Wolner, E., Simon, P. and Weigel, G. Decellularization protocols of porcine heart valves differ importantly in efficiency of cell removal and susceptibility of the matrix to recellularization with human vascular cells. J Thorac Cardiovasc Surg, 127, 399-405, 2004.

136. Rieder, E., Seebacher, G., Kasimir, M. T., Eichmair, E., Winter, B., Dekan, B., Wolner, E., Simon, P. and Weigel, G. Tissue engineering of heart valves: decellularized porcine and human valve scaffolds differ importantly in residual potential to attract monocytic cells. Circulation, 111, 2792-2797, 2005.

137. Roh, J. D., Sawh-Martinez, R., Brennan, M. P., Jay, S. M., Devine, L., Rao, D. A., Yi, T., Mirensky, T. L., Nalbandian, A., Udelsman, B., Hibino, N., Shinoka, T., Saltzman, W. M., Snyder, E., Kyriakides, T. R., Pober, J. S. and Breuer, C. K. Tissue-engineered vascular grafts transform into mature blood vessels via an inflammation-mediated process of vascular remodeling. Proc Natl Acad Sci U S A, 107, 4669-4674, 2010.

138. Ruffer, A., Purbojo, A., Cicha, I., Glockler, M., Potapov, S., Dittrich, S. and Cesnjevar, R. A. Early failure of xenogenous de-cellularised pulmonary valve conduits--a word of caution! Eur J Cardiothorac Surg, 38, 78-85, 2010.

139. Ruzmetov, M., Shah, J. J., Geiss, D. M. and Fortuna, R. S. Decellularized versus standard cryopreserved valve allografts for right ventricular outflow tract reconstruction: a single-institution comparison. J Thorac Cardiovasc Surg, 143, 543-549, 2012.

140. Sako, E. Y. Newer concepts in the surgical treatment of valvular heart disease. Curr Cardiol Rep, 6, 100-105, 2004.

141. Sands, M. P., Rittenhouse, E. A., Mohri, H. and Merendino, K. A. An anatomical comparison of human pig, calf, and sheep aortic valves. Ann Thorac Surg, 8, 407-414, 1969.

142. Sarikouch, S., Horke, A., Tudorache, I., Beerbaum, P., Westhoff-Bleck, M., Boethig, D., Repin, O., Maniuc, L., Ciubotaru, A., Haverich, A. and Cebotari, S. Decellularized fresh homografts for pulmonary valve replacement: a decade of clinical experience. Eur J Cardiothorac Surg, 2016.

143. Sawada, K., Terada, D., Yamaoka, T., Kitamura, S. and Fujisato, T. Cell removal with supercritical carbon dioxide for acellular artificial tissue. J Chem Technol Biotechnol, 943-949, 2008.

144. Schenke-Layland, K., Opitz, F., Gross, M., Doring, C., Halbhuber, K. J., Schirrmeister, F., Wahlers, T. and Stock, U. A. Complete dynamic repopulation of decellularized heart valves by application of defined physical signals-an in vitro study. Cardiovasc Res, 60, 497-509, 2003.

145. Schenke-Layland, K., Vasilevski, O., Opitz, F., Konig, K., Riemann, I., Halbhuber, K. J., Wahlers, T. and Stock, U. A. Impact of decellularization of xenogeneic tissue on extracellular matrix integrity for tissue engineering of heart valves. J Struct Biol, 143, 201-208, 2003.

146. Schmidt, D., Dijkman, P. E., Driessen-Mol, A., Stenger, R., Mariani, C., Puolakka, A., Rissanen, M., Deichmann, T., Odermatt, B., Weber, B., Emmert, M. Y., Zund, G., Baaijens, F. P. and Hoerstrup, S. P. Minimally-invasive implantation of living tissue engineered heart valves: a comprehensive approach from autologous vascular cells to stem cells. J Am Coll Cardiol, 56, 510-520, 2010.

147. Schnell, A. M., Hoerstrup, S. P., Zund, G., Kolb, S., Sodian, R., Visjager, J. F., Grunenfelder, J., Suter, A. and Turina, M. Optimal cell source for cardiovascular tissue engineering: venous vs. aortic human myofibroblasts. Thorac Cardiovasc Surg, 49, 221-225, 2001.

148. Schoen, F. J. Cardiac valves and valvular pathology: update on function, disease, repair, and replacement. Cardiovasc Pathol, 14, 189-194, 2005.

149. Siddiqui, R. F., Abraham, J. R. and Butany, J. Bioprosthetic heart valves: modes of failure. Histopathology, 55, 135-144, 2009.

150. Sidney, L. E., Branch, M. J., Dunphy, S. E., Dua, H. S. and Hopkinson, A. Concise review: evidence for CD34 as a common marker for diverse progenitors. Stem Cells, 32, 1380-1389, 2014.

151. Sierad, L. N., Shaw, E. L., Bina, A., Brazile, B., Rierson, N., Patnaik, S. S., Kennamer, A., Odum, R., Cotoi, O., Terezia, P., Branzaniuc, K., Smallwood, H., Deac, R., Egyed, I., Pavai, Z., Szanto, A., Harceaga, L., Suciu, H., Raicea, V., Olah, P., Simionescu, A., Liao, J., Movileanu, I., Harpa, M. and Simionescu, D. T. Functional Heart Valve Scaffolds Obtained by Complete Decellularization of Porcine Aortic Roots in a Novel Differential Pressure Gradient Perfusion System. Tissue Eng Part C Methods, 21, 1284-1296, 2015.

152. Sierad, L. N., Simionescu, A., Albers, C., Chen, J., Maivelett, J., Tedder, M. E., Liao, J. and Simionescu, D. T. Design and Testing of a Pulsatile Conditioning System for Dynamic Endothelialization of Polyphenol-Stabilized Tissue Engineered Heart Valves. Cardiovasc Eng Technol, 1, 138-153, 2010.

153. Sievers, H. H., Stierle, U., Schmidtke, C. and Bechtel, M. Decellularized pulmonary homograft (SynerGraft) for reconstruction of the right ventricular outflow tract: first clinical experience. Z Kardiol, 92, 53-59, 2003.

154. Simon, P., Kasimir, M. T., Seebacher, G., Weigel, G., Ullrich, R., Salzer-Muhar, U., Rieder, E. and Wolner, E. Early failure of the tissue engineered porcine heart valve SYNERGRAFT in pediatric patients. Eur J Cardiothorac Surg, 23, 1002-1006; discussion 1006, 2003.

155. Slazansky, M., Polzer, S., Man, V. and Bursa, J. Analysis of Accuracy of Biaxial Tests Based on their Computational Simulations. Strain, 52, 424-435, 2016.

156. Smits, A. I., Ballotta, V., Driessen-Mol, A., Bouten, C. V. and Baaijens, F. P. Shear flow affects selective monocyte recruitment into MCP-1-loaded scaffolds. J Cell Mol Med, 18, 2176-2188, 2014.

157. Somers, P., De Somer, F., Cornelissen, M., Thierens, H. and Van Nooten, G. Decellularization of heart valve matrices: search for the ideal balance. Artif Cells Blood Substit Immobil Biotechnol, 40, 151-162, 2012.

158. Spaggiari, G. M., Capobianco, A., Abdelrazik, H., Becchetti, F., Mingari, M. C. and Moretta, L. Mesenchymal stem cells inhibit natural killer-cell proliferation, cytotoxicity, and cytokine production: role of indoleamine 2,3-dioxygenase and prostaglandin E2. Blood, 111, 1327-1333, 2008.

159. Spina, M., Ortolani, F., El Messlemani, A., Gandaglia, A., Bujan, J., Garcia-Honduvilla, N., Vesely, I., Gerosa, G., Casarotto, D., Petrelli, L. and Marchini, M. Isolation of intact aortic valve scaffolds for heart-valve bioprostheses: extracellular matrix structure, prevention from calcification, and cell repopulation features. J Biomed Mater Res A, 67, 1338-1350, 2003.

160. Stamm, C., Khosravi, A., Grabow, N., Schmohl, K., Treckmann, N., Drechsel, A., Nan, M., Schmitz, K. P., Haubold, A. and Steinhoff, G. Biomatrix/polymer composite material for heart valve tissue engineering. Ann Thorac Surg, 78, 2084-2092; discussion 2092-2083, 2004.

161. Steinhoff, G., Stock, U., Karim, N., Mertsching, H., Timke, A., Meliss, R. R., Pethig, K., Haverich, A. and Bader, A. Tissue engineering of pulmonary heart valves on allogenic acellular matrix conduits: in vivo restoration of valve tissue. Circulation, 102, III50-55, 2000.

162. Stella, J. A., Liao, J. and Sacks, M. S. Time-dependent biaxial mechanical behavior of the aortic heart valve leaflet. J Biomech, 40, 3169-3177, 2007.

163. Stephens, E. H. and Grande-Allen, K. J. Age-related changes in collagen synthesis and turnover in porcine heart valves. J Heart Valve Dis, 16, 672-682, 2007.

164. Syedain, Z., Reimer, J., Schmidt, J., Lahti, M., Berry, J., Bianco, R. and Tranquillo, R. T. 6-month aortic valve implantation of an off-the-shelf tissue-engineered valve in sheep. Biomaterials, 73, 175-184, 2015.

165. Syedain, Z. H., Bradee, A. R., Kren, S., Taylor, D. A. and Tranquillo, R. T. Decellularized tissue-engineered heart valve leaflets with recellularization potential. Tissue Eng Part A, 19, 759-769, 2013.

166. Syedain, Z. H., Meier, L. A., Reimer, J. M. and Tranquillo, R. T. Tubular heart valves from decellularized engineered tissue. Ann Biomed Eng, 41, 2645-2654, 2013.

167. Takagi, K., Fukunaga, S., Nishi, A., Shojima, T., Yoshikawa, K., Hori, H., Akashi, H. and Aoyagi, S. In vivo recellularization of plain decellularized xenografts with specific cell characterization in the systemic circulation: histological and immunohistochemical study. Artif Organs, 30, 233-241, 2006.

168. Tavakkol, Z., Gelehrter, S., Goldberg, C. S., Bove, E. L., Devaney, E. J. and Ohye, R. G. Superior durability of SynerGraft pulmonary allografts compared with standard cryopreserved allografts. Ann Thorac Surg, 80, 1610-1614, 2005.

169. Thayer, P., Balachandran, K., Rathan, S., Yap, C. H., Arjunon, S., Jo, H. and Yoganathan, A. P. The effects of combined cyclic stretch and pressure on the aortic valve interstitial cell phenotype. Ann Biomed Eng, 39, 1654-1667, 2011.

170. Theodoridis, K., Tudorache, I., Calistru, A., Cebotari, S., Meyer, T., Sarikouch, S., Bara, C., Brehm, R., Haverich, A. and Hilfiker, A. Successful matrix guided tissue regeneration of decellularized pulmonary heart valve allografts in elderly sheep. Biomaterials, 52, 221-228, 2015.

171. Tudorache, I., Calistru, A., Baraki, H., Meyer, T., Hoffler, K., Sarikouch, S., Bara, C., Gorler, A., Hartung, D., Hilfiker, A., Haverich, A. and Cebotari, S. Orthotopic replacement of aortic heart valves with tissue-engineered grafts. Tissue Eng Part A, 19, 1686-1694, 2013.

172. Tudorache, I., Cebotari, S., Sturz, G., Kirsch, L., Hurschler, C., Hilfiker, A., Haverich, A. and Lichtenberg, A. Tissue engineering of heart valves: biomechanical and

morphological properties of decellularized heart valves. J Heart Valve Dis, 16, 567-573; discussion 574, 2007.

173. VeDepo, M. C., Buse, E. E., Quinn, R. W., Williams, T., Detamore, M. S., Hopkins, R. A. and Converse, G. L. Species-Specific Effects of Aortic Valve Decellularization. Acta Biomater, 2017.

174. VeDepo, M. C., Detamore, M., Hopkins, R. A. and Converse, G. L. Recellularization of decellularized heart valves: Progress toward the tissue-engineered heart valve. Journal of Tissue Engineering, 8, 2041731417726327, 2017.

175. Vincentelli, A., Wautot, F., Juthier, F., Fouquet, O., Corseaux, D., Marechaux, S., Le Tourneau, T., Fabre, O., Susen, S., Van Belle, E., Mouquet, F., Decoene, C., Prat, A. and Jude, B. In vivo autologous recellularization of a tissue-engineered heart valve: are bone marrow mesenchymal stem cells the best candidates? J Thorac Cardiovasc Surg, 134, 424-432, 2007.

176. Voges, I., Brasen, J. H., Entenmann, A., Scheid, M., Scheewe, J., Fischer, G., Hart, C., Andrade, A., Pham, H. M., Kramer, H. H. and Rickers, C. Adverse results of a decellularized tissue-engineered pulmonary valve in humans assessed with magnetic resonance imaging. Eur J Cardiothorac Surg, 44, e272-279, 2013.

177. Wang, S., Goecke, T., Meixner, C., Haverich, A., Hilfiker, A. and Wolkers, W. F. Freeze-dried heart valve scaffolds. Tissue Eng Part C Methods, 18, 517-525, 2012.

178. Weber, B., Scherman, J., Emmert, M. Y., Gruenenfelder, J., Verbeek, R., Bracher, M., Black, M., Kortsmit, J., Franz, T., Schoenauer, R., Baumgartner, L., Brokopp, C., Agarkova, I., Wolint, P., Zund, G., Falk, V., Zilla, P. and Hoerstrup, S. P. Injectable living marrow stromal cell-based autologous tissue engineered heart valves: first experiences with a one-step intervention in primates. Eur Heart J, 32, 2830-2840, 2011.

179. Williams, J. K., Miller, E. S., Lane, M. R., Atala, A., Yoo, J. J. and Jordan, J. E. Characterization of CD133 Antibody-Directed Recellularized Heart Valves. J Cardiovasc Transl Res, 8, 411-420, 2015.

180. Wong, M. L. and Griffiths, L. G. Immunogenicity in xenogeneic scaffold generation: antigen removal vs. decellularization. Acta Biomater, 10, 1806-1816, 2014.

181. Wong, M. L., Leach, J. K., Athanasiou, K. A. and Griffiths, L. G. The role of protein solubilization in antigen removal from xenogeneic tissue for heart valve tissue engineering. Biomaterials, 32, 8129-8138, 2011.

182. Wong, M. L., Wong, J. L., Athanasiou, K. A. and Griffiths, L. G. Stepwise solubilization-based antigen removal for xenogeneic scaffold generation in tissue engineering. Acta Biomater, 9, 6492-6501, 2013.

183.

184. Xue, Y., Sant, V., Phillippi, J. and Sant, S. Biodegradable and biomimetic elastomeric scaffolds for tissue-engineered heart valves. Acta Biomater, 48, 2-19, 2017.

185. Yacoub, M. H. and Takkenberg, J. J. Will heart valve tissue engineering change the world? Nat Clin Pract Cardiovasc Med, 2, 60-61, 2005.

186. Yamamoto, K., Takahashi, T., Asahara, T., Ohura, N., Sokabe, T., Kamiya, A. and Ando, J. Proliferation, differentiation, and tube formation by endothelial progenitor cells in response to shear stress. J Appl Physiol (1985), 95, 2081-2088, 2003.

187. Ye, X., Hu, X., Wang, H., Liu, J. and Zhao, Q. Polyelectrolyte multilayer film on decellularized porcine aortic valve can reduce the adhesion of blood cells without affecting the growth of human circulating progenitor cells. Acta Biomater, 8, 1057-1067, 2012.

188. Ye, X., Wang, H., Zhou, J., Li, H., Liu, J., Wang, Z., Chen, A. and Zhao, Q. The effect of Heparin-VEGF multilayer on the biocompatibility of decellularized aortic valve with platelet and endothelial progenitor cells. PLoS One, 8, e54622, 2013.

189. Ye, X., Zhao, Q., Sun, X. and Li, H. Enhancement of mesenchymal stem cell attachment to decellularized porcine aortic valve scaffold by in vitro coating with antibody against CD90: a preliminary study on antibody-modified tissue-engineered heart valve. Tissue Eng Part A, 15, 1-11, 2009.

190. Yu, B. T., Li, W. T., Song, B. Q. and Wu, Y. L. Comparative study of the Triton X-100-sodium deoxycholate method and detergent-enzymatic digestion method for decellularization of porcine aortic valves. Eur Rev Med Pharmacol Sci, 17, 2179-2184, 2013.

191. Zeltinger, J., Landeen, L. K., Alexander, H. G., Kidd, I. D. and Sibanda, B. Development and characterization of tissue-engineered aortic valves. Tissue Eng, 7, 9-22, 2001.

192. Zhai, W., Chang, J., Lin, K., Wang, J., Zhao, Q. and Sun, X. Crosslinking of decellularized porcine heart valve matrix by procyanidins. Biomaterials, 27, 3684-3690, 2006.

193. Zhai, W., Lu, X., Chang, J., Zhou, Y. and Zhang, H. Quercetin-crosslinked porcine heart valve matrix: mechanical properties, stability, anticalcification and cytocompatibility. Acta Biomater, 6, 389-395, 2010.

194. Zhou, J., Fritze, O., Schleicher, M., Wendel, H. P., Schenke-Layland, K., Harasztosi, C., Hu, S. and Stock, U. A. Impact of heart valve decellularization on 3-D ultrastructure, immunogenicity and thrombogenicity. Biomaterials, 31, 2549-2554, 2010.

195. Zhou, J., Hu, S., Ding, J., Xu, J., Shi, J. and Dong, N. Tissue engineering of heart valves: PEGylation of decellularized porcine aortic valve as a scaffold for in vitro recellularization. Biomed Eng Online, 12, 87, 2013.

196. Zhou, J., Nie, B., Zhu, Z., Ding, J., Yang, W., Shi, J., Dong, X., Xu, J. and Dong, N. Promoting endothelialization on decellularized porcine aortic valve by immobilizing branched polyethylene glycolmodified with cyclic-RGD peptide: an in vitro study. Biomed Mater, 10, 065014, 2015.

197. Zhou, J., Ye, X., Wang, Z., Liu, J., Zhang, B., Qiu, J., Sun, Y., Li, H. and Zhao, Q. Development of decellularized aortic valvular conduit coated by heparin-SDF-1alpha multilayer. Ann Thorac Surg, 99, 612-618, 2015.

APPENDIX A: FIGURES

CHAPTER 1: Figure 1.1

CHAPTER 2: Figure 2.1 – 2.3

CHAPTER 3: Figure 3.1 – 3.8

CHAPTER 4: Figure 4.1 – 4.5

CHAPTER 5: Figure 5.1 – 5.4

CHAPTER 6: Figure 6.1 – 6.3

CHAPTER 7: Figure 7.1

Supplemental Figure 1

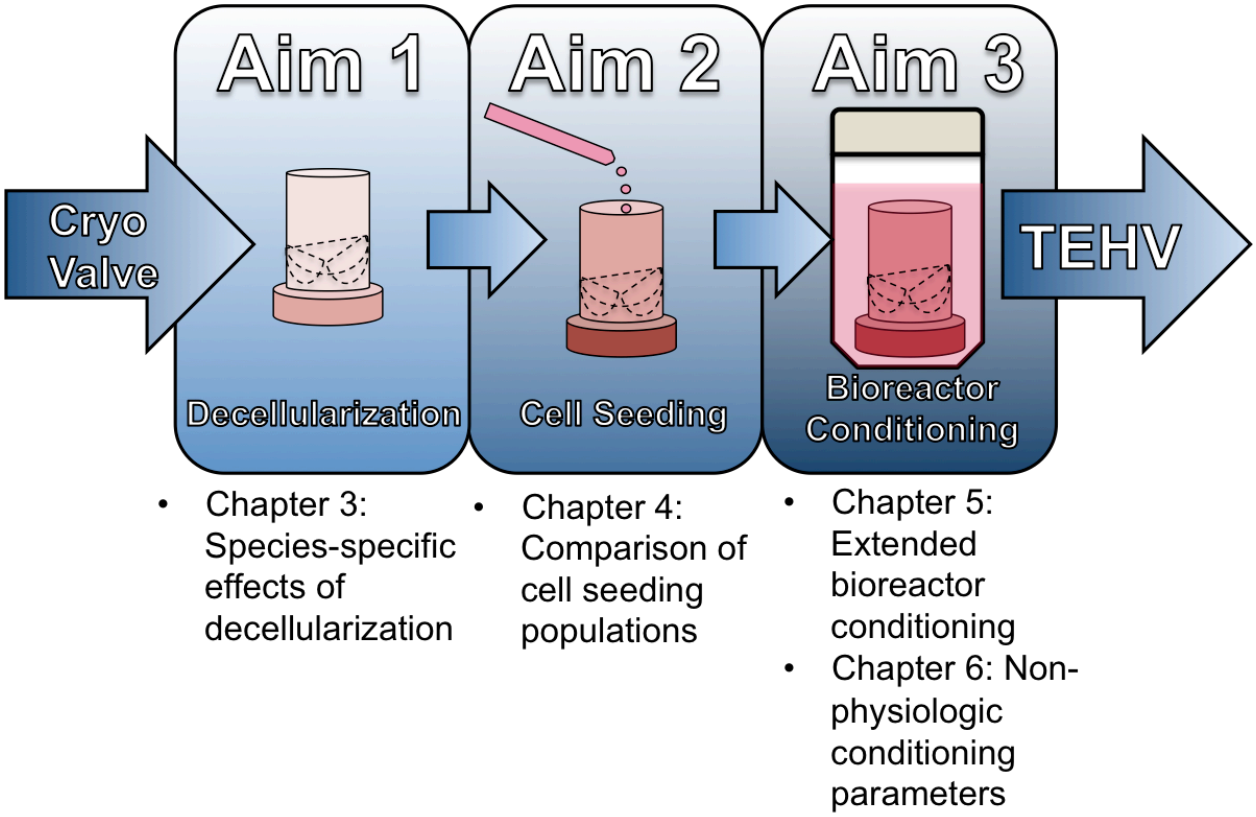

Figure 1.1: Schematic of the Aims of the thesis following the progression of the TEHV

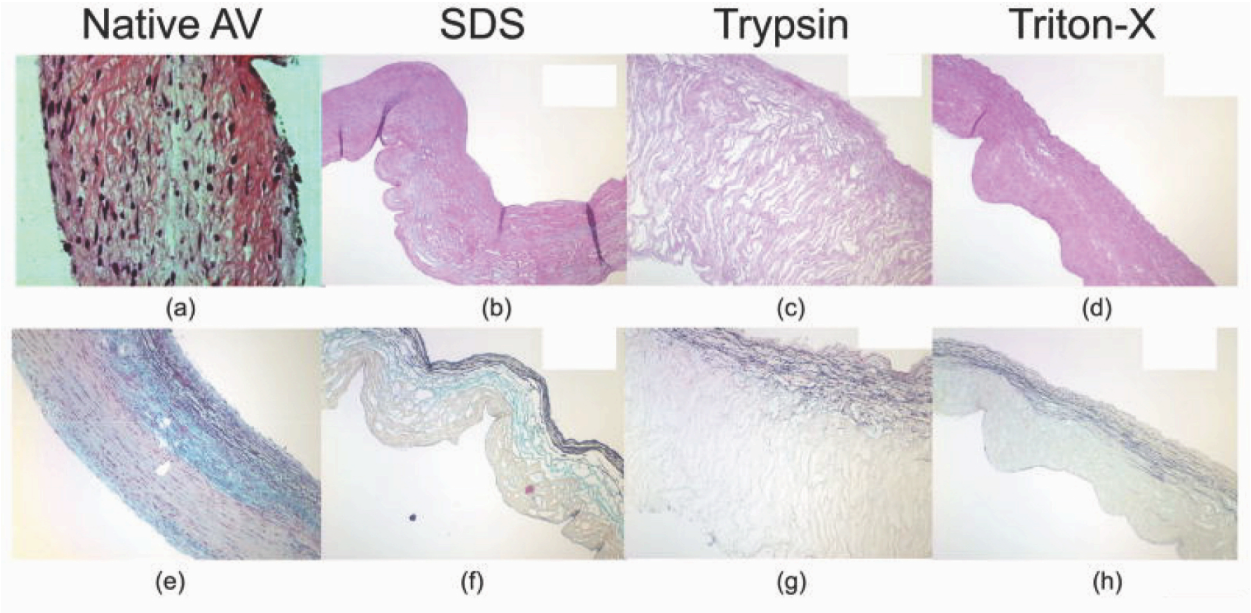

Figure 2.1: Effects of various decellularization methods

(a–d) H&E and (e–h) Movat's pentachrome staining highlighting the effects of decellularization by SDS (b, f), trypsin (c, g), and Triton X-100 (d, h) compared to native tissue (a, e). All three methods show effective removal of cellular and nuclear material. SDS slides show preservation of leaflet structure and ECM components. Trypsin slides show a "loosening" of the ECM network and loss of structural proteins. Triton X-100 slides show good preservation of leaflet structure but loss of GAGs from the ECM.

Source: Figure reprinted from Liao et al.[101] with permission. Copyright 2008 Elsevier: Biomaterials.

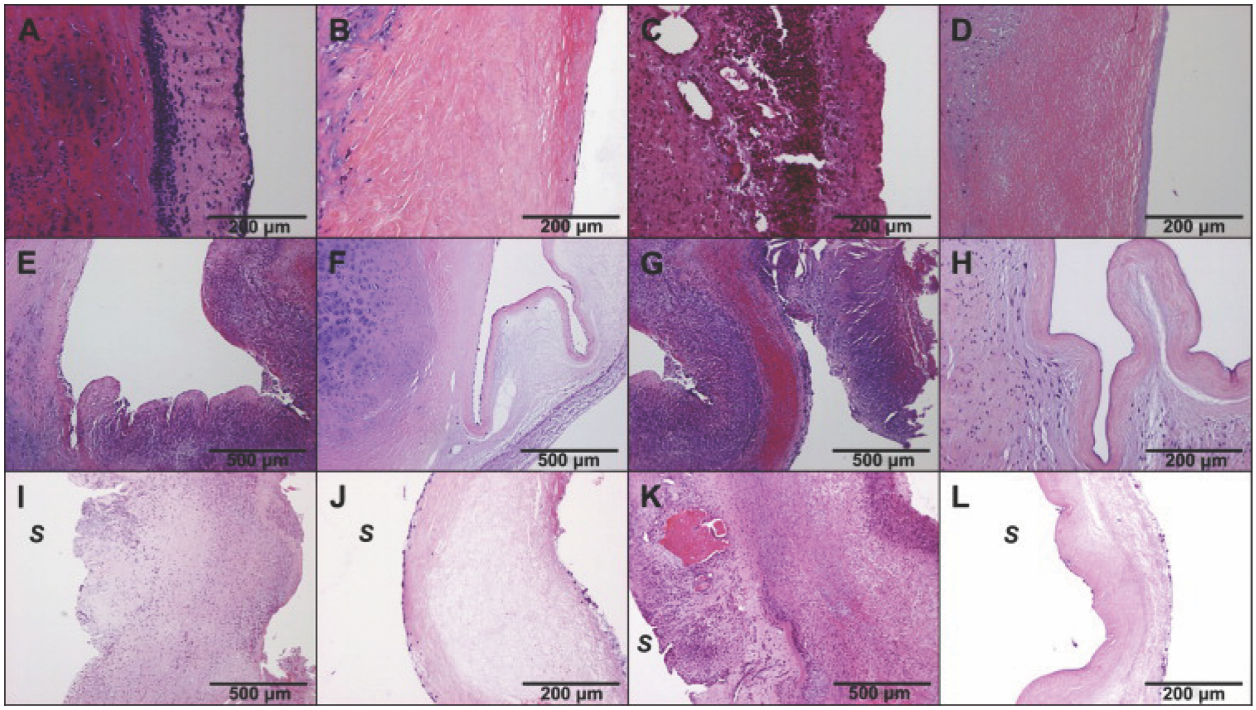

Figure 2.2: Limited autologous recellularization of cryopreserved and decellularized valves *in vivo*

H&E-stained sections highlighting the autologous recellularization of decellularized (dAV) and cryopreserved (cAV) aortic valves after implantation in sheep. Histology of aortic wall: cAV after 3 months (a) and after 9 months (c) with signs of rejection and leukocyte infiltration; dAV after 3 months (b) and after 9 months (d) without any signs of rejection and with partial re-endothelialization and ingrowth of interstitial cells. The same findings are shown in the aortic sinus: cAV degeneration after
3 months (e) and after 9 months (g); dAV sinus without signs of rejection and with partial re-endothelialization and recellularization of leaflet base after 3 months (f) and even more recellularization after 9 months (h). Leaflets from the cAV show massive degeneration and destruction after 3 months (i) and after 9 months (k); dAV distal leaflets show partial re-endothelialization after 3 months (j) and after 9 months (l). (S) shows sinus side of the leaflet.
Source: Figure reprinted from Baraki et al.[13] with permission. Copyright 2009 Elsevier: Biomaterials.

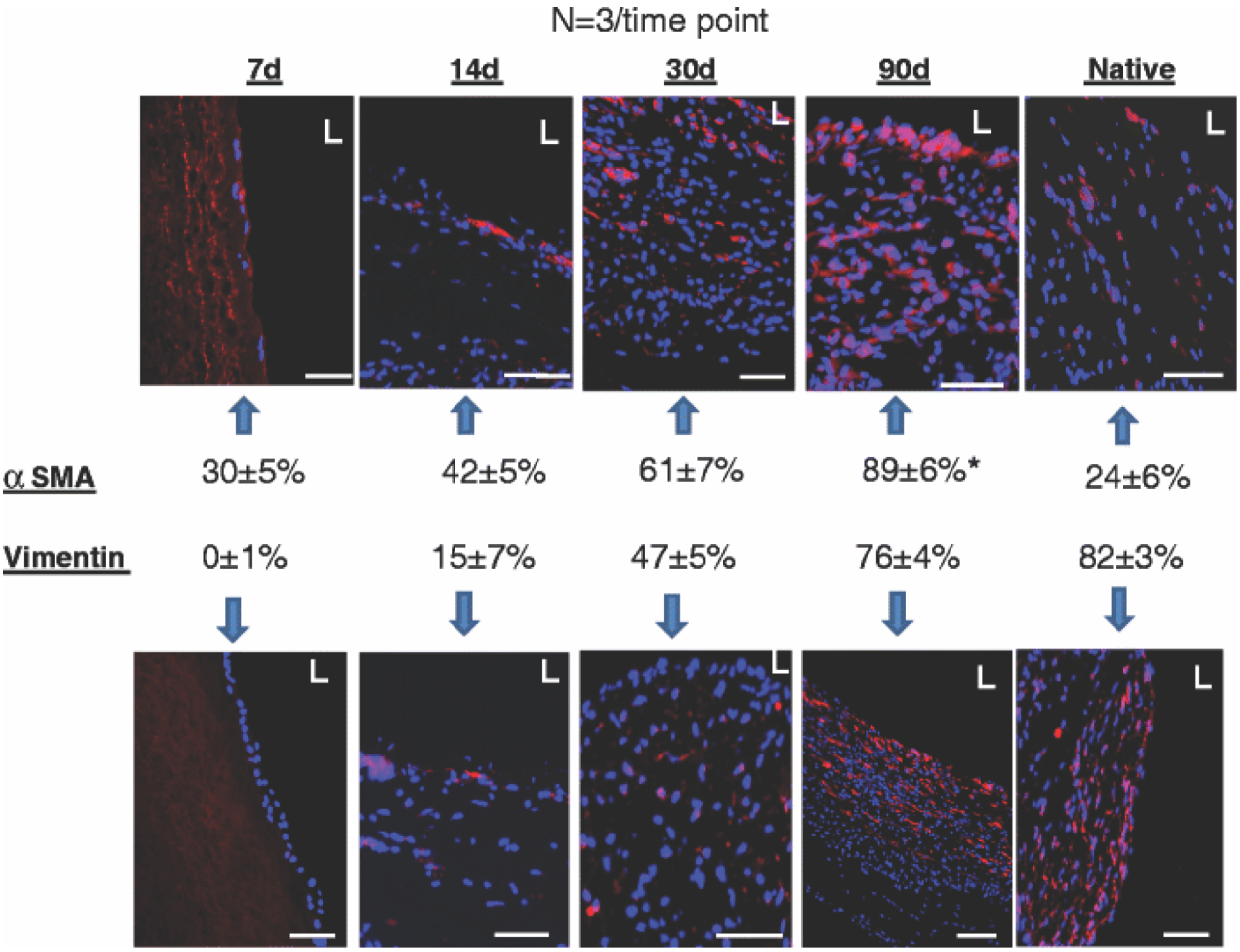

Figure 2.3: Recellularization of CD133 conjugated heart valve leaflets

Immunological staining demonstrating successful recellularization of leaflets from pulmonary valves conjugated with CD133 and implanted in the pulmonary position in sheep. Texas Red–labeled secondary antibodies show αSMA (top row) and vimentin (bottom row), and the nuclei are DAPI counterstained. Percentage values are the percent of cells with positive expression compared to the total number of cells which represent the mean calculated from all three leaflets. Note the high αSMA expression in the tissue-engineered leaflets compared to native leaflets. L denotes lumen. * indicates $p < 0.05$. Scale bars are 100 μm.

Source: Figure reprinted from Williams et al.[179] with permission. Copyright 2015 Springer Science: Journal of Cardiovascular Translational Research.

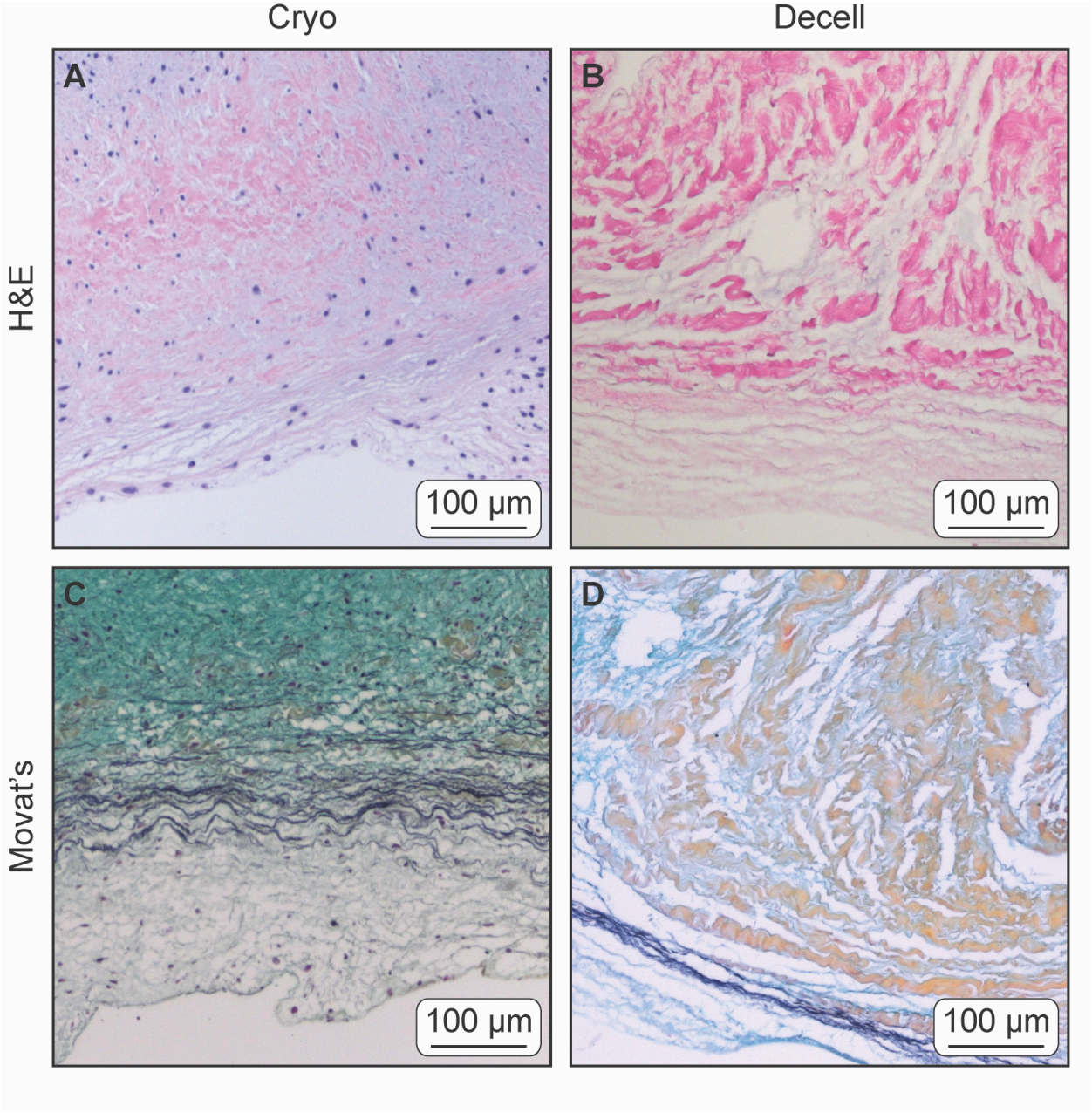

Figure 3.1: Histology of human aortic valves

Representative histology of cryopreserved (cryo) and decellularized (decell) human aortic valve leaflets stained with H&E (A, B) or Movat's Pentachrome (C, D).

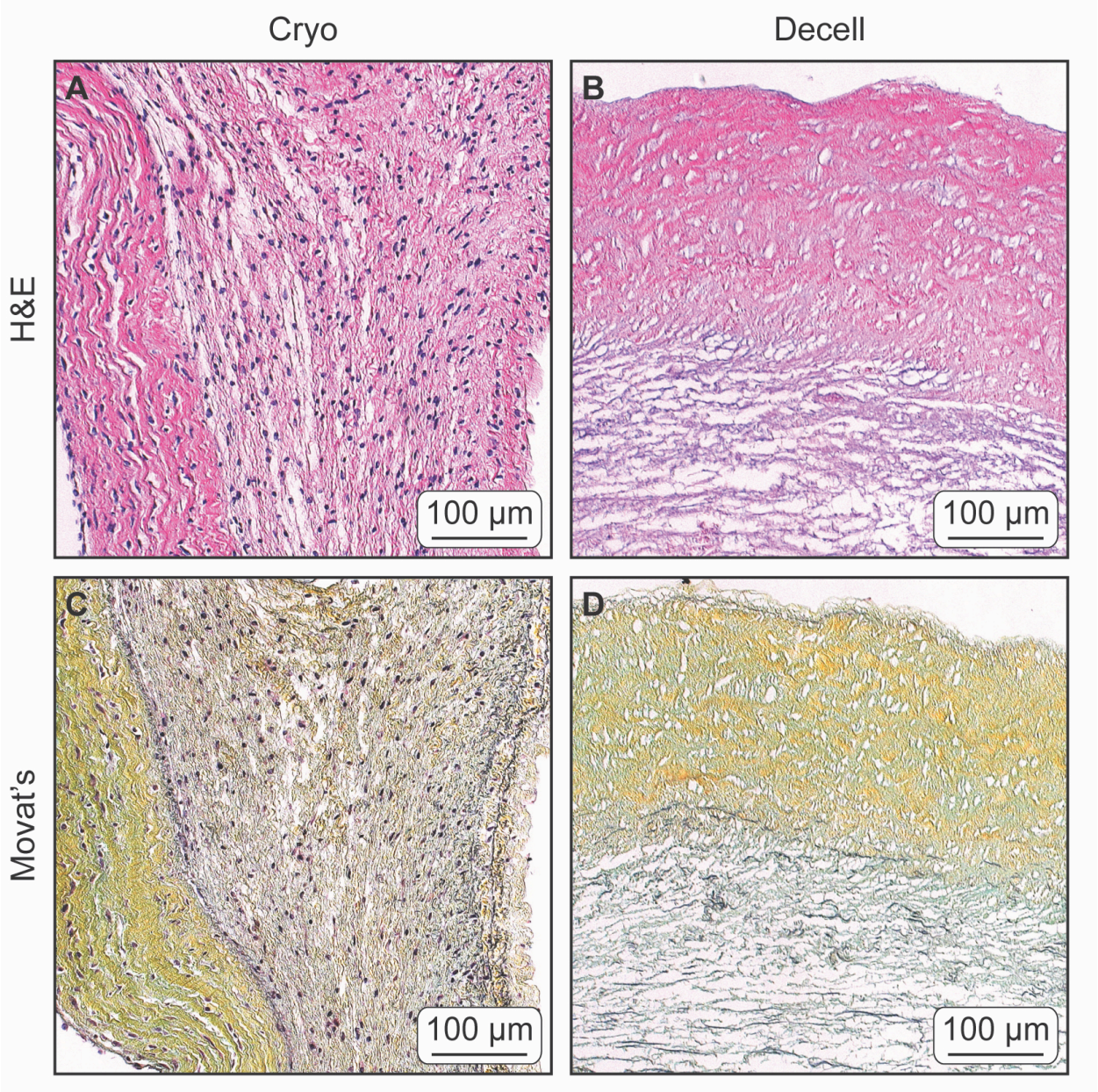

Figure 3.2: Histology of ovine aortic valves

Representative histology of cryopreserved (cryo) and decellularized (decell) ovine aortic valve leaflets stained with H&E (A and B) or Movat's Pentachrome (C and D).

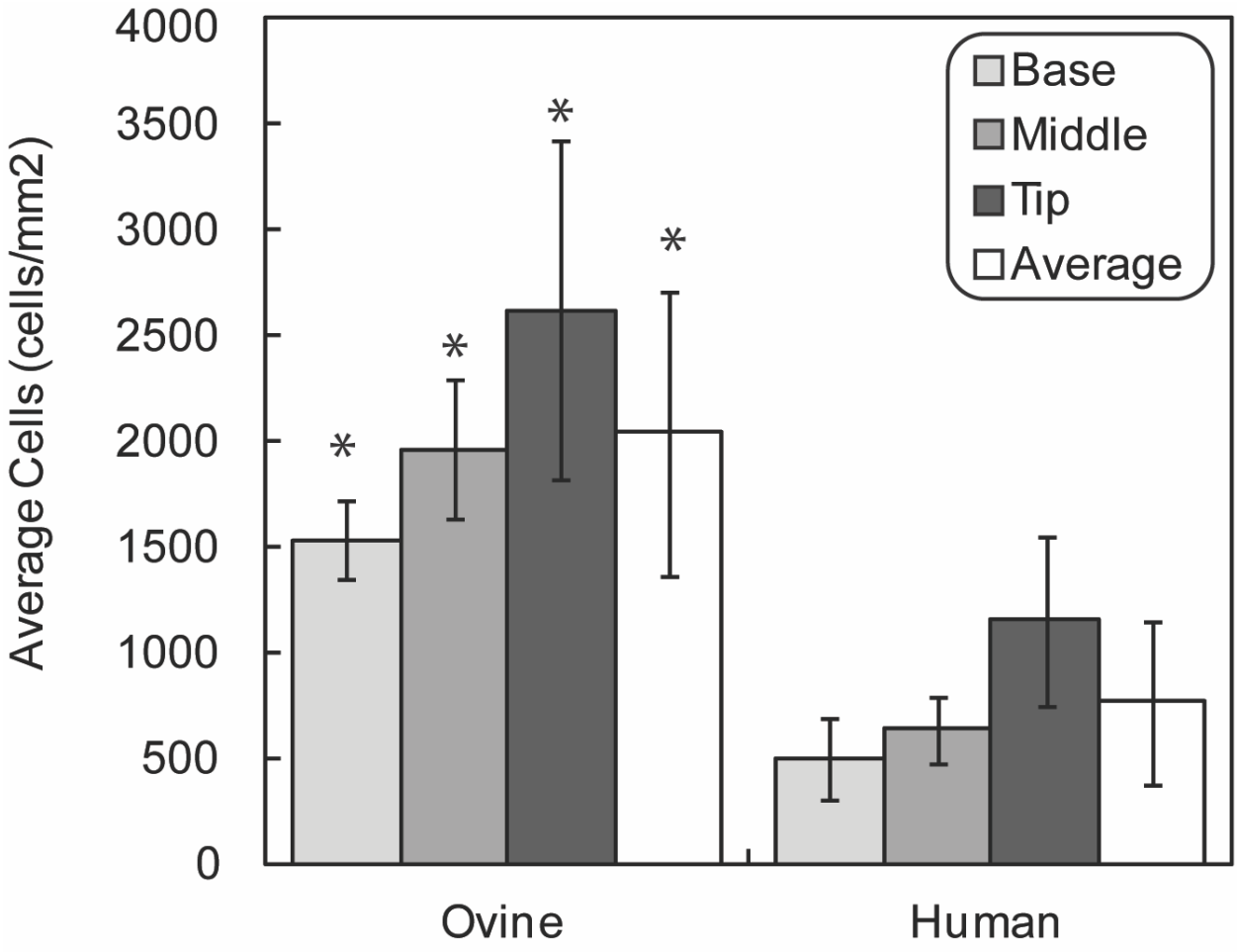

Figure 3.3: Cell density of ovine and human aortic valves

Cells per mm^2 of ovine and human cryopreserved leaflets. Cellularity was measured at the base, middle, and tip of each leaflet and reported as the mean with SD error bars. The reported Average is the mean of all three regions. * Denotes a statistically significant difference between species ($p < 0.001$, t-Test).

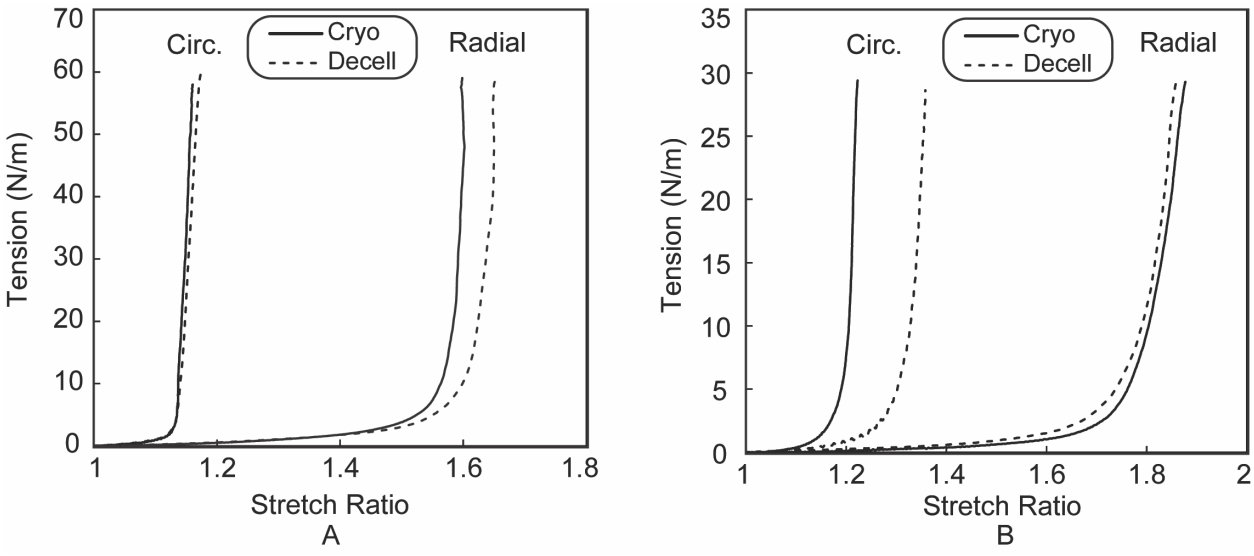

Figure 3.4: Tension-stretch curves for human and ovine aortic valves

Representative tension-stretch curves for human (A) and ovine (B) cryopreserved and decellularized leaflets under biaxial loading.

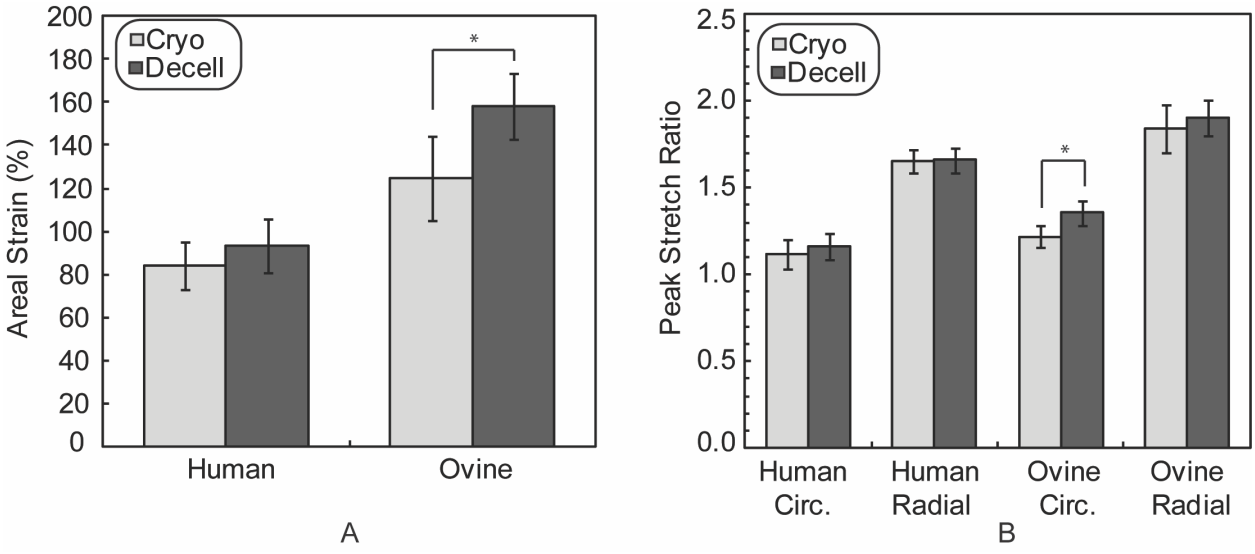

Figure 3.5: Areal strain and peak stretch ratio of human and ovine aortic valves

Areal strain (A) and peak stretch ratio (B) of human and ovine, cryopreserved and decellularized aortic valve leaflets. Peak stretch ratios were measured along the circumferential and radial axes. Mean values are reported and error bars represent standard deviation. * Denotes a statistically significant difference between groups of the same species ($p < 0.05$, t-Test).

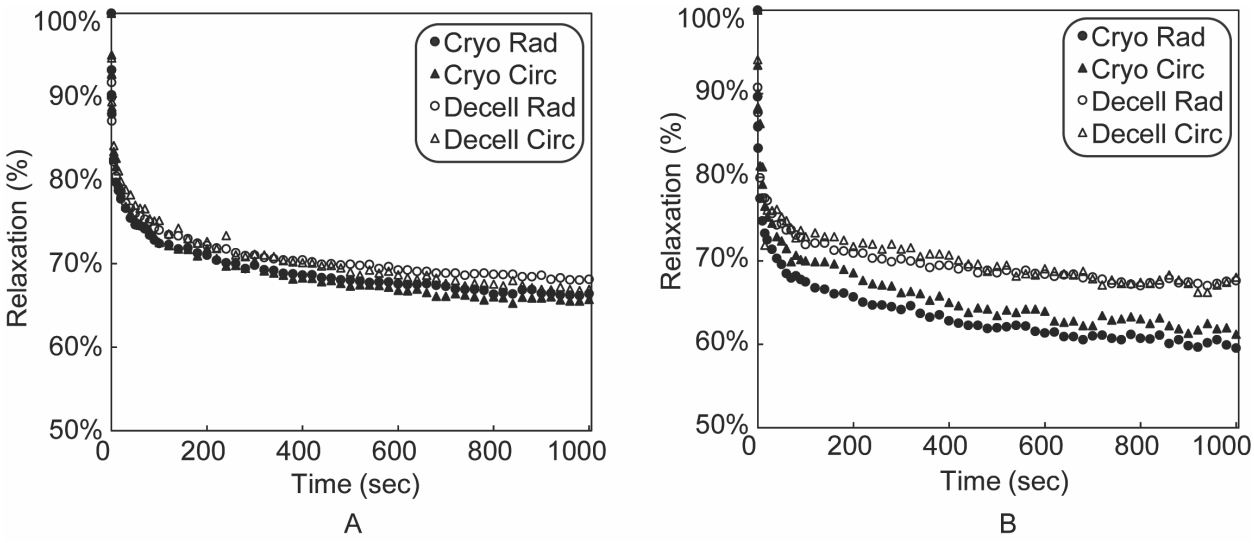

Figure 3.6: Sample stress relaxation curves from human and ovine aortic valves

Representative relaxation curves from human (A) and ovine (B) cryopreserved and decellularized aortic valve leaflets under biaxial loading.

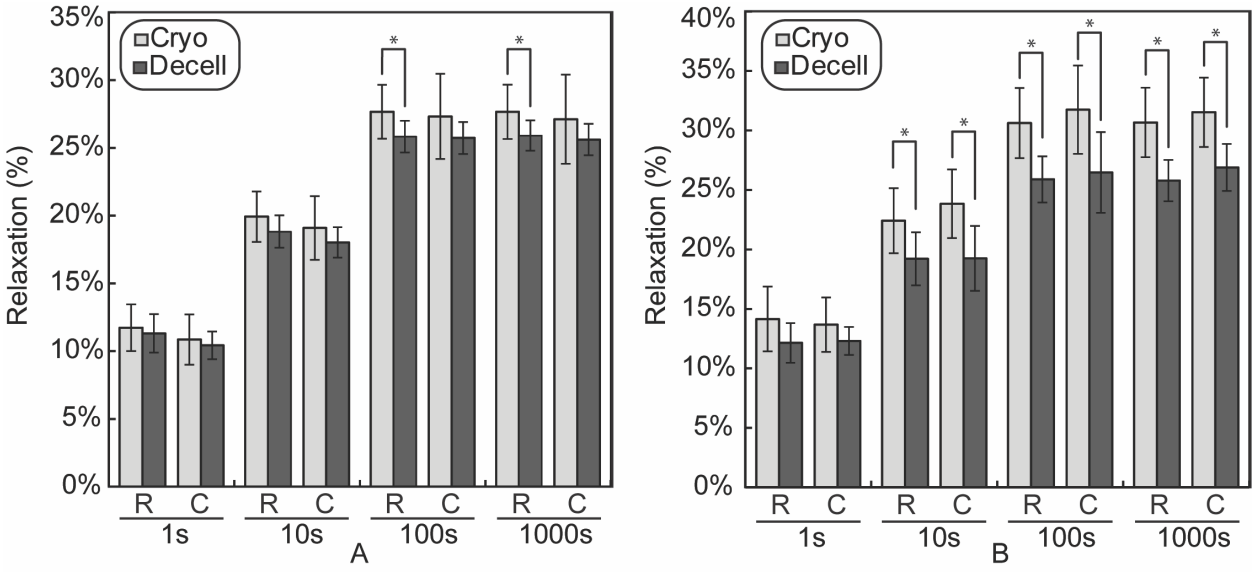

Figure 3.7: Stress relaxation of human and ovine aortic valves

Relaxation of human (A) and ovine (B), cryopreserved (cryo) and decellularized (decell) aortic valve leaflets at 1s, 10s, 100s, and 1000s. Per cent relaxation was measured along both the radial (R) and circumferential (C) axes. Mean values are reported and error bars represent standard deviation. * Denotes a statistically significant difference between groups of the same species ($p < 0.05$, t-Test).

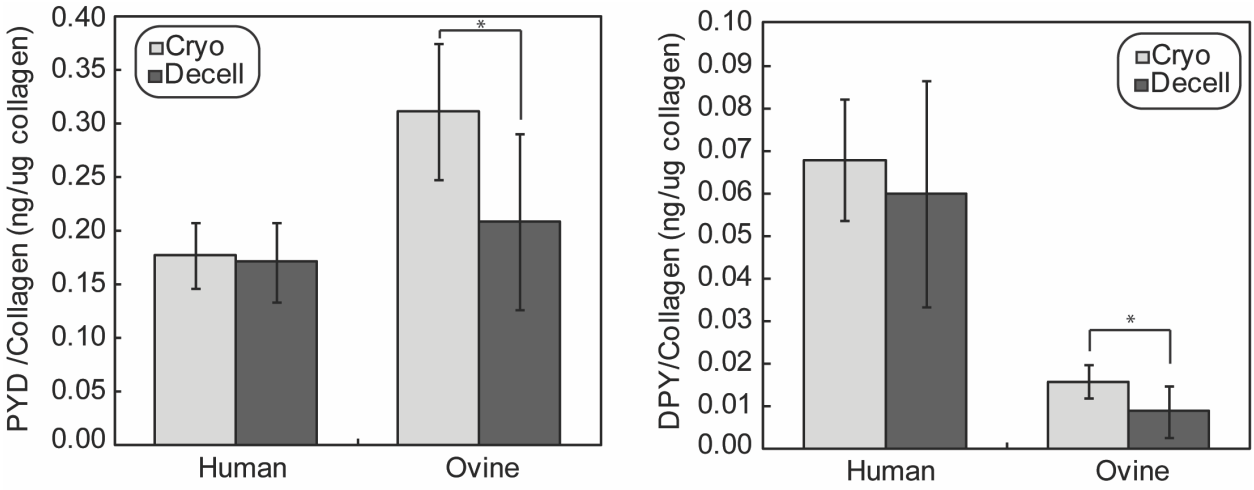

Figure 3.8: Concentration of collagen crosslinking in human and ovine aortic valves

Concentration of the collagen crosslinking compounds PYD and DPY in human and ovine aortic leaflets before and after decellularization. Crosslinking concentration is reported per ug of collagen within the leaflet ECM. Mean values are reported and error bars represent standard deviation. * Denotes a statistically significant difference between groups of the same species ($p < 0.05$, t-Test).

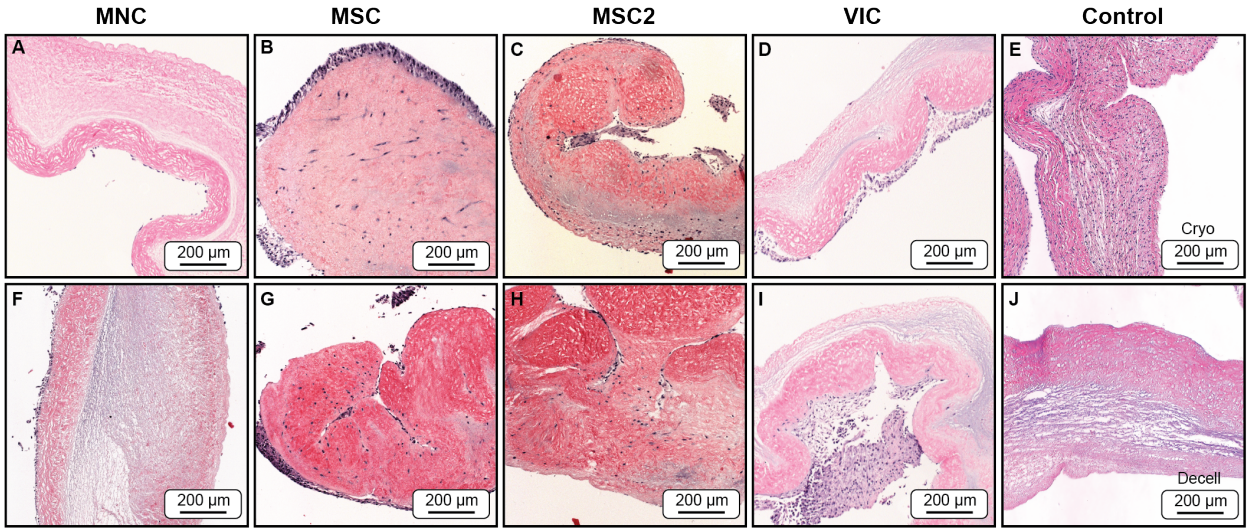

Figure 4.1: Histology of TEHVs seeded with MNC, MSC, MSC2 or VIC populations

Representative H&E stained sections showing various degrees of recellularization from the four groups of the tissue engineered valve leaflets, two weeks post seeding. MNC valves (A,F) showed no signs of interstitial recellularization and minimal cells on the leaflet surface. MSC valves (B,G) and MSC2 (C,H) valves displayed increased interstitial recellularization of the distal leaflet and slight cell clumping on the leaflet surface. VIC valves (D,I) showed no cell infiltration and a high degree of cell clumping along the leaflet surface. Positive and negative controls (E & J, respectively) are presented as cryopreserved (cryo) and decellularized (decell) ovine valve samples. Images within the same processing group (e.g. A & F) are taken from separate valves under the same processing conditions to show reproducibility. All images are taken from the distal third region of the leaflet.

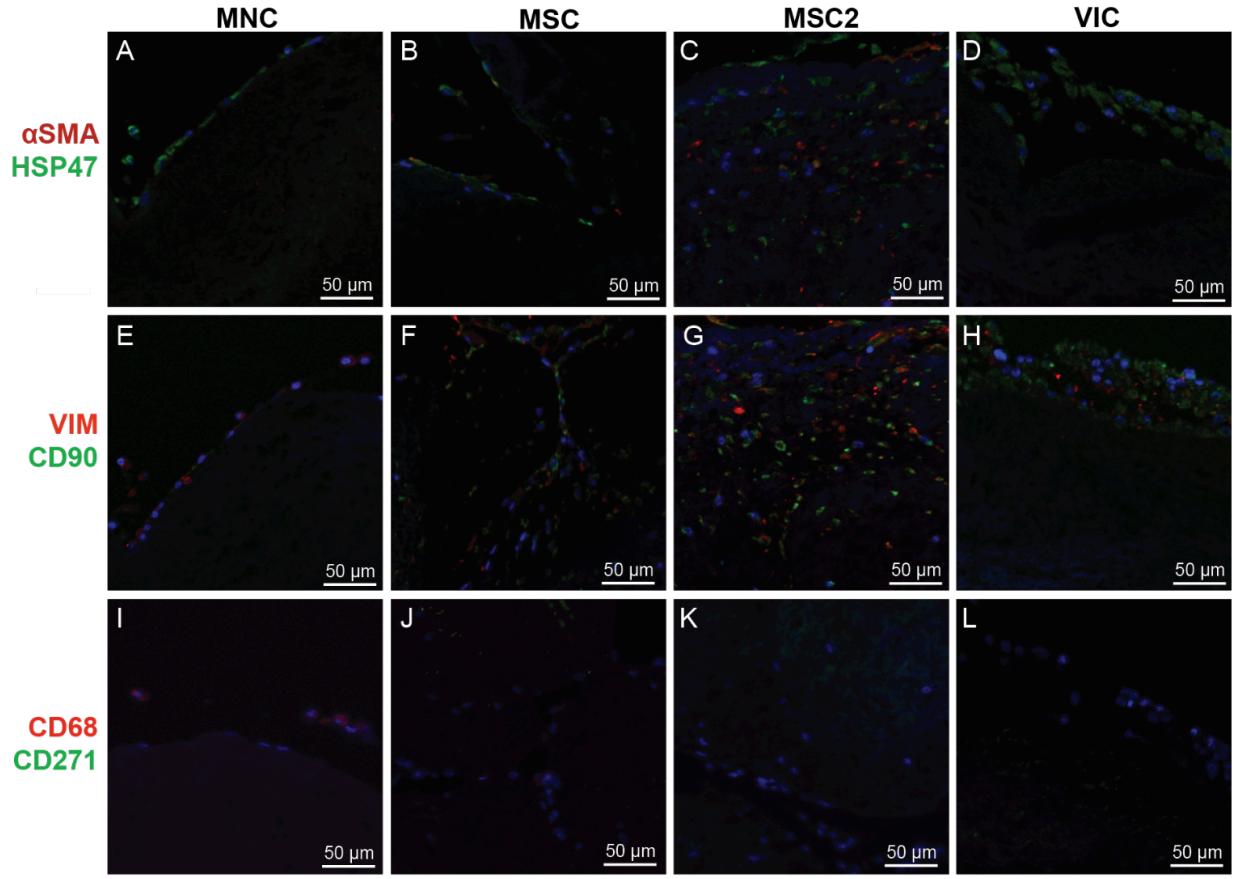

Figure 4.2 IHC staining of TEHVs seeded with MNC, MSC, MSC2 or VIC populations

Immunohistochemical sections of seeded valve leaflets dual stained for the expression of: cell nuclei (blue) (all), αSMA (red) & HSP47 (green) (A-D), VIM (red) & CD90 (green) (E-H), and CD68 (red) & CD271 (green) (I-L). *MNC* leaflets (A,E,I) showed positive expression for HSP47, VIM, and CD68. *MSC* leaflets (B,F,J) and *MSC2* leaflets (C,G,K) both showed positive expression for HSP47, αSMA, VIM, and CD90, although the *MSC2* leaflets appear to have increased expression. *VIC* leaflets (D,H,L) showed positive expression for HSP47, VIM, and CD90.

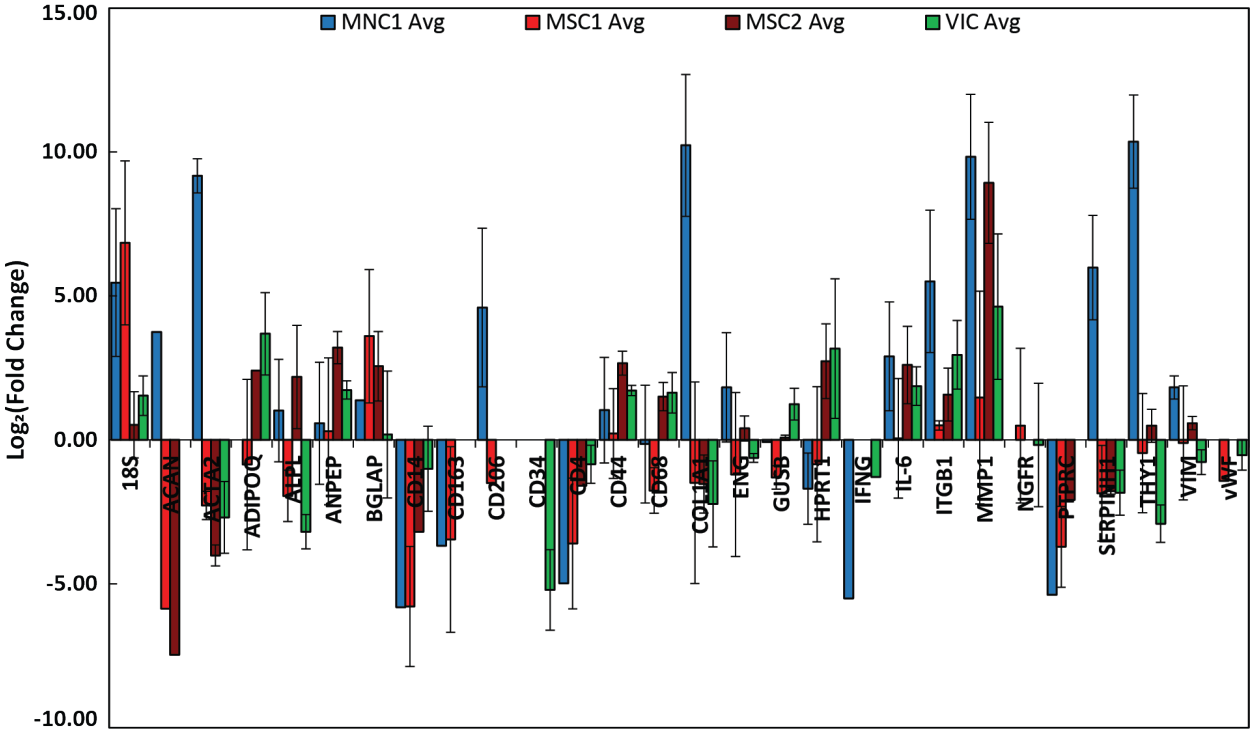

Figure 4.3: Gene expression of cells from TEHVs seeded with MNC, MSC, MSC2 or VIC populations

Relative fold change in the gene expression of cells from MNC, MSC, MSC2 and VIC seeded heart valves in relation to their respective pre-seeded cell populations. Changes in gene expression are displayed as the Log_2 of the average relative fold change within a group. Error bars represent the standard deviation.

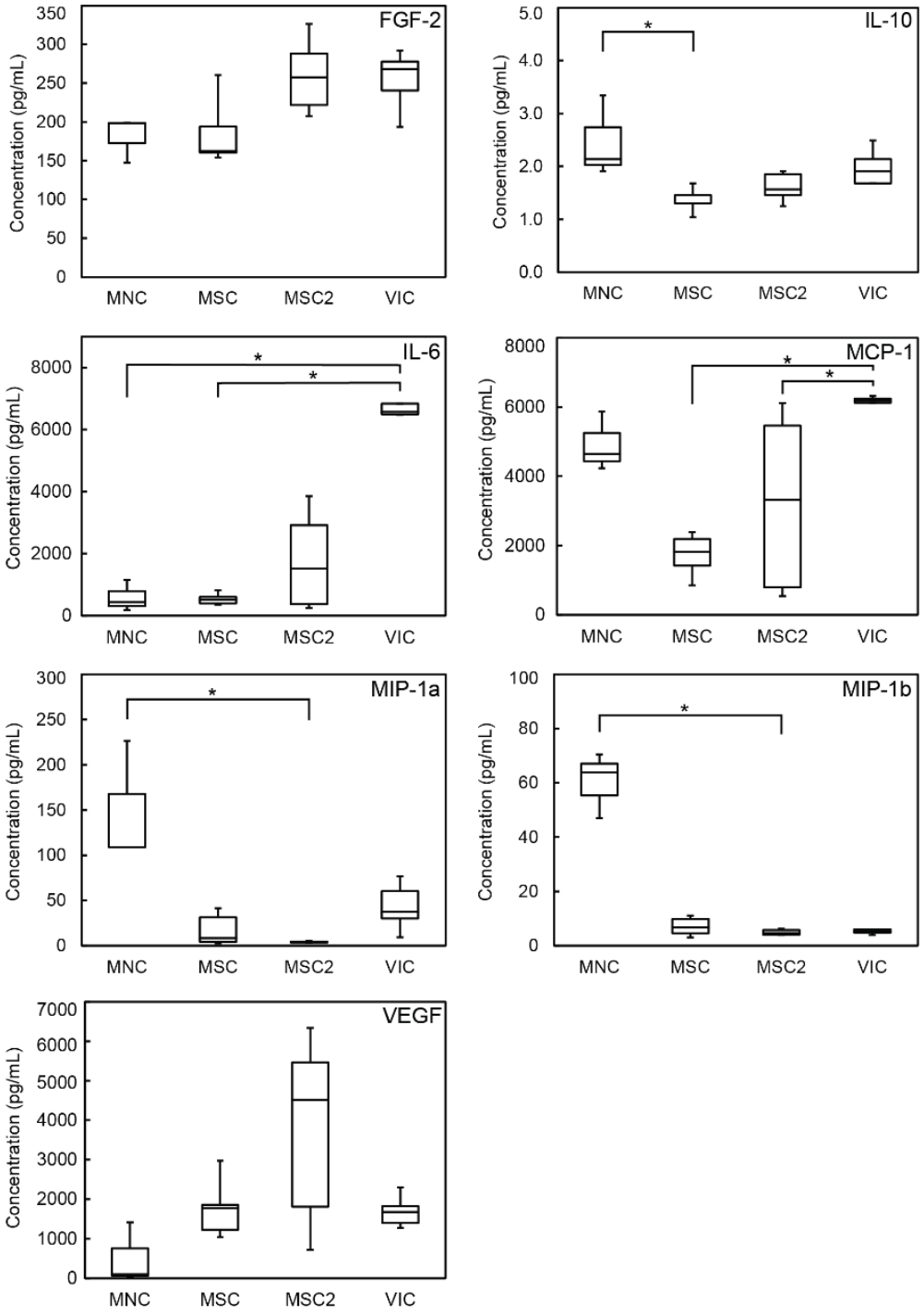

Figure 4.4: Cytokine production of TEHVs seeded with MNC, MSC, MSC2 or VIC populations

Box and whisker plots of cytokine concentrations from the bioreactor media of the tissue engineered valve groups, two weeks post seeding. The box boundaries represent the first and third quartiles, the horizontal line indicates the median, and the whiskers indicate the maximum and minimum values. * denotes a significant difference between groups ($p < 0.05$).

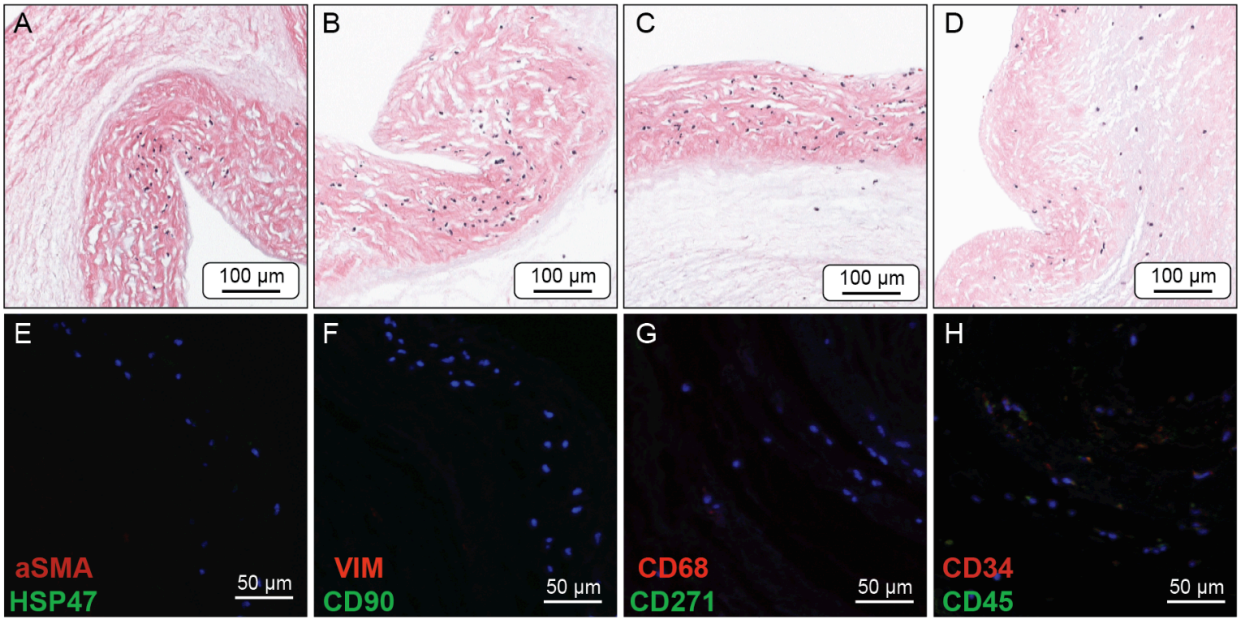

Figure 4.5: Histology and IHC of short term MNC seeded valves

H&E (A-D) and IHC (E-H) stained sections of MNC short heart valve leaflets, 3 days post seeding. IHC sections were stained for cell nuclei (blue) (E-H), αSMA (red) & HSP47 (green) (E), VIM (red) & CD90 (green) (F), CD68 (red) & CD271 (green) (G), and CD34 (red) & CD45 (green) (H). H&E staining revealed clusters of cell infiltration into the fibrosa along the length of the leaflet (A-D). IHC revealed positive expression of CD68, CD34, and CD45 (G,H).

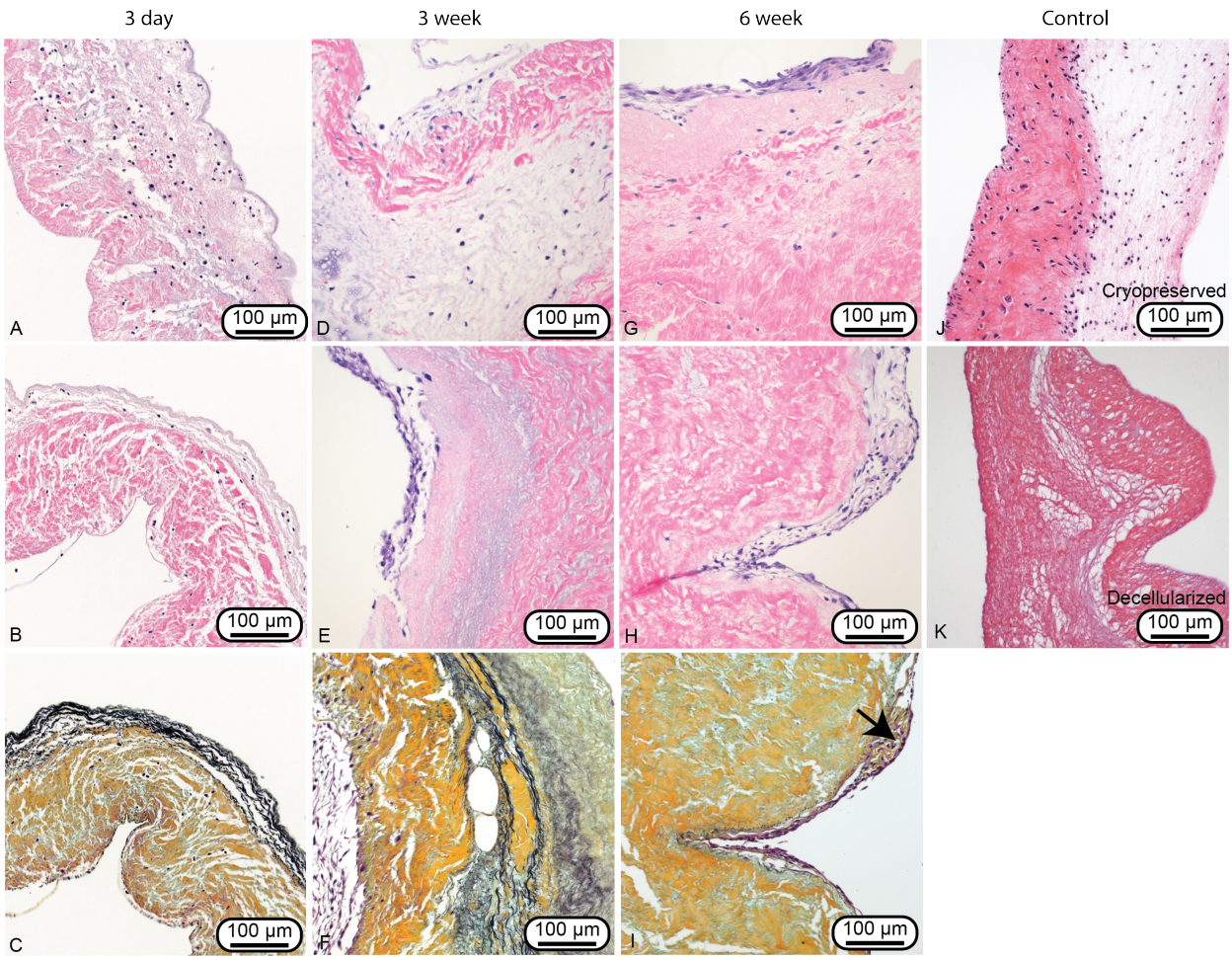

Figure 5.1: Histology of MNC seeded TEHVs after extended conditioning

Representative H&E (A,B,D E,G,H) and Movat's Pentachrome (C, F, I) images of 3 day (A-C), 3 week (D-F) and 6 week (G-I) bioreactor conditioned heart valve leaflets. 3 day conditioned leaflets exhibited high interstitial recellularization. 3 week and 6 week conditioned valves exhibited decreased interstitial recellularization but increased numbers of cells on the leaflet surface, often in multi-layered clumps. Images of cryopreserved (J) and decellularized (K) human valve sections provide positive and negative control images for recellularization, respectively. Movat's Pentachrome staining demonstrated preservation of leaflet structural proteins (collagen, gold; elastin, black; GAG, blue) and evidence of collagen deposition in the 6 week conditioned valves (black arrow).

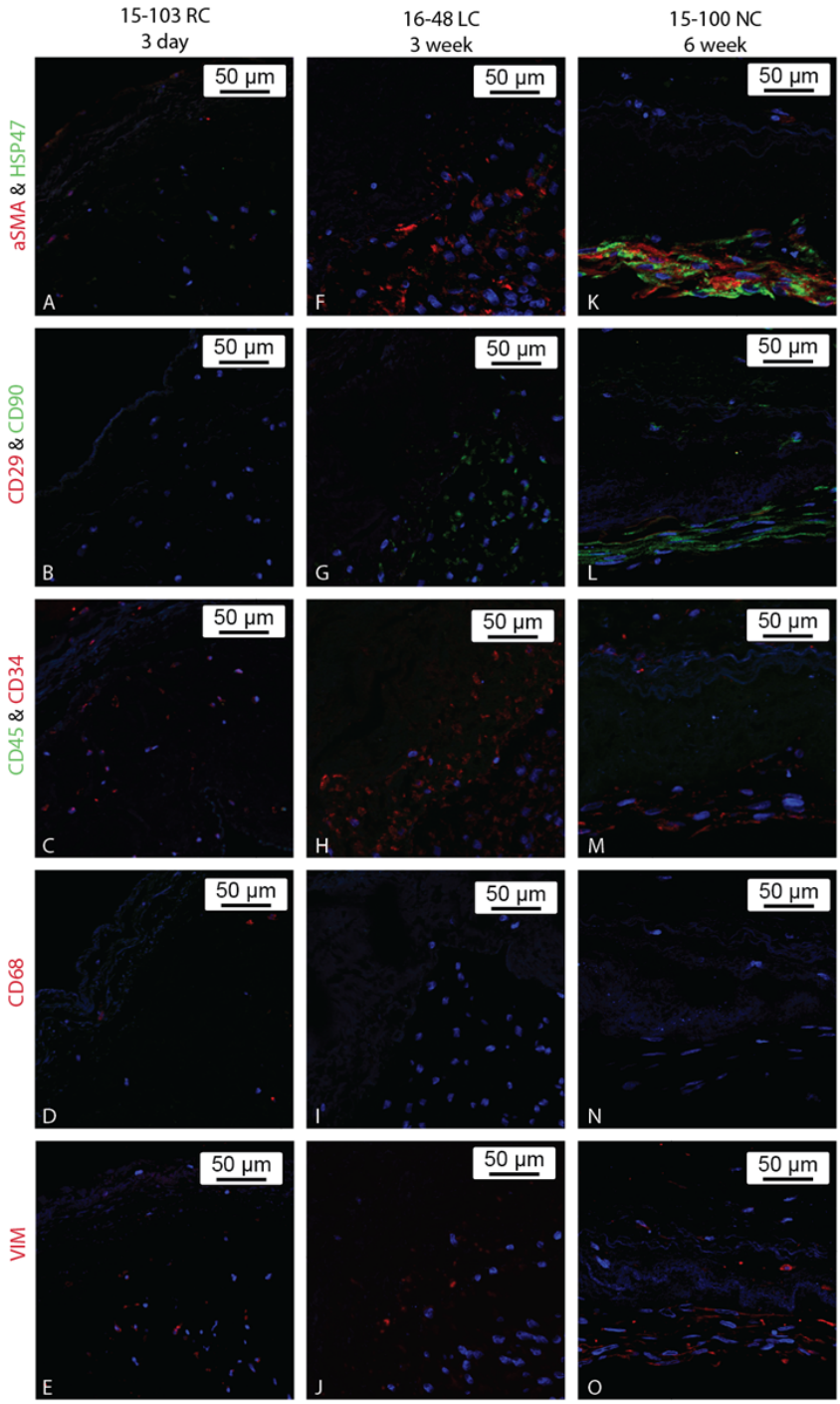

Figure 5.2: IHC of MNC seeded TEHVs after extended conditioning

IHC stained sections of 3 day (A-E), 3 week (F-J) and 6 week (K-O) bioreactor conditioned heart valve leaflets. Sections were stained for αSMA (red) & HSP47 (green) (A,F,K), CD29 (red) & CD90 (green) (B,G,L), CD45 (green) & CD34 (red) (C, H, M), CD 68 (red) (D, I, N), and VIM (red) (E, J, O).

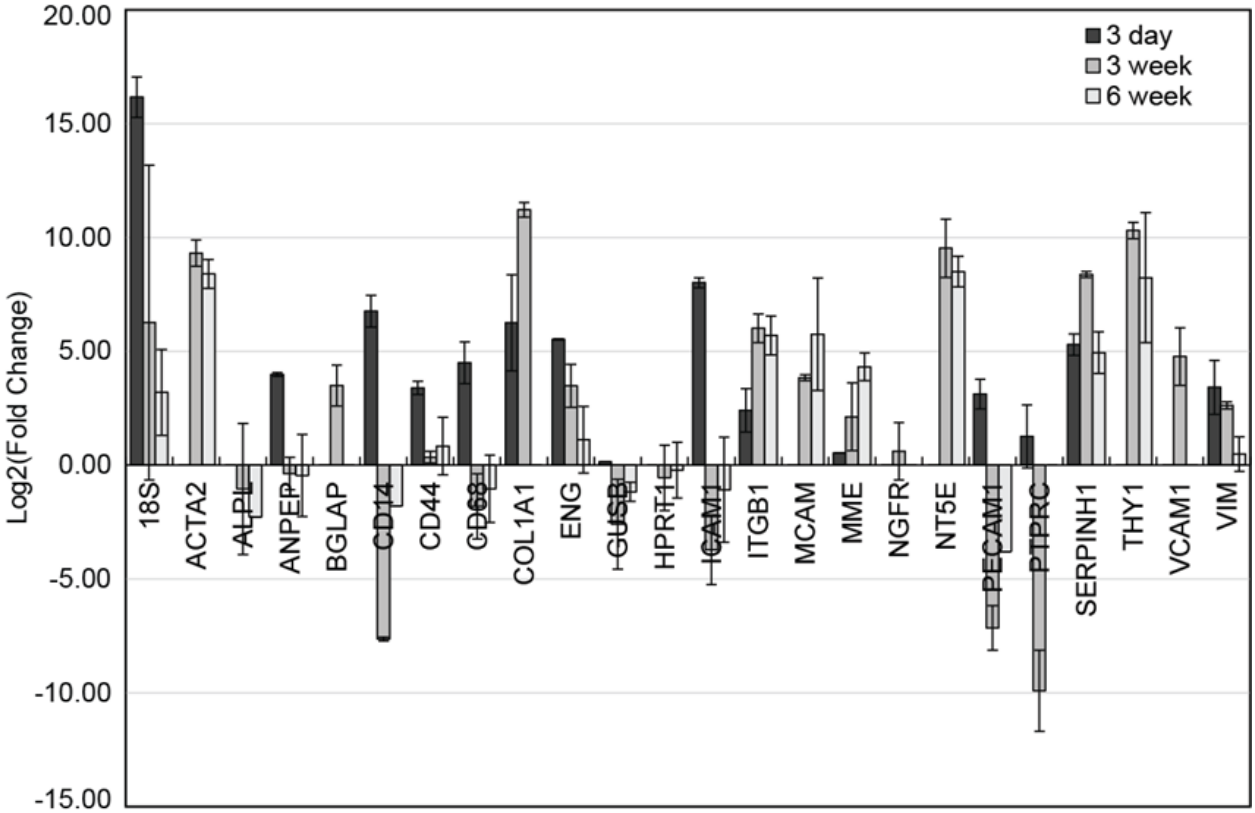

Figure 5.3: Gene expression of MNC seeded TEHVs after extended conditioning

Relative fold change in the gene expression between 3 day, 3 week, and 6 week conditioned heart valves in relation to their respective pre-seeded cell populations. Changes in gene expression are displayed as the Log_2 of the average relative fold change within a group. Error bars represent the standard deviation.

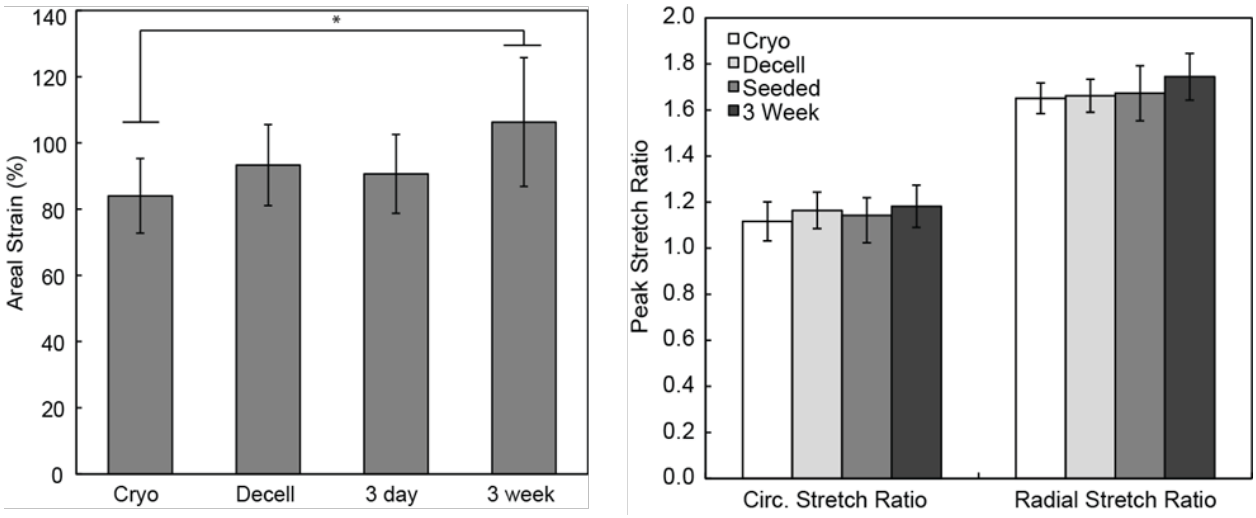

Figure 5.4: Mechanical properties of MNC seeded TEHVs after extended conditioning

Mechanical properties, areal strain and directional peak stretch ratios, of the 3 day and 3 week conditioned heart valve leaflets. Previously reported data for cryopreserved (cryo) and decellularized (decell) human aortic valves are included for comparison [ref]. * indicates a statistically significant difference ($p < 0.05$).

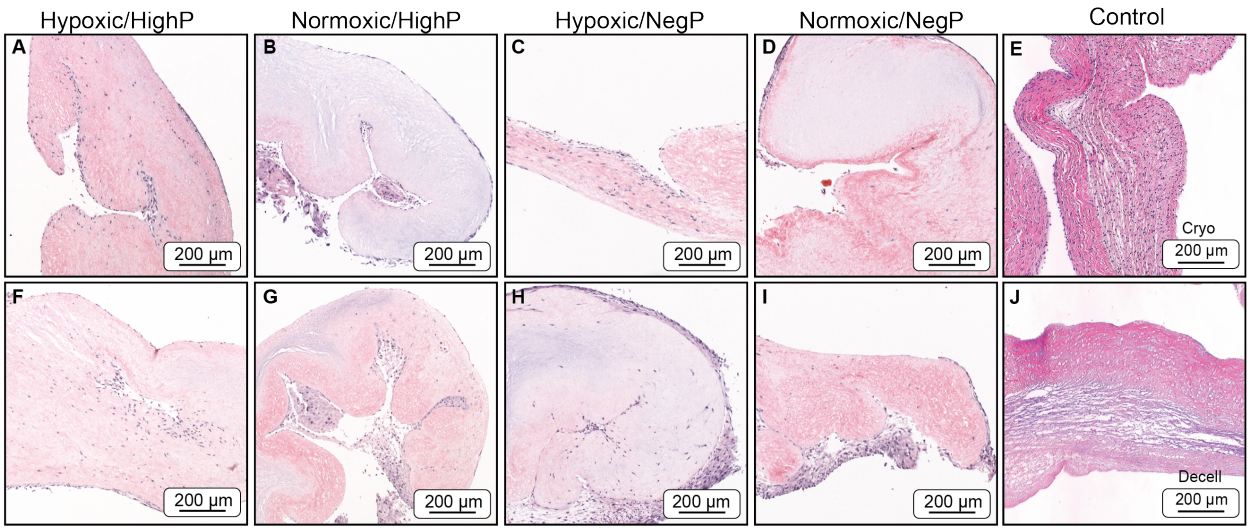

Figure 6.1: Histology of TEHVs from various bioreactor conditioning groups

Representative H&E stained sections of tissue engineered valve leaflets from the Hypoxic/HighP (A,E), Normoxic/HighP (B,F), Hypoxic/NegP (C,G) and Normoxic/NegP (D,H) groups. Positive and negative controls (E & J, respectively) are presented as cryopreserved (cryo) and decellularized (decell) ovine valve samples. All images are taken of the distal tip of the leaflet. Both the Hypoxic/HighP valves and the Hypoxic/NegP valves exhibited a high degree of recellularization with cells infiltrated into the leaflet matrix. Conversely, Normoxic/HighP valves and Normoxic/NegP valves exhibited minimal cellular infiltration and an increased amount of cells clumped together on the leaflet surface.

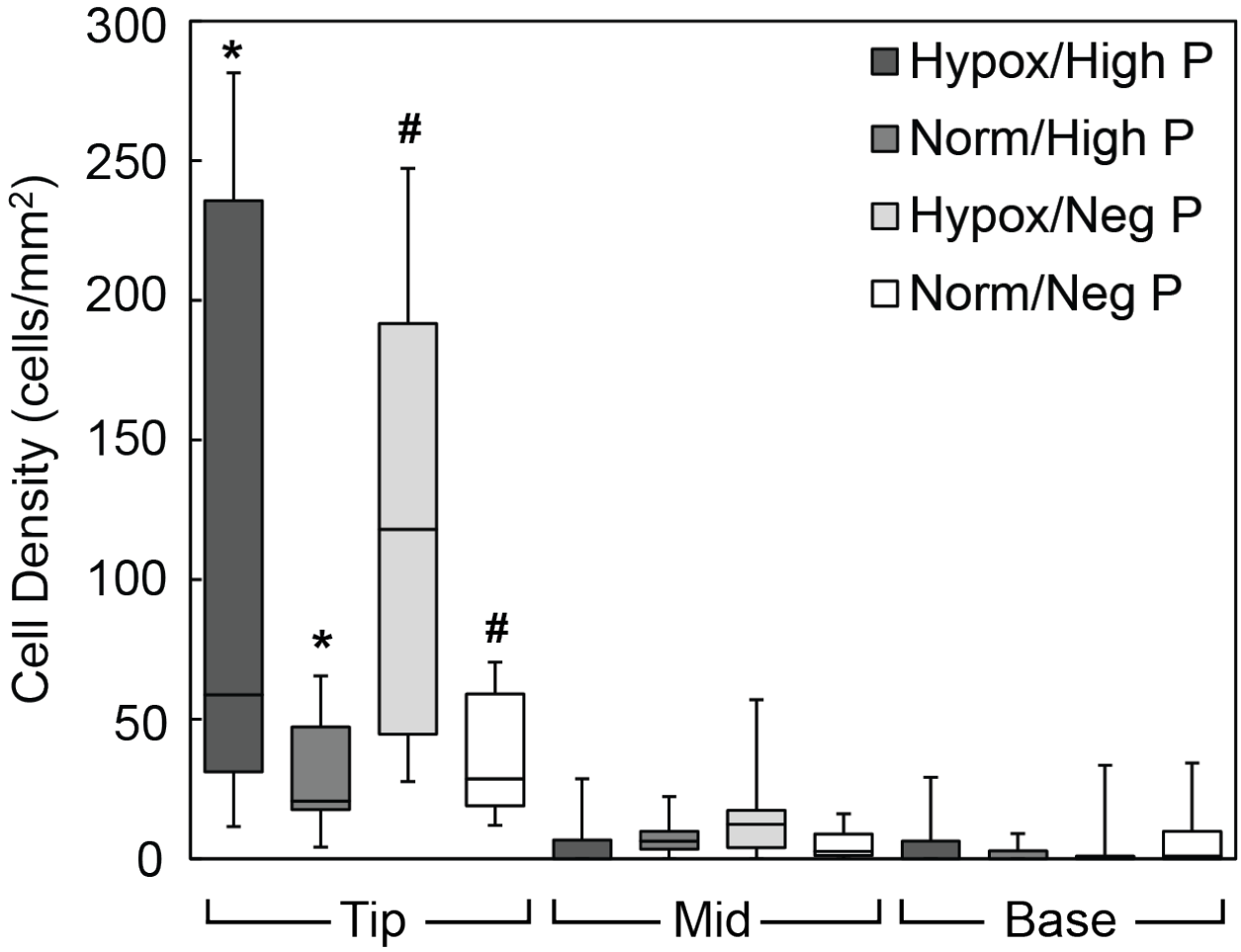

Figure 6.2: Cell density of TEHVs after bioreactor conditioning

Box and whisker plot of the cellular density of the tissue engineered valve leaflets from the various bioreactor conditioning groups. Cellularity was measured at the tip, middle, and base regions of the leaflet. The box boundaries represent the first and third quartiles, the horizontal line indicates the median, and the whiskers indicate the maximum and minimum values. Significance was analyzed between hypoxic/normoxic conditioning, within individual pressure conditioning groups. Symbols of the same type (*, #) indicate significance between groups ($p < 0.05$).

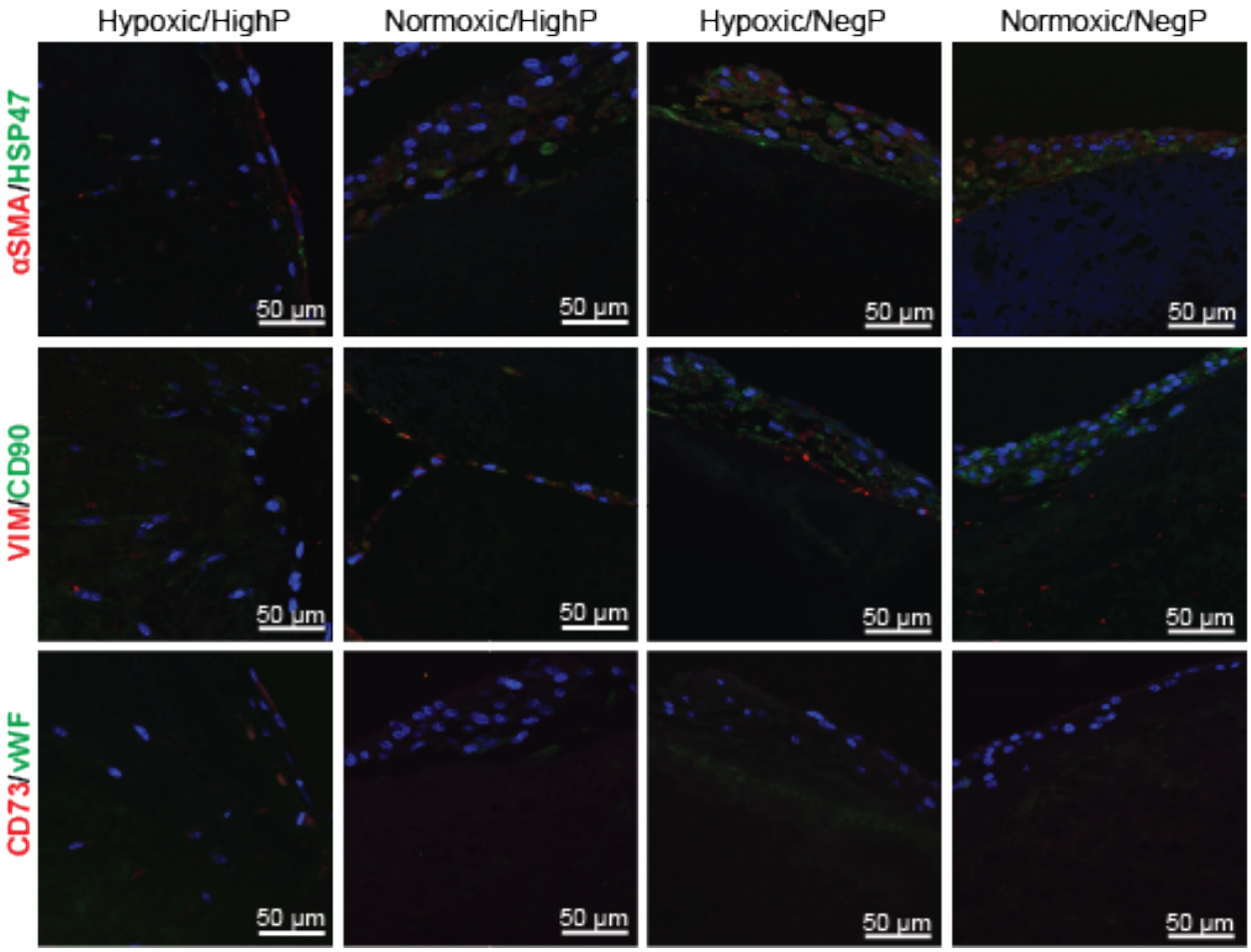

Figure 6.3: Protein expression of TEHVs from bioreactor conditioning groups

Immunohistochemical sections of bioreactor conditioned valve leaflets dual stained for the expression of: cell nuclei (blue) (all), αSMA (red) & HSP47 (green) (A-D), VIM (red) & CD90 (green) (E-H), and CD73 (red) & vWF (green) (I-L). All groups show positive expression for αSMA, HSP47, VIM, and CD90. The Hypoxic/HighP group shows positive expression for CD73. None of the groups stained positive for vWF.

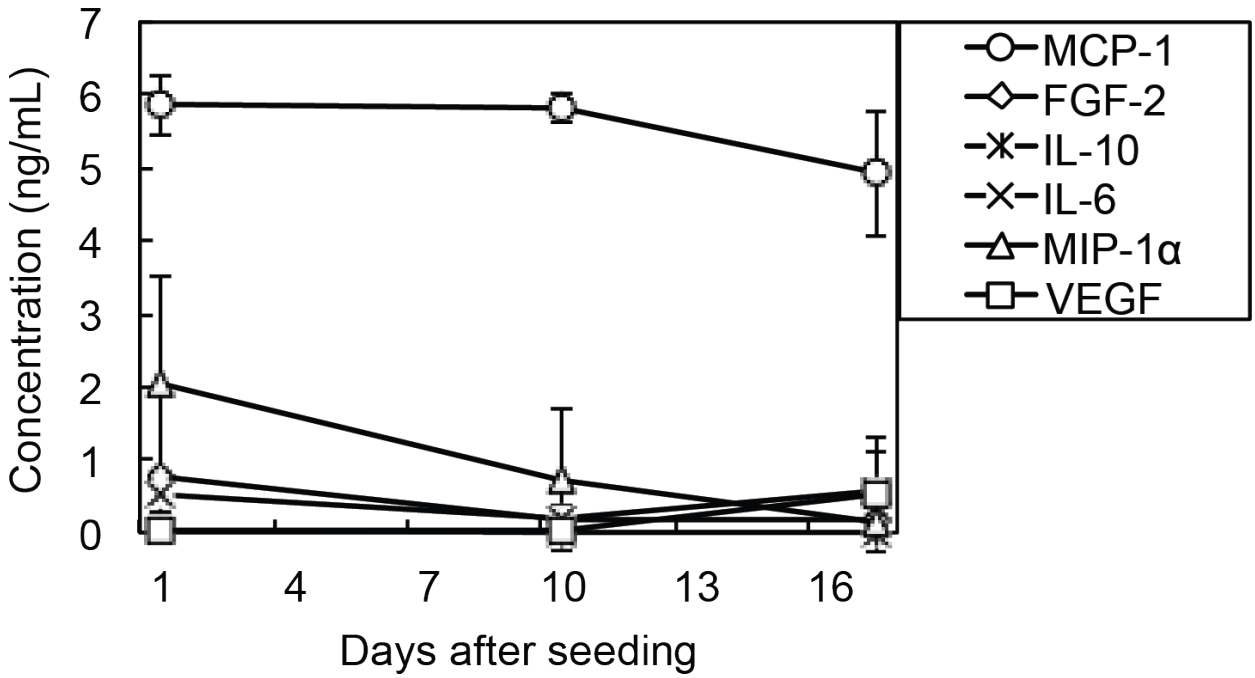

Figure 7.1: Cytokine production of MNC seeded TEHVs

Temporal cytokine production of MNC seeded TEHVs. During culture, the entire media was changed at day 1 and half the media was changed at day 10. Values represent the mean of the samples and error bars represent the standard deviation.

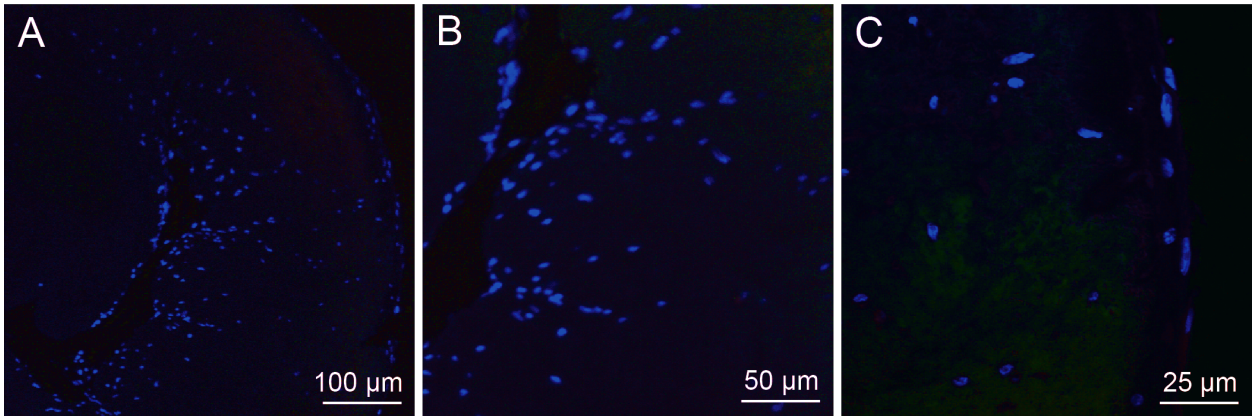

Supplemental Figure 1: Secondary antibody only staining for immunohistochemistry

Representative images of negative control slides for immunohistochemical staining using DAPI staining and secondary antibodies only (Alexa Fluor 488 or Alexa Fluor 594). The images represent different magnifications at 100x (A) 200x (B), and 400x (C). DAPI staining shows positive expression of cell nuclei. The lack of red or green staining indicates little to no background staining by the secondary antibodies.

APPENDIX B: TABLES

CHAPTER 1: No Tables

CHAPTER 2: Table 2.1-2.6

CHAPTER 3: Table 3.1

CHAPTER 4: Table 4.1 – 4.2

CHAPTER 5: Table 5.1

CHAPTER 6: Table 6.1-6.3

CHAPTER 7: No Tables

Table 2.1: Various methods for the decellularization of heart valves

Decellularization Method	Treatments/Chemicals	General Effectiveness	General Effect on Valve ECM	Ref
Anionic Detergent	SDS or Sodium deoxycholate	Lack of visible cell nuclei; ~95% DNA removal	Increased areal strain & peak stretch ratio; Decreased flexural stiffness; Preservation of GAGs. Can disrupt ECM fiber structure.	19, 29, 56, 58, 87, 101, 172, 194
Non-Ionic Detergent	Triton X-100;	Lack of visible cell nuclei	Increased areal strain and peak stretch ratio; Decreased flexural stiffness; Loose ECM network; Histological reduction of GAG, laminin, fibronectin, and collagen	63, 87, 101, 116, 157
	Triton X-100 + Sodium cholate	~30% DNA removal	Increased extensibility & decreased stiffness; GAG reduction; Preservation of elastin and collagen components	118, 159
Multi-detergent	Triton X-100 + Sodium deoxycholate	Lack of visible cell nuclei; 98% DNA removal	Histologic preservation of structure and ECM components	87, 190
	Osmotic Shock + Triton X-100 + NLS salt + Ethanol	Lack of visible cell nuclei; >97% dsDNA removal	Increased areal strain & peak stretch ratio; Decreased stress relaxation; Reduced GAG content	32, 173
Enzymatic	Trypsin + EDTA	Incomplete cell removal	Decreased mechanical properties; Histologic tissue damage & loss of basement membrane; Histologic reduction of GAG, laminin, fibronectin, and collagen;	63, 101, 116, 145, 157, 172, 194
	Trypsin + SDS	Lack of visible cell nuclei; 96% DNA removal	Reduction of GAG and αGal antigen; Preservation of mechanical properties	108
	Trypsin + Sodium deoxycholate	Visible cell remnants; 98% DNA removal	Histologic disruption of ECM components	190
Enzymatic Combinations	Trypsin + Osmotic shock + Triton X-100	Lack of visible cells	Misalignment of collagen fibers	82, 194
	Trypsin + Osmotic shock	Visible cell remnants	Histologic loss of collagen; GAG reduction; Decreased mechanical strength	157
Glycol Radiation	PEG + Gamma irradiation	Lack of visible cell nuclei; >92% cusp DNA removal	Preserved leaflet ultrastructure; Removal of αGal antigen	122
Osmotic shock	Hypotonic/Hypertonic Tris buffer	Many visible cell remnants	Histologic reduction in MHC antigens; Loss of non-collagen proteins	116, 157
Sequential Antigen Removal	Dithiothreitol, potassium chloride, amidosulfobetaine-14	Lack of visibile cell remnants and reduced antigenicity	Preservation of Young's modulus and ultimate tensile strength. Preservation of collagen and elastin. Decreased GAGs.	130, 181, 182
Supercritical Fluid	CO2; Ethanol	Lack of visible cell nuclei; 90% phospholipid removal	Stiffening of tissue; Tissue dehydration	143

ECM: extracellular matrix; SDS: sodium dodecyl sulfate; NLS: N-Llauroylsarcosine sodium salt. PEG: polyethylene glycol. MHC: major histocompatibility complex.

The general effectiveness and general effect on ECM are overall observations and individual results may vary based on the protocol or tissue used.

Table 2.2: Summary of in situ results for the implantation of non-conditioned decellularized valve scaffolds in various animal models and clinical trials.

Recell Method	Tissue	Conditioning	Implant model	Details	Results
In Situ - No Conditioning	mPV[79]	None	**Mouse** PV	Decell valve attached to donor heart and implanted in another mouse	Leaflets were thickened with many aSMA+ cells present early, though less aSMA+ cells present later
	rbAV[167] pAV[78]	None	**Canine** PV[78] Aorta[167]	Decell xenogenic valves implanted in canines	Rabbit valve leaflets degenerated. Porcine valves re-endothelialized with minimal cell infiltration near leaflet surface
	oAV[13] pAV[84, 125] oPV [72, 99, 131] pPV[99]	None	**Ovine** AV[13] PV [72, 99, 125, 131] Aorta[84]	Decell xenogeneic and allogeneic valves implanted in sheep	Re-endothelialization. Recell of valve wall. Minimal recell of leaflet. Xenograft comparable to allograft.
	pAV[69, 75, 76, 125]	None or stented[69]	**Porcine** AV[69] PV[75] Aorta[125]	Decell allogeneic valves implanted in pigs	Aorta implants led to loss of leaflets. PV implants led to good recell of surface and interior of leaflet. AV implants showed recell of conduit wall only.
	hPV[27, 120] hAV[39] pPV[28, 56, 95, 96, 127, 138, 142, 154, 176]	None	**Human** PV AV[39]	Decell allogeneic and xenogeneic valves implanted in humans	Allogeneic performed better than xenogeneic. Recell of valve wall and endothelialization evident. No evidence of leaflet recell unless by inflammatory cells.

αSMA: alpha-activated smooth muscle actin.
The results are overall observations and the outcome of individual studies may vary. Lower case letters in acronyms denote species (o = ovine, p=porcine, h=human, m=mouse, rb=rabbit).

Table 2.3: Summary of methods for in situ recellularization of decellularized valve scaffolds with chemical conditioning.

Recell Method	Tissue	Conditioning	Implant model	Details	Results
In Situ - Chemical Conditioning	rAV[6] oAV[57] pAV[122]	Valves treated with FN[6], FN + SDF-1a[57] or FN + HGF[122]	rIVC[6] oPV[57] cPV[122]	FN treated valves implanted	FN alone led to luminal recell. FN + SDF-1a led to moderate leaflet recell. FN + HGF led to great recell of the entire leaflet.
	pPV[83, 179]	CD133 conjugated to valve surface	oPV	Valves conjugated with CD133 and implanted	Early endothelial layer and leaflet interstitial recell with aSMA+ cells. MMP proteins present.
	bPV[71] hPV[71] oPV[23, 132]	Valves treated with collagen conditioning solution	bPV[71] oPV [131, 132]	Valves treated in conditioning soln. before implant	Treated valves re-endothelialized but no distal leaflet recell. Treated valves decreased antibody production in baboons.

FN: fibronectin; SDF-1α: stromal cell–derived factor 1α; HGF: hepatocyte growth factor; αSMA: alpha-activated smooth muscle actin; MMP: matrix metallopeptidase.
The results are overall observations and the outcome of individual studies may vary. Lower case letters in acronyms denote species (o = ovine, p=porcine, h=human, r=rat, c=canine, b=baboon).

Table 2.4: Summary of in vitro recellularization methods of decellularized valve scaffolds with no conditioning steps applied.

Recell Method	Cell Source	Conditioning	Implant model	Details	Results
In Vitro – No conditioning	ECs [18, 63, 135, 136]	None	None	Leaflets seeded statically	EC coverage. No internal leaflet repopulation
	Fibroblast-like cells [40, 94, 191]	None	None	Leaflets seeded statically	Mild cell infiltration in leaflet interior. Cells aSMA+ and VIM+
	MFs & ECs [90, 161]	None	cPV[90] oPV[161]	Valve seeded statically - no conditioning	Complete surface coverage and partial interstitial repopulation
	MNC or MSC [175]	None	oPV	Cells injected into valve and implanted	Complete cell surface coverage for both groups. MNC leaflets were damaged. MSC leaflets were healthy with aSMA+ cells

EC: endothelial cell; αSMA: alpha-activated smooth muscle actin; VIM: vimentin; MF: myofibroblast; MNC: mononuclear cell; MSC: mesenchymal stem cell.
The results are overall observations and the outcome of individual studies may vary. Lower case letters in acronyms denote species (o = ovine, c = canine).

Table 2.5: Various methods for in vitro recellularization of decellularized valve scaffolds with mechanical conditioning.

Recell Method	Cell Source	Conditioning	Implant model	Details	Results
In Vitro - Mechanical Conditioning	MFs and ECs [103, 104, 144]	Cultured at pulmonary pressure and flow	None	Valves seeded with EC or MF then EC then cultured	EC seeding led to surface coverage. MF & EC seeding led to great recell with appropriate phenotype.
	MSC [34]	Cultured at static, negative, or negative then positive pressure.	None	Seeded valves cultured under various pressures	Negative & positive pressure led to EC coverage and moderate cell infiltration of HSP47,+ VIM+, & aSMA+ cells
	oMSC[85] oEC[171]	Cultured in pulsatile flow bioreactor then implanted	Ovine Aorta[85] oAV[171]	Seeded valves conditioned before implant	TE valves showed complete endothelium at explant. Partial recellularization of leaflets.
	hMNCs [27]	Cultured in perfusion bioreactor	Human PV	Seeded valves conditioned before implant in two patients	*In vitro* seeding led to complete EC monolayer. Both patients showed somatic growth, valve growth, and no valve degradation at 3.5y.

MF: myofibroblast; EC: endothelial cell; MSC: mesenchymal stem cell; HSP47: heat shock protein 47; VIM: vimentin; αSMA: alpha-activated smooth muscle actin; TE: tissue-engineered; MNC: mononuclear cell.
The results are overall observations and the outcome of individual studies may vary. Lower case letters in acronyms denote species (o = ovine, h = human).

Table 2.6: Various methods for in vitro recellularization of decellularized valve scaffolds with chemical conditioning.

Recell Method	Cell Source	Conditioning	Implant model	Details	Results
In Vitro - Chemical Conditioning	rMSC [68] mMF [160] hMF [160] hEC [160]	Valves coated with P3/4HB before seeding	None	Hybrid valves seeded *in vitro*	Hybrid valves had increased mechanics. *In vitro* seeding led to cell coverage, but no infiltration.
	rMF[42] hECs[195, 196] hMF [73]	Leaflets modified with PEG plus TGF-B1, VEGF, or RGD peptides	None	PEG-peptide modified leaflets seeded with cells	PEGylation increased mechanics and cell surface density, regardless of additional peptide. No cellular infiltration.
	gMSC [123]	Encapsulation of cells in PEG before seeding	Goat aorta	PEG encapsulated cells seeded on decell scaffold then implanted in goats	PEG-cell seeding increased tensile strength, increased ratio of endothelial cells, and decreased thrombosis
	rMSC[197] hEPC[187, 188]	Polyelectrolyte layers of heparin & SDF1a/ chitosan/ VEGF adsorbed onto valve	None[187, 188] rAorta[197]	Valve scaffolds coated with polyelectrolyte multilayers then seeded with cells	Treated valves led to reduced platelet activation. Chitosan and VEGF increased EC adherence, and proliferation in vitro. SDF-1a had increased endothelial layer after implant *in vivo*
	oECs [170]	Valves coated in CCN1	oPV	Valves coated in CCN1 and before implant	Treated valves had good recell *in vivo*. Cell coverage higher on ventricularis with mild infiltration of VIM^+ & $aSMA^+$ cells
	rMSCs [189]	Valves conjugated with CD90 antibody	None	Treated leaflets cultured in shear flow chamber with MSCs	Treated leaflets had increased cell attachment distributed across surface
	pVIC[16] hMSC[77]	Valves treated with fibronectin before seeding	None	Treated leaflets seeded statically	Leaflet surface coverage and mild cell infiltration by appropriate phenotypes
	oECs[47]	Valves treated with fibronectin before seeding	oPV	Treated valves seeded then implanted	Treated valves had complete EC layer and good interstitial repopulation
	hECs [49-51]	Valve treated with Pronectin F before seeding	hPV	Treated valves seeded and implanted in 11 patients	100% survival at 10y. 3m biopsy of valve wall showed endothelialization and partial recell by fibroblast cells.

MSC: mesenchymal stem cell; MF: myofibroblast; EC: endothelial cell; P3/4HB: poly(3-hydroxybutyrate-co-4-hydroxybutyrate); PEG: polyethylene glycol; TGF-β1: transforming growth factor beta 1; VEGF: vascular endothelial growth factor; EPC: endothelial progenitor cell; SDF-1α: stromal cell–derived factor 1α; VIM: vimentin; αSMA: alpha-smooth muscle actin; VIC: valvular interstitial cell.
The results are overall observations and the outcome of individual studies may vary. Lower case letters in acronyms denote species (o=ovine, p=porcine, h=human, m=mouse, r=rat, g=goat).

Table 3.1: Biochemical concentrations of human and ovine aortic valves

Species	Condition	Collagen (µg/mg tissue)	Elastin (µg/mg tissue)	sGAG (µg/mg tissue)	Total Protein (µg/mg tissue)
Ovine	Decell	24.52 (7.72)	6.64 (1.52)	**0.39 (0.47)****	133.42 (64.27)
	Cryo	25.78 (2.85)	6.78 (1.45)	**1.62 (1.20)****	153.47 (46.65)
Human	Decell	22.28 (8.46)	**4.77 (1.73)***	**0.78 (0.21)***	167.20 (67.58)
	Cryo	19.35 (2.25)	**6.52 (1.43)***	**1.73 (0.41)***	160.17 (47.01)

Biochemical makeup of human and ovine aortic valve ECM before (cryo) and after decellularization (decell). Mass measurements of samples were made using wet tissue. Values reported as mean (standard deviation).
* statistically significant difference between groups of the same species ($p < 0.05$, t-Test)
**statistically significant difference between groups of the same species ($p < 0.05$ Mann-Whitney Test).

Table 4.1: Mechanical properties of TEHVs seeded with MNC, MSC, MSC2, or VIC populations.

Cell Type	Areal Strain (%)	Circ. Stretch Ratio	Radial Stretch Ratio
MNC	124.01 ± 19.06 [a,b,c]	1.27 ± 0.11	1.77 ± 0.13
MSC	153.83 ± 28.12 [b,d]	1.37 ± 0.11 [b]	1.85 ± 0.12
MSC2	134.48 ± 8.43	1.30 ± 0.07	1.81 ± 0.06
VIC	151.99 ± 18.24 [c]	1.39 ± 0.05 [a]	1.82 ± 0.13
Cryo	124.53 ± 19.73 [d,e]	1.21 ± 0.06 [a,b,c]	1.84 ± 0.14
Decell	158.09 ± 15.40 [a,e]	1.36 ± 0.07 [c]	1.90 ± 0.11

Biaxial mechanical properties of MNC, MSC, MSC2, and VIC seeded ovine aortic valves. Previously reported data for cryopreserved (cryo) and decellularized (decell) ovine aortic valves are included for comparison [24]. Data is reported as mean ± standard deviation. Superscript letters of the same type indicate a significant difference between groups ($p < 0.05$).

Table 4.2 Biochemical concentrations of TEHVs seeded with MNC, MSC, MSC2, or VIC populations.

Cell Type	GAG	Collagen	Tot. Protein
MNC	0.93 ± 0.31	73.50 ± 8.29 [a,b]	203.2 ± 28.5
MSC	0.99 ± 0.32	68.00 ± 18.80 [c,d]	216.2 ± 88.4
VIC	1.04 ± 0.25	64.49 ± 10.18 [e,f]	197.2 ± 50.5
2x MSC	0.917 ± 0.26	70.40 ± 12.64 [g,h]	248.6 ± 45.1 [a,b]
Cryo	1.62 ± 1.20 [a]	39.49 ± 7.11 [a,c,e,g]	153.5 ± 46.6 [a]
Decell	0.39 ± 0.47 [a]	40.25 ± 3.79 [b,d,f,h]	133.4 ± 64.3 [b]

Biochemical concentrations of MNC, MSC, MSC2, and VIC seeded ovine aortic valves. Previously reported data for cryopreserved (cryo) and decellularized (decell) ovine aortic valves are included for comparison [24]. Data is reported as mean ± standard deviation. Superscript letters of the same type indicate a significant difference between groups ($p < 0.05$).

Table 5. 1: Biochemical concentrations of MNC seeded TEHVs after extended conditioning

Test Group	Collagen (µg/mg wet tissue)	GAG (µg/mg wet tissue)
Cryo	48.24 ± 4.92	1.73 ± 0.41*
Decell	44.33 ± 11.59	0.78 ± 0.21*
3wk	47.89 ± 14.82	0.58 ± 0.25
6wk	39.73 ± 11.22	0.64 ± 0.23

Biochemical data for 3 week and 6 week conditioned heart valve leaflets. Previously reported data for cryopreserved (cryo) and decellularized (decell) human aortic valves are included for comparison [ref]. Data reported as the mean ± standard deviation. * indicates a significant difference between groups ($p < 0.05$)

Table 6. 1: Gene expression of TEHVs from bioreactor conditioned groups

Marker	Gene	Hypox/ HighP	Norm/ HighP	Hypox/ NegP	Norm/ NegP
VIC	VIM	↑	↑	↑	↑
	ACTA2	↓	↓↓	↓	↓↓
MSC	THY1	↓	↓	↑	↑↑
	CD44	↑	↑	↑	↑
	ITGB1	↓	↓	↑	↑
	ANPEP	↑	↑	↑↑	↑↑
ECM Remodeling	HSP47	↓	↓	↑	↑
	COL1A1	↓	↓	↑	↑
	COL3A1	↓	↓	↑	↑
	MMP1	↑↑↑	↑↑↑	↑↑↑	-
Cell Proliferation	MKI67	↓	↓	↑	-
Apoptosis	BAX	↑	↑	↑	↑↑
Hypoxia	EPAS1	↓	↓	↓	↓
HSC	CD34	-	-	-	-
Endothelial	vWF	-	↑↑	-	-
	ENG	↓	↓	↑	↑
Leukocyte	PTPRC	↓↓	↓	-	-
Macrophage	CD14	↓	↓	↑	-
Chondrocyte	ACAN	↓↓↓	↓↓↓	↓↓	-
Osteoblast	ALPL	↓	↓	↓	-
Adipocyte	ADIPOQ	↑	↓	-	-

Gene expression of the tissue engineered heart valves from each bioreactor conditioning group. Data is qualitatively presented as the fold change in expression for each gene of the tissue engineered valves relative to their matched pre-seeded cell populations.

Note: changes in gene expression in bioreactor conditioned tissues were evaluated relative to their matched pre-seeded cell populations. Fold change in expression is presented qualitatively based on the scale described below.

"↑" or "↓" = Fold change (increased or decreased, respectively) in range 1 to 9.99.

"↑↑" or "↓↓" = Fold change (increased or decreased, respectively) in range 10 to 99.99.

"↑↑↑" or "↓↓↓" = Fold change (increased or decreased, respectively) in range 100 to 295.

"– " = No expression

Table 6.2: Biochemical concentrations of TEHVs from bioreactor conditioned groups

	GAG (μg/mg wet tissue)	**Collagen** (μg/mg wet tissue)	**Total Protein** (μg/mg wet tissue)
Hypox/High P	0.649 ± 0.173	54.59 ± 15.64 [a,b]	131.93 ± 44.44
Norm/High P	0.427 ± 0.204	63.61 ± 13.54 [c,d]	139.47 ± 38.28
Hypox/Neg P	0.516 ± 0.172	50.17 ± 9.32 [e,f]	106.20 ± 35.13
Norm/Neg P	0.474 ± 0.157	53.43 ± 4.90 [g,h]	128.47 ± 32.88
Cryo	1.622 ± 1.199 [a]	25.78 ± 2.85 [a,c,e,g]	153.47 ± 46.65
Decell	0.390 ± 0.473 [a]	24.52 ± 7.72 [b,d,f,h]	133.42 ± 64.27

Concentration of GAG, collagen, and total protein measured within the extracellular matrix of the tissue engineered heart valve groups. Data is presented as the mean ± standard deviation. Superscript letters of the same type indicate a significant difference between groups ($p < 0.05$).

Table 6.3: Recellularization comparison of donor matched hypoxic/normoxic conditioned TEHVs

Donor	Pressure Conditioning	Hypoxic Valve Cell Density (cells/mm^2)	Normoxic Valve Cell Density (cells/mm^2)	Fold Change
Donor 1	Positive	259.53 ± 22.96	30.96 ± 30.09	8.38
Donor 2	Positive	44.92 ± 13.75	38.41 ± 17.63	1.17
Donor 3	Positive	41.11 ± 19.00	22.80 ± 19.82	1.80
Donor 4	Negative	38.25 ± 9.41	18.18 ± 13.83	2.10
Donor 5	Negative	160.93 ± 106.26	70.38 ± 0.06	2.29
Donor 6	Negative	142.35 ± 42.27	24.70 ± 19.81	5.76

Measured cell densities at the distal tip region of each donor matched hypoxic and normoxic valve. Measurements were made on a per leaflet basis. Data is presented as the average per valve ± standard deviation. The fold change displays the cell density of the hypoxic valve compared to the normoxic valve. Superscript letters of the same type indicate a significant difference between matched valves ($p < 0.05$).